# IDENTIFICATION AND CHARACTERISATION OF MICRORNAS INVOLVED IN THE PATHOGENESIS OF HIV–ASSOCIATED NON-HODGKIN'S LYMPHOMA

**Miss Taahira Goolam Hoosen**
(GLMTAA001)

submitted in fulfilment of the requirements for the award of degree of

M.Sc. Med: Haematology

Department of Pathology
Division of Haematology
Faculty of Health Sciences
UNIVERSITY OF CAPE TOWN

Supervisor: Dr. Shaheen Mowla

13 March 2017



# DECLARATION

I hereby certify that this dissertation submitted for the M.Sc. Med (Haematology) degree at the University of Cape Town is based on my original work and has not been previously submitted for another degree at this or any other university. I waive copyright of the dissertation in favour of the University of Cape Town. I declare that this work is not plagiarised and that each contribution to and quotation in this dissertation from the work of others has been cited and referenced using the Harvard referencing style.

Signed

**13 March 2017**

Miss Taahira Goolam Hoosen — Date

# ABSTRACT

Background: Since its discovery about three decades ago, the Human Immunodeficiency Virus (HIV) has claimed over millions of lives globally. Although our understanding of the mode of transmission and action of this causative agent for the Acquired Immune Deficiency Syndrome (AIDS) has increased through research, and treatment regimens developed and improved, in certain parts of the world the pandemic continues to expand. Sub-Saharan Africa, which is the epicentre of this global health concern, accounts for approximately 66% of the total number of individuals affected, with South Africa enduring the heaviest burden.

South Africa has the world's largest antiretroviral therapy (ART) programme and as such, HIV infected people are living longer, and consequently the incidence of HIV co-morbidities has increased dramatically. HIV/AIDS defining cancers are such co-morbidities with Non-Hodgkin's lymphomas (NHL) being the second most common HIV-associated cancer. Diffuse Large B-cell lymphoma (DLBCL) and Burkitt's lymphoma (BL) are the main subtypes and both present aggressively in HIV positive patients with rapid progression. The use of highly active antiretroviral therapy (HAART) has decreased the incidence of DLBCL in HIV positive patients, however the prevalence of these cancers still remain high in some settings.

It has been suggested that the pathogenesis of these cancers in HIV infected individuals is complex and different to that in HIV uninfected individuals, with the possibility that the virus may have an oncogenic role. This has already been demonstrated in the case of the HIV/AIDS-defining cancer Kaposi Sarcoma. However, the same has not been unequivocally demonstrated in HIV-associated NHL. In light of this, the mechanisms through which viruses and viral components promote cellular transformation is an area of active research.

One of these mechanisms manipulated by viruses is through the dysregulation of cellular microRNAs (miRNAs) which are small non-coding RNA molecules that are key regulators of gene expression. While they are essential for normal cellular functioning, their expression has been found to be deregulated in diseases including cancer. Several studies have described specific miRNA signatures for NHLs including for DLBCL and BL but none have been described for the HIV-association of these cancers.

Aim: The aim of this project was to identify and characterise miRNAs involved in the

pathogenesis of HIV-associated NHLs. This thesis reports on the changes in expression of miRNAs in B-cells exposed to an attenuated form (structurally intact but non-infectious) of HIV.

Methods: We designed a custom miRNA microarray to identify deregulated miRNAs in the BL cell line Ramos that were exposed to HIV compared to microvesicle treated cells. It was initially planned to use both normal B-cells (L1439A) and BL cells for analysis but Ramos was selected due to technical reasons for this step. Thereafter we validated selected miRNAs by quantitative real-time PCR (qPCR) using single-tube TaqMan® Assays which was predominantly performed in the lymphoblastoid cell line L1439A, which is derived from a healthy donor. We then focused on further characterising the role of one miRNA in the development of HIV-associated NHL by using prediction programmes to predict its putative gene targets and then confirmed its target by using qPCR and western blot analyses.

Results: Extensive and comprehensive analysis of the array data led to the identification of a large number of miRNAs which were differentially expressed, with 32 being selected for further studies. These 32 miRNAs include 16 upregulated and 16 downregulated miRNAs, and were selected because they displayed changes in expression by two or more folds. Thereafter, four miRNAs, namely miR-363-3p, miR-222-3p, miR-200c-3p and miR-575, were chosen for validation based on their reported involvement in cancer for validation. The results of two miRNAs (miR-575 (upregulated) ($p \leq 0.05$) and miR-200c-3p (downregulated) ($p \leq 0.05$)) were found to be consistent with the results obtained from the miRNA microarray whilst the other two were opposite to that result (both downregulated) ($p \leq 0.05$).

Using online tools as well as the published literature, several potential target genes of miR-575 were identified, namely *DENND5A, CDK1, CSTA* and *ATAD5*. One particular target, the BH3-like motif containing inducer of cell death (*BLID*), which is involved in apoptosis, has previously been confirmed as a gene target in non small cell lung cancer. Using qPCR, we found that *BLID* messenger RNA (mRNA) was downregulated in normal B-cells when exposed to HIV-1 AT-2. Unfortunately, the BLID protein could not be detected using western blot analysis despite several attempts at detecting varying concentrations of the protein and using two different positive control cell lines.

Conclusion: The reverse correlation, between miR-575 and *BLID* mRNA expression in the same cell line and under the same treatment conditions, supports the notion that the downregulation of miR-575 may be physiologically relevant. However, this could not be further verified as the BLID protein could not be detected in the L1439A cells, even in the microvesicle treated control cells. Future studies should look at further characterisation of miR-575 in the pathogenesis of HIV-associated NHLs by investigating other predicted gene targets of the miRNA. This will then be followed by loss and gain of function assays to confirm the miRNA:mRNA relationship. Furthermore, functional analyses, such as measure of apoptosis, expression of key regulators of the cell cycle, and other cellular events characteristic of cancer should be carried out to define the role of the miR-575 in the development of HIV-associated lymphoma.

# ACKNOWLEDGEMENTS

*"... I took the road less travelled and it has made all the difference in my life...."*
*Robert Frost*

This incredible journey would not have been possible without the following gracious people.

Firstly, I would like to thank my family for the constant support and motivation towards always educating and empowering myself. Being away from home is tough especially when you are the glue that keeps it all together but your voices, prayers and wishes for my dreams keeps me going strong. Praise to God for all that he has provided & helped me through those days when I wanted to give up!

The next person is a dear friend and colleague who is a constant inspiration to us all but especially to me. His courage and thirst for making a difference inspires me to be the best I can be daily. His support & wisdom has enabled me to never give up and seek new ways of thinking both for myself to grow in my career as well as in the way we make a difference through our NPO. Thank you Habib!

The next group of people are responsible for making this Masters endeavour possible.

- The Haematology lab: All my skills in the lab have been taught to me by my colleagues thank you to Beatrice, Leo, Lungile, Grant, Noni, Gift and Kirsty for the patience, and willingness to always assist when you could. A special thank you to Rashaad, Colleen, Jean & Princess for being the kind people that you are!
- CPGR: Dr. Wendy Kröger, Jacqueline Meyer and Nicki Adams for their assistance
- Dr. Wendy Burgers and Prof. Jeff Lifson for the kind donation of AT2-HIV-1 virions
- Fadwah Booley for assistance and use of the Roche Light Cycler machine
- Prof. Sharon Prince Lab: Kind donation of breast cancer cells & expertise
- National Research Foundation: For making this journey possible & less stressful

Lastly and most importantly, no research journey is easy but it helps when your supervisor is understanding and nurtures you to make the most out of the journey. Thank you Shaheen for always being supportive, guiding and imparting your valuable knowledge.

# CONTENTS

# LIST OF FIGURES

# LIST OF TABLES

# ABBREVIATIONS

3’ UTR – 3’ untranslated region

ABC – activated B-cell

AGO2 – Argonaute 2

AID – activation-induced cytidine deaminase

AIDS – Acquired Immune Deficiency Syndrome

ART – antiretroviral therapy

AT-2 – aldriothiol-2,2

BCL2 – B-cell lymphoma 2

B-CLL – B-cell chronic lymphocytic leukeamia

BL – Burkitt’s lymphoma

BLID – BH3-like motif containing inducer of cell death

BRCC2 – breast cancer cell type 2

cDNA – complementary DNA

CSR – class switch recombination

Ct – critical threshold

DEPC – diethyl pyrocarbonate

DGCR8 – DiGeorge Syndrome critical region 8

DLBCL – Diffuse large B-cell lymphoma

DMEM – Dulbecco’s Modified Eagle Medium

DMNT – DNA Methyltransferases

DMSO – dimethyl sulphoxide

dsRBD – double stranded RNA binding domain

EBV – Epstein Barr Virus

EtBr – Ethidium bromide

EtOH - Ethanol

FBS – fetal bovine serum

FC – fold change

GAPDH – Glyceraldehyde-3-Phosphate Dehydrogenase

GCB – germinal centre B-cell

gDNA – genomic DNA

GTP – guanosine triphosphate

HAART – highly active antiretroviral therapy

HIV – Human immunodeficiency virus

IGH – immunoglobulin heavy chain

KS – Karposi Sarcoma

KSHV – Karposi Sarcoma Herpes virus

miRNA – microRNA

mRNA – messenger RNA

NHL – Non-Hodgkin's lymphoma

NOS – not otherwise specified

NTC – no template control

PACT – protein activator of PKR

PBMC – peripheral blood mononuclear cell

PBS – phosphate buffered saline

PML-BCL – primary mediastinal large B-cell lymphoma

Pre-miRNA – precursor miRNA

Pri-miRNA – primary miRNA

P/S – penicillin/streptomycin

qPCR – quantitative polymerase chain reaction

R-CHOP – rituximab, cyclophosphomide, doxorubicin, vincristine and oral prednisone

RISC – RNA inducing silencing complex

RNAi – RNA interference

RNAP – RNA polymerase

RPL27 – 60S ribosomal protein 27

RPMI – Roswell Park Modified Institute

RSS – RNA silencing suppressor complex

RT – reverse transcription

RT-qPCR – real time qPCR

SHM – somatic hypermutation

Tat - Trans-Activator of Transcription

TLDA - TaqMan® Low Density Array

TLR8 – Toll like receptor 8

$T_m$ – melting temperature

TRBP – Tar RNA binding protein

UV – ultraviolet

vmiRNA – viral miRNA

# CHAPTER 1: INTRODUCTION

## 1.1 MICRORNAS

MicroRNAs (miRNAs) are a group of small (17-25 nucleotides) of non-coding RNA molecules that bind to the 3' untranslated region (UTR) of protein coding transcripts. These highly conserved molecules first discovered in 1993 (Lee *et al.,* 1993), are thought to regulate up to 30% of human protein coding genes (Sassen *et al.,* 2008). Research in the last decade has shown that miRNAs regulate gene expression post-transcriptionally, either by complete degradation of messenger RNA (mRNA) through the RNA interference (RNAi) pathway or by inhibiting protein translation (Sassen *et al.,* 2008; Lee *et al*., 1993). The latter mode of regulation is however, dependent on the degree of miRNA-mRNA target sequence complementarity.

### 1.1.1 Biogenesis of miRNAs

Functional miRNAs are formed from longer precursor molecules (designated as mir) encoded by miRNA genes (Figure 1.1) that undergo two ribonuclease reactions. This process firstly begins in the nucleus whereby the primary transcripts (pri-mir) are several kilobases long which is polyadenylated at the 3' end and contains a 7-methylguanosine cap at the 5' end (Lee *et al.,* 2002). Initiated via transcription by RNA polymerase (RNAP) II, a stem loop structure is created which is then cleaved into several precursor miRNAs (pre-mir). As shown in Figure 1.1, cleavage of miRNAs are performed by a 500-650 kDa microprocessor complex that consists of the RNAP III enzyme, Drosha and its co-factor, the double stranded RNA binding domain (dsRBD) protein DiGeorge Syndrome critical region 8 (DGCR8) molecule (Gregory *et al.,* 2004). At this stage pre-miRNAs (60-100 nucleotides) contain a two nucleotide overhang that is bound to exportin-5 and Ran-guanosine triphosphate (GTP). These molecules not only protect the pre-miRNA from cellular digestion but also mediates its translocation from the nucleus into the cytoplasm (Guttler & Gorlich, 2011).

The second ribonuclease reaction takes place in the cytoplasm by the RNAP II enzyme, Dicer along with dsRBD protein Tar RNA binding protein (TRBP) and protein activator of PKR (PACT) (Figure 1.1). A mature miRNA (designated as miR) approximately 22-25 nucleotides in length is produced with a two nucleotide overhang on each 3' end by removal of the stem

loop structure. Two strands are therefore produced in which the mature guide miRNA forms part of the functional centre of the RNA-inducing silencing complex (RISC) and the other passenger miRNA becomes degraded (Sand *et al.*, 2011).

The nomenclature of miRNAs are distinct in that they are assigned sequential numerical identifiers with abbreviated three or four letter prefixes to designate the species (e.g. hsa-miR for *Homo sapiens* and mmu-miR for the mouse species) whilst paralogous sequences whose mature miRNAs differ at only one or two positions are given lettered suffixes (e.g. hsa-miR-200c) and finally distinct hairpin loci that give rise to identical mature miRNAs have numbered suffixes (e.g. hsa-miR-10-1). The two mature strands produced can also either be excised from opposite arms of the same hairpin precursor and are designated by the suffixes, 5p or 3p, indicating which arm the mature miRNA arises from (Griffith-Jones *et al.,* 2006).

Mature miRNAs recognise their target messenger RNAs (mRNAs) by sequence complementarity between nucleotides 2-8 of the miRNA at the 5' end (known as the seed region) and complementary nucleotides in the 3' untranslated region (3' UTR) of mRNAs which determine their function (Kuhn *et al.,* 2008). RISC along with Argonaute 2 (AGO2) associated with cellular miRNA fragments bind to the 3' UTR of their target mRNA (Wang *et al.*, 2009). Thereafter, the miRNA/RISC complex anneals to this region and mRNA degradation is performed should complete complementarity be found. Alternatively, translational repression can occur when there is limited complementarity with this complex (Reinhart *et al*., 2000).

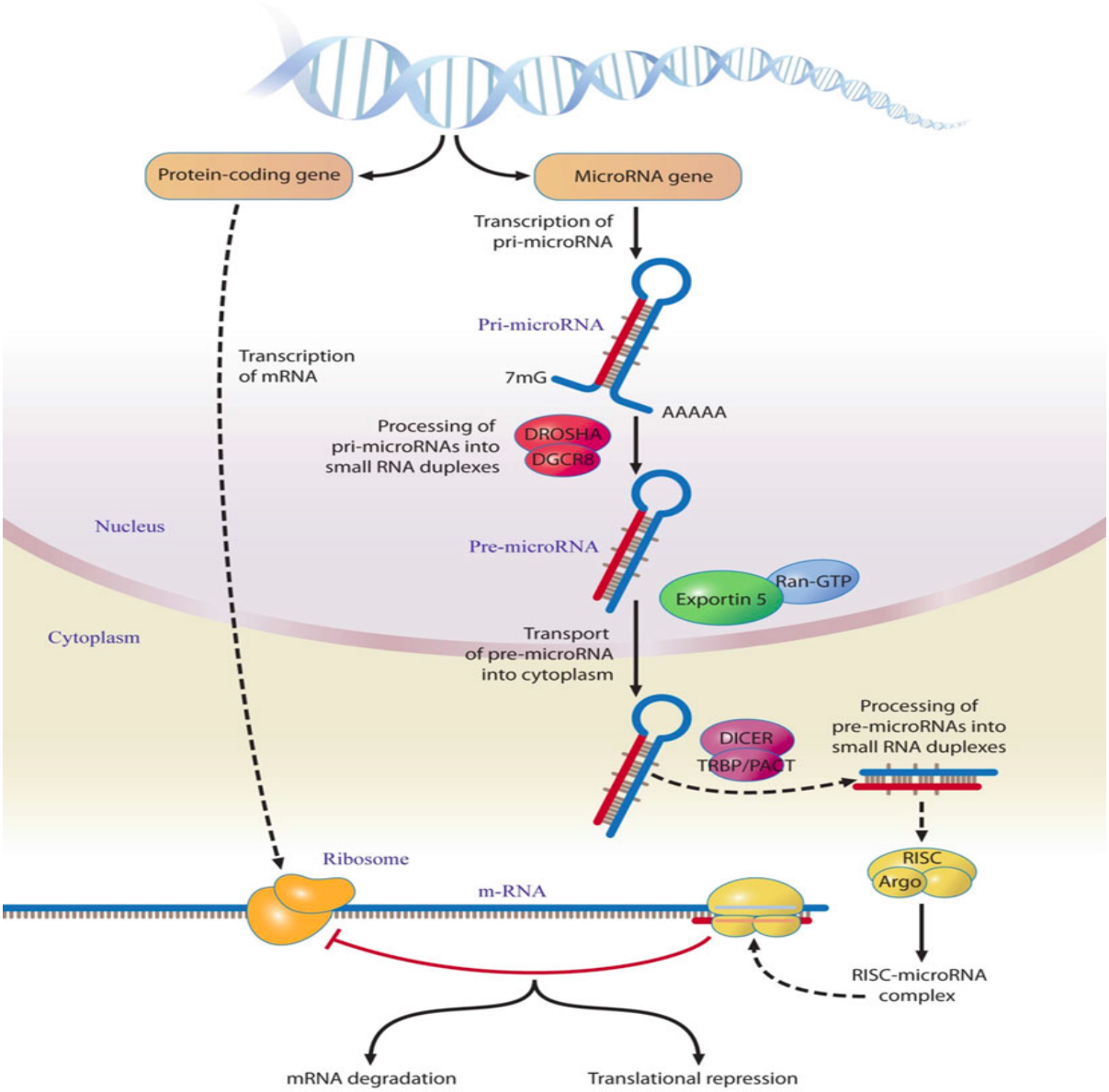


**Figure 1.1: Biogenesis of miRNAs.** Two maturation processes are involved by RNase enzyme action by Dicer and Drosha. The first reaction takes place in the nucleus whilst the second takes place in the cytoplasm to produce two miRNAs strands. The mature guide strand performs either translational repression or degradation of mRNA (Reproduced from Sand, 2014).

### 1.1.2 Biological Function of miRNAs

The first miRNA, lin-4 was discovered in the nematode, *Caenorhabditis elegans*. The role of lin-4 was reported to be involved in developmental timing (Lee *et al*., 1993). Thereafter, Reinhart *et al.,* (2000) discovered let-7 in the same organism, which led to the subsequent identification of homologs in humans and other animals (Pasquinelli *et al*., 2000). Since the discovery by Lee and colleagues, miRNAs have been found in other species and the conservation across species suggests a fundamental biological role. To date, 2588 mature

miRNAs have been identified in the human genome and the number is ever increasing *(http://www.mirbase.org)*.

The biological function of many miRNAs to date are not known or are poorly understood. Studies among invertebrates have however, shown that miRNAs regulate a range of cellular processes including developmental timing (Lee *et al.,* 1993) and neuronal differentiation in *C. elegans* (Johnston & Hobert, 2003), whilst cell proliferation has been shown in the *bantam* gene of *Drosophila* (Brennecke *et al.,* 2003). In mammals, roles for miRNAs in embryogenesis and stem cell maintenance have been identified in mouse models (Bernstein *et al.,* 2003), but computational biology has been largely relied upon to infer miRNA targets and functions, especially in humans (Liu *et al.,* 2012). In addition, several studies have demonstrated deregulated expression of miRNAs in a wide range of diseases, including cancer. It remains unknown however, if this deregulated expression is a cause or consequence of pathogenesis.

### 1.2 ROLE OF MIRNAS IN CARCINOGENESIS

Cancer is a complex disease that involves an ongoing battle between oncogenes and tumour suppressor genes which is ultimately won by oncogenes. It is caused by the alteration of gene expression and structural abnormalities of both coding and non-coding genes (Calin & Croce, 2006; Fabbri, 2013). This altered gene expression is known to lead to uncontrolled cell proliferation, and it is becoming increasingly evident that miRNAs play a role in the development and pathogenesis of cancer. This statement can be supported by three observations.

Firstly, the earliest miRNAs discovered in *C. elegans* and *Drosophila* were shown to control cell proliferation and apoptosis (Lee *et al.,* 1993; Brennecke *et al.,* 2003). Deregulation of these fundamental biological miRNAs have suggested that these regulatory molecules may contribute to proliferative diseases such as cancer.

Secondly, the discovery of human miRNAs have been located at fragile sites in the genome or regions that were commonly amplified or deleted in human cancers. This is supported by the first genome wide location analysis of 186 miRNAs (Calin *et al*., 2004). It was reported that 98 out of 186 (52.5%) miRNAs were located in cancer associated genomic regions or fragile sites, in minimal regions of loss of heterozygosity, regions of amplification and common

breakpoint regions. Deregulated expression levels were further shown in conjunction with their location. These fragile sites were found to contain oncogenes and tumour-associated viruses that in turn would influence the development of cancer (Calin *et al.,* 2004).

Lastly, widespread deregulated expression of miRNAs was found in malignant tumour cell lines compared to normal tissue. The first comprehensive profile of cancers with miRNA expression analysis was conducted in 2006. A total of 540 samples were analysed which included 363 solid tumours from six malignancies compared to 177 normal tissue samples. It was found that 36 miRNAs were upregulated and 21 were downregulated, with several of these being well characterised miRNAs such as, miR-17-5p, miR-20a, miR-21, miR-92, miR-106a and miR-155 (Volinia *et al.*, 2006). These observations together suggest a direct link between miRNAs and cancer of which evidence supporting their further roles are provided in the next section.

### 1.2.1 OncomiR & tumour suppressor miRNAs

The potential role of miRNAs in the development of cancer was found in early observations, however the first suggested direct link was only reported in 2002 by Calin *et al.,* (2004) in B-cell chronic lymphocytic leukeamia (B-CLL). Two miRNAs, *miR15* and *miR16* were found to be downregulated in the majority (68%) of cases when compared to normal tissue. Though the first profile of cancers with miRNA expression analysis was performed in 2006, significant deregulated miRNA expression was first shown in a variety of human cancers (breast, pancreatic and liver cancers and B-cell lymphoma), by Lu *et al.,* (2005) in the previous year. Significant global reduction of miRNAs was observed when compared to normal tissues in this study. A total of 334 samples were analysed with particular interest in 217 mammalian miRNAs (Lu *et al.,* 2005). Despite the significant finding, the question remained whether miRNAs were a cause or consequence of cancer. Evidence was later provided by Kumar *et al.,* (2007) that miRNAs promoted tumourigenesis in lung cancer. Using knock out mice that contained the missing allele of the microprocessing enzymes, Drosha and Dicer, they were able to show that the mice had developed an increased tumour burden (Kumar *et al.,* 2007). This supported earlier discoveries, that reduced let-7 expression was associated with lung cancer (Takamizawa *et al.,* 2004) and that it was a negative regulator of the oncogene, RAS which is involved in cell growth, differentiation and survival (Johnson *et al.,* 2005).

Subsequent studies thereafter began to identify miRNAs as having either an oncogenic (oncomiR) or tumour suppressor miR role (Volinia *et al.,* 2006; Gaur *et al.,* 2007). Gaur *et al*., (2007) revealed that miRNA expression correlates to cell proliferation indices, and therefore indicate that those miRNAs are important in regulating proliferation. They were able to identify a total of 145 miRNAs as either candidate oncomiRs or tumour suppressor miRs in four different cell lines. Although many studies have found miRNAs to be downregulated in cancer, miRNAs which are upregulated have also been found in many types of cancers. A key issue though, is the level of expression that can be considered biologically significant (Calin *et al.,* 2006). In addition, it has also been found that miRNAs can also regulate gene expression through other mechanisms such as through epigenetic factors, other non-coding RNAs, or by directly binding to proteins (transcription factors or receptors), and the triggering of cell signal transduction (Fabbri, 2013). Over the years it has also become apparent that miRNAs are tissue specific and may have more than one mRNA target (Zhou *et al.,* 2013a). This suggests that a single miRNA may have multiple roles supporting further exploration into their biological function as an oncomiR or tumour suppressor miR depending on their gene target and tissue of origin (Esquela-Kerscher & Slack, 2006; Sand, 2014).

### 1.2.2 Deregulation of miRNAs in lymphomas

The deregulation of several miRNAs, and their target genes, has been associated with the development of lymphomas (Lawrie, 2012; Thapa *et al.,* 2011; Farazi *et al.,* 2013; Lim & Marra, 2013). Expression profiling studies of miRNAs have identified miRNAs that are associated with different types of B-cell lymphomas including Burkitt's lymphoma (BL), Diffuse Large B-cell lymphoma (DLBCL) and Follicular lymphoma (FL) (Onnis *et al.,* 2010; Bueno *et al.,* 2011; Lenze *et al.,* 2011; Robertus *et al.,* 2010). Additionally, animal models further provides evidence for miRNA involvement in lymphomagenesis (Lawrie, 2012; Sandhu *et al.,* 2013). This has led to the recent identification of specific miRNA signatures for different types of B-cell lymphomas (Di Lisio *et al.,* 2012; Lim & Marra, 2013).

The dysregulation of miRNAs in the above cancers can be caused by several mechanisms, which range from copy number alterations to chromatin modifications (Lim & Marra, 2013). Translocations are a frequent cause which can result in the gain or loss of miRNA function (Calin *et al*., 2004). The disruption of miRNA expression patterns can also be caused by deregulation of transcription factor activity, such as MYC, seen in BL (Spender & Iman, 2014). Furthermore, disruption of Drosha and Dicer expression at the post-transcriptional level can

occur resulting in alterations at the miRNA biogenesis level (Lim & Marra, 2013). Lastly, viral infections can be associated with lymphomagenesis, such as the Epstein-Barr virus (EBV) and human immunodeficiency virus (HIV), which may lead to alteration in miRNA expression (Lim & Marra, 2013).

## 1.3 HIV-ASSOCIATED LYMPHOMAS

### 1.3.1 HIV and non-Hodgkin lymphoma

An estimated 36.7 million people globally were living with HIV in 2016 with 1.1 million deaths attributed to AIDS-related illnesses (UNAIDS, 2016). Sub-Saharan Africa accounts for the bulk of this burden with 24.2 million (66%) infected people with South Africa bearing the brunt of the burden hosting an alarming 6.8 million people of the global total (UNAIDS, 2016). South Africa has the largest antiretroviral therapy (ART) programme for the treatment of HIV (Abayomi *et al.,* 2011). The standard treatment is the combination of three or more antiretroviral drugs known as highly active antiretroviral therapy (HAART) (also known as combination ART) (Egger *et al.,* 2002). Whilst HIV infects and destroys the host's $CD4^+$ T–cells causing a loss of immune regulation leading to Acquired Immune Deficiency Syndrome (AIDS), a clear link between HIV and certain types of cancers has been identified which are described as HIV/AIDS-defining cancers.

Non-Hodgkin lymphoma (NHL) in particular is a well defined HIV/AIDS associated disease and the risk of developing NHL increases by 60-165 folds (based on different reports, wehre the variation is dependent on the setting and the level of health care available) in HIV positive patients when compared with HIV negative patients (reviewed by Vishnu & Aboulafia, 2012; Bohlius *et al.,* 2009; Cote *et al.,* 1997). In addition, the types of NHL that affect HIV positive individuals are distinct from the types that affect the HIV negative population (Abayomi *et al.,* 2011) (Figure 1.2). Several factors have been implicated in the development of these particular cancers which not only include the dysregulated immune system but also the involvement of the tumour environment (Fowler & Saksena, 2013; reviewed by Grewal *et al.,* 2015; Dolcetti *et al.,* 2016), the late introduction of ART in developing countries, and the contribution of different strains of HIV to the type of lymphoma (Grewal *et al.,* 2015). South Africa has the predominant strain subtype C which has the most immunosuppression associated lymphoma subgroups (Dietrich *et al.,* 1993).

B-cells are a critical component of the adaptive immune system protecting the host from pathogens. Whilst HIV does not infect B-cells, studies have shown that HIV and/or its encoded proteins may induce polyclonal B-cell activation by indirect mechanisms (Schnittman *et al.,* 1986; Moir & Fauci, 2009; Perise-Barrios *et al.,* 2012). B-cells can firstly be influenced by HIV-1 infected macrophages, dendritic cells and T-cells in the extranodal sites where NHL usually occurs (Schnittman, 1986; Sparano, 2001). They can also be prompted to overproduce stimulatory cytokines (reviewed by Epeldegui *et al.,* 2010; Haij *et al.,* 2015) that may result in B-cell activation via activation induced-cytidine deaminase (*AID*) associated DNA modification errors and oncogenic translocations (Huysentruyt & McGrath, 2010; Perise-Barrios *et al.,* 2012). Whilst the above evidence has been shown *in vitro*, they have also been observed in patients infected with HIV (Lane *et al.,* 1983; Titanji *et al.,* 2006; Moir & Fauci, 2009; Perise-Barrios *et al.,* 2012).

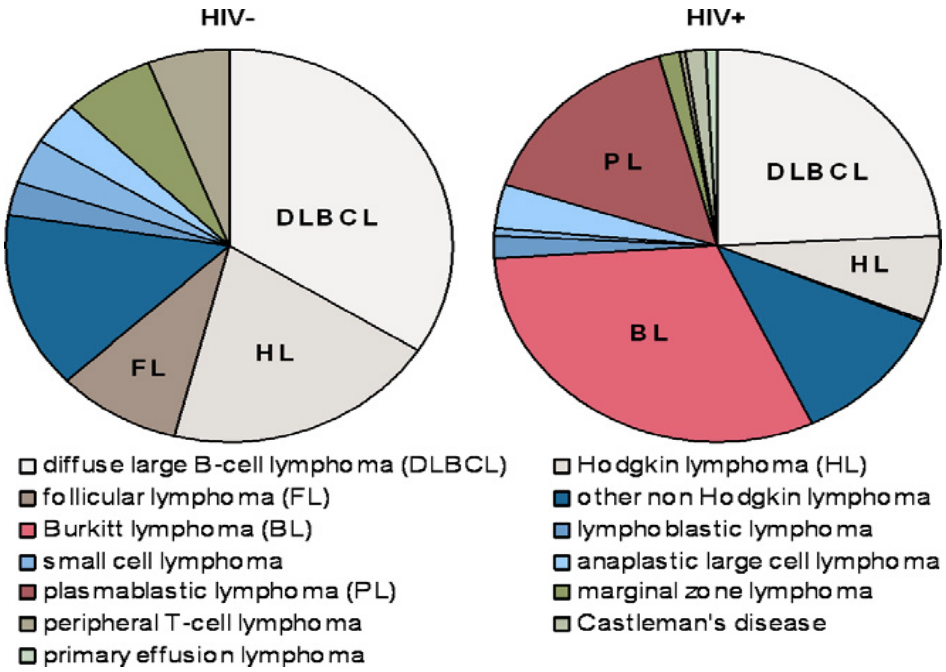


**Figure 1.2: The distribution of lymphoma in HIV negative and HIV positive populations.**
Certain lymphomas such as Burkitt's lymphoma have an increased incidence in the HIV positive population (Reproduced from Abayomi *f* 2011).

Patients living with AIDS have been shown to exhibit hyperimmunoglobulineamia, depletion of memory B-cells, and altered differentiation of naïve B-cells that could result in class switch recombination (CSR) of non specific immunoglobulins, supporting the indirect mechanisms promoted by the virus (Lane *et al.,* 1983; Titanji *et al.,* 2006; Moir & Fauci, 2009; Perise-Barrios *et al.,* 2012). Interestingly however, the immune systems of patients on HAART are not restored suggesting additional dysregulatory pathways of B-cells (Jacobson *et al.,* 2002;

Abudulai *et al.,* 2016). This evidence collectively has lead to the description and identification of several changes in B-cell subsets in association with HIV-1 plasmavireamia (Figure 1.3) (Moir & Fauci, 2009). These alterations include differences in cell surface markers during stages of B-cell differentiation in both the periphery and bone marrow but the mechanism behind this is largely unknown.

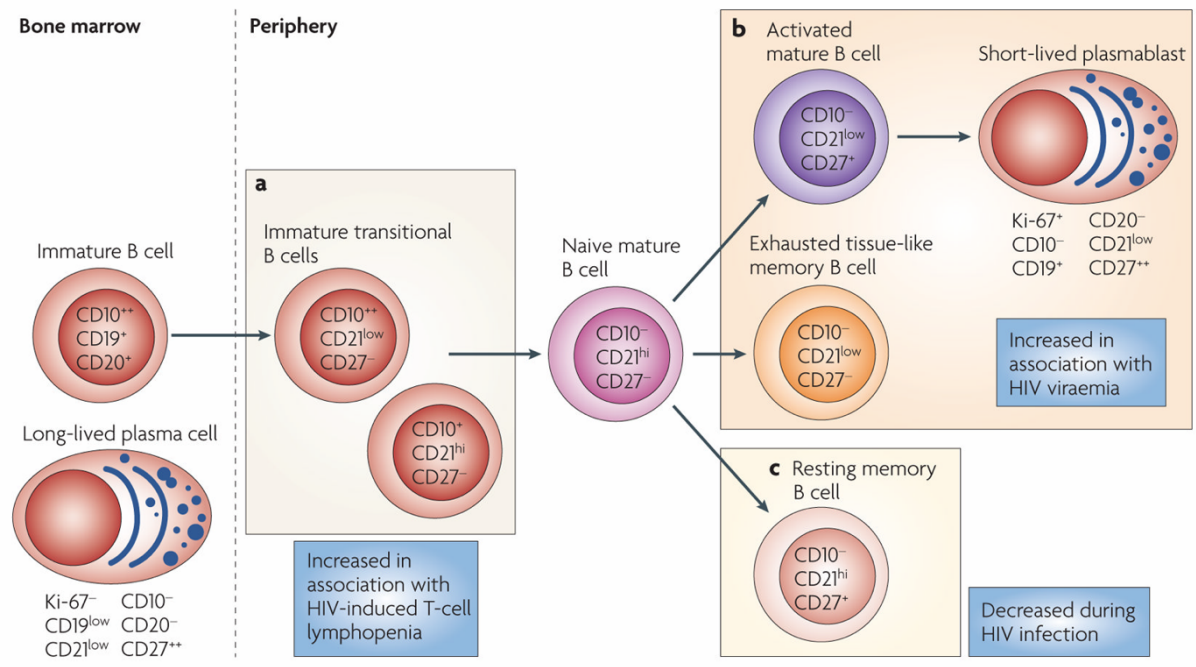


**Figure 1.3: Alterations in human B-cells induced by HIV-1.**
Cell surface markers differ during the stages of B-cell differentiation induced by HIV infection (Reproduced from Moir & Fauci, 2009).

Consistent with the notion that an additional factor may be implicated in B-cell dysregulation, HIV-encoded viral proteins have provided some evidence for direct interference. For instance, HIV-1 Nef has been shown to be delivered into B-cells through interactions between the receptor CD21 and HIV-infected macrophages (Moir *et al.,* 2000) and through the gp120 proteins and dendritic cells (Swinger *et al.,* 1999). This has been shown both *in vivo* and *in vitro* but the mechanism here once again is not clear. Later on, Perise-Barrios *et al.,* (2012) confirmed the phenotypical dysregulation and activation of peripheral primary B-cells after direct HIV-1 contact. Further evidence was shown by Viau *et al.,* (2007) using XenoMouse® mice models. In our lab this emerging idea is further supported whereby ectopic expression of Nef showed an increase in both oncogene, *c-MYC* and *AID* in lymphoma cultured cells (Mdletshe, 2015). These observations however prompt further in-depth analyses and investigation.

As mentioned earlier, certain types of cancers are more prevalent in the HIV positive population (Figure 1.2). The two most prevalent HIV-associated NHLs, which differ in histology, molecular alterations, prognosis and treatment, are Diffuse Large B-cell lymphoma (DLBCL) and Burkitt's lymphoma (BL). Both these lymphomas will be discussed further in the sections below.

#### *1.3.1.1 HIV-associated Diffuse Large B-Cell Lymphoma*

Accounting for more than 80% of lymphoma cases in the world, DLBCL is the most common form of NHL in the adult population (representing 30-40% of all NHLs) (Campo *et al.,* 2011). Whilst it has a high incidence rate in the general population (40%) (Müller *et al.,* 2005), amongst HIV positive patients it has an even higher prevalence rate of 50% with 80% of cases associated with the Epstein-Barr virus (EBV) (reviewed by Gloghini *et al.,* 2013). Affecting the B-cells, DLBCL represents a heterogeneous group of diseases comprising of different genetic abnormalities, molecular subgroups, clinical characteristics, therapy responses and prognoses. Histological studies have revealed DLBCL to present with large cells having vesicular nuclei, prominent nucleoli, basophilic cytoplasm and a high B-cell proliferation rate (Mazan-Mamczarz & Gartenhaus, 2013). The standard treatment for DLBCL consists of immunochemotherapeutic agents rituximab, cyclophosphomide, doxorubicin, vincristine and oral prednisone (R-CHOP) (Wang & Castillo, 2011). Based on molecular and genetic characteristics, three subtypes of DLBCL have been defined, namely germinal centre B-cell like (GCB), activated B-cell like (ABC) and primary mediastinal large B-cell lymphoma (PML-BCL) (Puvvada *et al.,* 2013). These three subtypes differ significantly in their clinical outcome after treatment. A five-year survival rate of 59%, 30% and 64% has been reported in patients with GCB, ABC, and PML-BCL DLBCL, respectively (Lenz *et al.,* 2008).

Deregulated miRNAs have been shown to be associated with the pathogenesis, diagnosis, prognosis and potential treatment of DLBCL (Troppan *et al.,* 2014). In addition, miRNAs have been described for the three subtypes mentioned above and reviewed extensively by Lim & Marra (2013), Zheng *et al.,* (2016) and Ni *et al.,* (2016) to name but a few. Examples of these deregulated miRNAs include miR-331-3p, miR-3934-3p, miR-589-5p, miR-210, miR-138-1-3p for the GCB type and miR-221-3p, miR-92a-1-5p, miR-21-3p, miR155-5p for the non-GCB types (Lim *et al.,* 2015).

#### *1.3.1.2 HIV-associated Burkitt's Lymphoma*

BL is an aggressive cancer that occurs relatively rarely in the general population, but has an increased frequency (200-1000 fold) (due to geographical location and age groups) (Muller *et al.,* 2005) and an estimated 40% prevalence rate amongst HIV positive patients (Corti *et al.,* 2013; Gloghini *et al*., 2013). First described in African children by Dr. Dennis Burkitt, BL affects B-cells that express a germinal centre phenotype (Burkitt, 1958). Clinical representations include a high B-cell proliferative rate and extra-nodal tumours affecting the bones of the jaws and the abdominal area (Ziegler, 1982; Corti *et al.,* 2013; Mangani *et al*., 2013).

As mentioned earlier, a compromised immune system (CD4 count < 200 cell/μL) and advanced stages of HIV have been associated with the development of NHL. However, the risk of developing BL in HIV infected patients has been found to be linked to a less immunodeficient status (CD4 counts of >200 cell/μL) (Corti *et al.,* 2013; Gloghini *et al.,* 2013). A competent immune system therefore seems to play a role in the development of this lymphoma (Donadoni *et al.,* 2013). Also mentioned earlier, the introduction of HAART has reduced the incidence of NHL subtypes such as DLBCL amongst HIV positive individuals (Aboulafia *et al.,* 2004). However, this has not been demonstrated for HIV-associated BL, especially in poorly resourced settings, where the cancer continues to progress unabated (Carbone & Gloghini, 2005; Lim *et al.,* 2005; Gloghini *et al.,* 2013). The mechanisms for this is currently unknown and suggests that the pathogenesis of BL in HIV positive patients is unique and needs elucidation.

Three variants of BL have been described namely, sporadic, endemic and HIV-associated. The sporadic variant affects any age group and is most often found in the western world. Endemic BL affects mostly children and is most commonly found in equatorial Africa, and is associated with malaria and EBV infection. The last type is associated with immunodeficiency, such as infection with HIV. Co-infection with EBV is found in more than 40% of cases but the hallmark of the disease for all variants is the translocation of the transcription factor, c-MYC to the highly active immunoglobulin heavy chain (IGH) locus, resulting in overexpression of this known oncoprotein (Figure 1.4) (Dang, 2012; Ott *et al.,* 2013; Spender & Inman, 2014).

As found in DLBCL, several miRNAs have also been shown to be deregulated in BL (Onnis *et al.,* 2010; reviewed by Di Lisio *et al.,* 2012). In a study that compared BL tissue with normal

lymph nodes, 43 miRNAs were found to be deregulated with 26 upregulated (miR-17-92 cluster; miR-210; miR-575; miR-202) and 17 downregulated (miR-29b, let-7d, miR-155, miR-15a, let-7e), suggesting a significant impact on tumour transcription profiles (Bueno *et al.,* 2011).

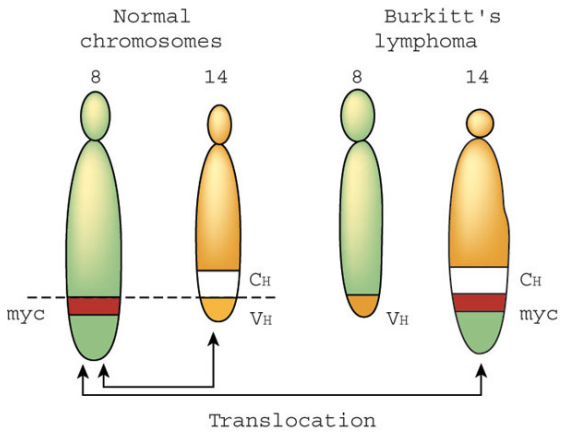


**Figure 1.4: Translocation of the c-MYC transcription factor (8;14) (q24;q25) as the most common translocation in Burkitt's lymphoma.**
The translocation results in the overexpression of c-MYC that is involved in cell proliferation resulting in lymphoma development (Reproduced from Nossal, 2003).

## 1.4 VIRUSES AND MIRNAS

miRNA mediated gene silencing has been shown to play important roles in viral pathogenesis (Nathans *et al.,* 2009; reviewed by Flor & Blom, 2016). This can be done by cellular miRNAs targeting viral RNAs or cellular RNAs that encode proteins necessary for promoting viral replication (Sun *et al.,* 2011). In this way, the replication of viruses can be inhibited and latency ensues. This has been demonstrated for several viruses including the primate foamy virus type-1, (Lecellier *et al.,* 2005), the H1N1 Influenza A virus (Song *et al.,* 2010) as well as the Hepatitis C virus (Jopling *et al.,* 2005).

Additionally, several viruses have been found to encode their own miRNAs, known as vmiRNAs, to regulate the host's system (Bennasser *et al.,* 2004; Harwig *et al.,* 2014). For instance, herpes viruses have been shown to encode up to 35 distinct miRNAs which have roles in regulating cellular genes involved in cell cycle regulation, apoptosis and immunity (Grundoff & Sullivan, 2011). Among retroviruses only the bovine leukeamia virus has been shown to express miRNAs (Kincaid *et al.,* 2012). This retrovirus was shown to encode a RNA polymerase III-transcribed miRNA cluster that is functionally similar to the human miR-29

which contributes to the development of B-cell tumours. It has been suggested that miRNAs expressed by RNA viruses have not been detected due to the fact that cleavage by Drosha leads to degradation of the pri-miRNA precursor, which in the case of most RNA viruses would likely be genomic RNA or viral mRNA (Skalsky & Cullen, 2010). Whilst recent deep sequencing technology has led to the discovery and identification of vmiRNAs and miRNA-like sequences in HIV-1 infected T-cells (Yeung *et al.,* 2009; Schopman *et al.,* 2012; Holland *et al.,* 2013), the miRNA coding potential of HIV remains controversial.

Viruses have been shown to exploit host miRNAs by manipulating their expression to their own advantage to transform cells. For instance, the herpes virus saimiri (HVS) has been shown to express a non-coding RNA (ncRNA) which degrades cellular miR-27, and this is linked to the transformation of T-cells (Guo & Steitz, 2014). Cellular miR-197 was found to be downregulated in EBV-positive BL tumours compared to EBV-negative BL tumours, predicted to regulate *BCL6* which is implicated as a key regulator of B-cell differentiation (Ambrosio *et al.,* 2014). In this study, miR-127 was overexpressed by the EBV encoded nuclear antigen 1 (EBNA1) leading to impaired B-cell differentiation and possibly responsible for lymphoma development. EBV also upregulates miR-155, an oncogenic miRNA (Yin *et al.,* 2008).

### 1.4.1 HIV and miRNAs

The first report of a potentially HIV encoded miRNA was in 2004 using computer algorithms (Bennasser *et al.,* 2004), and was later confirmed by other groups (Omoto & Fujii*.,* 2005; Pfeffer *et al.,* 2005; Whisnant *et al.,* 2013; Klase *et al.,* 2013). The miRNA, MiR-TAR promotes HIV-1 persistence (Klase *et al.,* 2013), whilst Kaul *et al.,* (2009) identified hiv1-mir-H1 that was found to suppress *c-MYC* and downregulate cellular miR-149 that targets the HIV viral protein, Vpr. Another HIV encoded miRNA was identified namely miR-H3 (Zhang *et al.,* 2014) whilst vmiR88 and vmiR99 where found in the sera and exosomes of HIV-1 positive individuals (Bernard *et al.,* 2014). Along with Vpr mentioned above, HIV-1 seems to regulate its own replication by using *nef* miRNA, Nef-U3-miR-N367 (Omoto *et al.,* 2004). Other potential vmiRNAs have been found to be similar in sequence to cellular miR-195, miR-30d, miR-30e, miR-374a and miR-424 (Holland *et al.,* 2013). These vmiRNAs together may represent therapeutic strategies to limit progression to AIDS but warrants further investigation.

### 1.4.2 Modulation of cellular miRNAs by HIV

It has been proposed that HIV can modulate the expression of cellular miRNAs to promote its replication (Yeung *et al.,* 2005; Triboulet *et al.,* 2007) and contributes to HIV-1 latency in primary CD4+ T-cells. Some of these cellular miRNAs include miR-28, miR-125b, miR-150, miR-223 and miR-382 (Huang *et al.,* 2007) that target the 3'UTR of HIV-1 transcripts promoting productive infection towards latency. Furthermore, the knockdown of several miRNA processing pathway proteins including Dicer, Drosha and DGCR8 were shown to increase viral replication (Benasser & Jeung, 2006). There is also evidence to suggest that the HIV-1 encoded protein Tat can act to suppress the miRNA processing system (Benasser & Jeung, 2006). In addition, HIV-transcripts were shown to be co-localised with the RNA interference pathway effector proteins in P-bodies (Nathans *et al.,* 2009).

Work by Munshi *et al.,* (2014) further suggests that miRNA expression can be predicted for HIV disease progression and therapy. They compared miRNA expression in peripheral blood mononuclear cells (PBMC) between healthy and HIV-1 infected individuals and found high levels of cellular miR-150 and miR-146b-5p to be a predictor of increased disease progression. Further studies have also identified an association between HIV-1 vireamia and cellular miRNAs (Ma *et al* 2014; Farberov *et al.,* 2015; Monteleone *et al.,* 2015). Specific miRNA signatures for four classes of HIV-1 based on their $CD4^+$ T-cell counts and viral loads were found in early 2008 by Houzet *et al*. They reported an overall general downregulation of most of the miRNAs *in vivo* (Houzet *et al.,* 2008). Recently, the miR-29 family was found to influence the clinical progression of the infection. When the miRNAs levels in HIV positive patients were compared with HIV negative patients, a significant upregulation was found ($p \leq 0.001$) (Monteleone *et al.,* 2015).

What has been a contested topic is understanding why some patients infected with HIV-1 are able to maintain a viral load below the limit of detection, known as elite controllers (EC) (Witmer *et al.,* 2012; Seddiki *et al.,* 2013; Reynoso *et al.,* 2014; Egana-Gorrono *et al.,* 2014). Understanding the mechanisms behind this may be able to provide diagnostic and prognostic value. Reynoso *et al.,* (2014) showed that 16 miRNAs were differentially expressed *in vitro* between the plasma of chronically HIV infected patients compared to healthy donors. However, specifically miR-29b-3p and miR-33a-5p were found to be overexpressed in EC in MT2 and primary $CD4^+$ T-cells and was associated with reduced viral production. In addition, Zhu *et al.,* (2012) showed that six out of a set of 18 miRNAs were significantly related to CD4

T-cell count decline as an indicator for identifying the outcome of HIV disease at the chronic stage.

In contrast, increased virion release was observed upon upregulated miRNA levels of let-7c, miR-34a and miR-124a that was associated with a downregulation of p21 in HeLa-CCR5 cells. This downregulation of p21 was also found to be associated in a recent study with the overexpression of miR-106b and miR-20 (Guha *et al.,* 2016) whilst miR-9 induced B-lymphocyte induced maturation protein 1 (BLIMP-1) repression indicative of progressive HIV-1 infection (Seddiki *et al.,* 2013).

To date Sun *et al.,* (2011) has reported the first comprehensive miRNA microarray analysis of *in vitro* HIV-1 infected $CD4^+$ cells with several cellular miRNAs found to be downregulated (miR-29a/b; miR-155, miR-21) and miR-223 being upregulated. However, though it is widely accepted that HIV does not play a direct oncogenic role in HIV-associated cancers, emerging evidence in HIV-associated Karposi Sarcoma (KS) has contested this supporting role of HIV in promoting the progression and initiation of KS through several mechanisms. Of these, HIV-1 Nef and the oncogene Karposi Sarcoma Herpes Virus (KSHV) K1 was demonstrated to synergistically promote angiogenesis by inducing miR-718 to regulate the PTEN/AKT/mTOR signalling pathway (Xue *et al.,* 2014). Furthermore, Yan *et al.,* (2014) recently showed that HIV-1 Vpr upregulated miR-942-5p that directly targets IκBα whilst HIV-1 Tat was shown to promote KSHV vIL-6-induced angiogenesis and tumourigenesis by regulating the PI3K/PTEN/AKT/GSK- 3β signalling pathway (Zhou *et al.,* 2013b).

The findings discussed above provide the first insights into an emerging potential role for HIV in modulating cellular miRNAs in the context of cancer, more specifically, NHLs. Research is limited in this area with a few recent reviews discussing the possibility of the role of miRNAs in the pathogenesis of HIV associated NHLs (Klase *et al.,* 2012; Swaminathan *et al.,* 2013; Grewel *et al.,* 2015) but further validation is required in larger cohort sizes with detailed *in vitro* analyses at the molecular level.

### 1.5 RATIONALE

Currently, miRNAs have been suggested as serum biomarkers (Di Leva *et al.,* 2014; Manterola *et al.,* 2015) for prognosis and diagnosis of cancers as well as predictors of treatment outcomes

(Shepshelovich *et al.*, 2015; Ni *et al.,* 2016). The development of novel and more targeted anti-cancer therapies by exploiting the involvement of miRNAs in cancer is promising (Vasilatou *et al.,* 2009). Two possible scenarios can be forecasted in the near future where miRNAs can be used as treatment to target oncogenes or drugs can be developed to target those miRNAs which affect tumour suppressor genes. Already, pharmaceutical companies are exploring miRNA based therapy and a few miRNAs have entered preclinical and clinical stage of testing (Christopher *et al.,* 2016).

As mentioned earlier, recent evidence suggests that HIV proteins and miRNAs may have a direct role for the development of HIV-associated malignancies such as DLBCL and BL. In light of the findings linking HIV-1 and cellular miRNA modulation, it is predicted that one of the mechanisms for the development and/or progression of lymphoma in HIV positive individuals is via the modulation of miRNAs in B-cells (Curreli *et al.,* 2013). Based on literature, we have constructed a venn diagram in Figure 1.5 to align those miRNAs that are differentially expressed in DLBCL and BL. We have then overlapped these miRNAs within each disease and then with HIV. Collectively we hope to identify a miRNA signature for HIV-associated DLBCL and BL which can contribute towards identifying dysregulated cellular pathways. This will aid in our understanding of the HIV and miRNAs link to potentially develop therapeutic drug targets in this sparse area of research (Huang *et al.,* 2015).

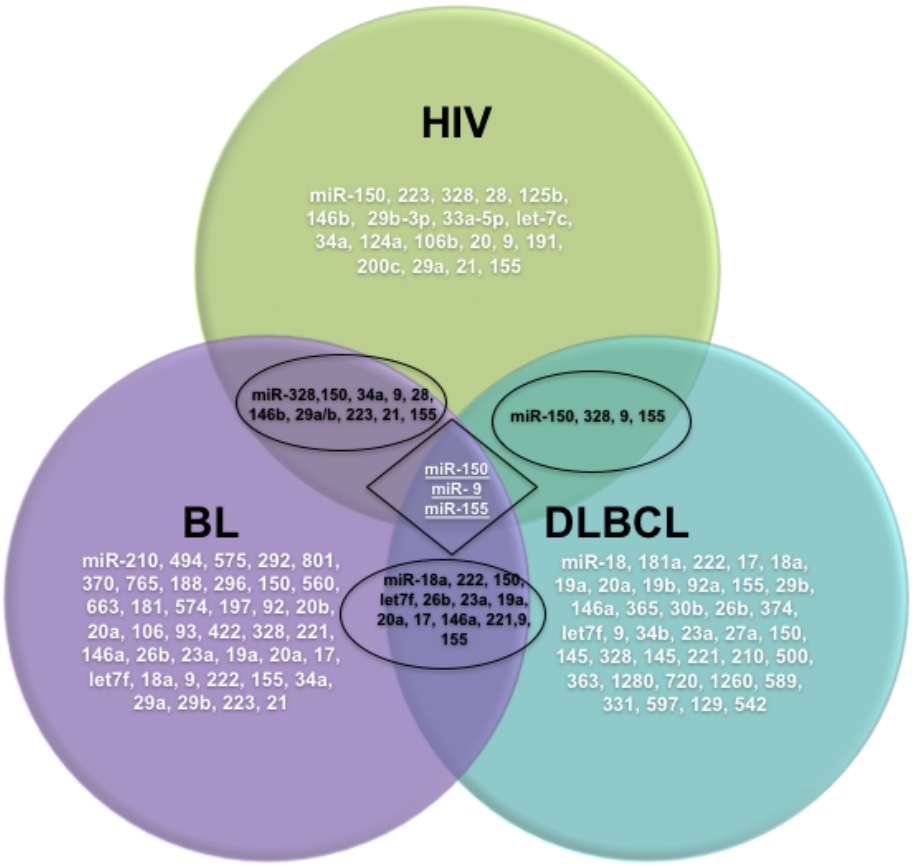

**Figure 1.5: Venn diagram representing the overlap of differentially expressed miRNAs identified in DLBCL and BL with the possible association in HIV-associated NHLs.**
Several miRNAs have been implicated in the pathogenesis of BL and DLBCL as well as associated with HIV infection. The smaller circles represent the overlap between DLBCL, BL and HIV respectively whilst the diamond shape represent the overlap of all three diseases. These miRNAs could be predicted in the pathogenesis of HIV-associated B-cell NHL, BL and DLBCL.
BL – Burkitt's lymphoma; DLBCL – Diffuse large B-cell lymphoma; HIV – Human Immunodeficiency Virus; miRNA – microRNA; NHL – non-Hodgkin's lymphoma.

References: Sampson *et al.,* (2007); Chang *et al.,* (2008); Leucci *et al.,* (2008); Malumbres *et al*., (2009); Imig *et al.,* (2010); Jima *et al.,* (2010); Robertus *et a*l., (2010); Bueno *et al.,* (2011); Sun *et al.,* (2011); Di Lisio *et al.,* (2012); Forte *et al.,* (2012); Witmer *et al.,* (2012); Chiang *et al.,* (2013); Seddiki *et al.,* (2013); Egana-Gorrono *et al.,* (2014); Reynoso *et al.,* (2014); Zhu *et al.,* (2014); Guha *et al.,* (2016)

## 1.6 AIMS & OBJECTIVES

The aim of this project was to identify and characterise miRNAs involved in the pathogenesis of HIV-associated non-Hodgkin's lymphoma. Previous research in our laboratory had found that B-cells derived from healthy individuals respond differently to cancerous cells when exposed to components of HIV, such as Tat and Nef. Therefore, in this project, the response of both types of cells was investigated. Following identification of differentially expressed miRNAs, selected miRNAs and their predicted or confirmed targets were further characterised. This project ultimately aimed to identify cellular miRNAs whose expressions are altered by HIV and which could potentially contribute to the development or progression of HIV-associated lymphomas. The objectives of the project were as follows:

- To identify miRNAs that are differentially expressed in human B-cells exposed to HIV, compared to microvesicle treated control cells by utilising a miRNA microarray
- To validate selected miRNAs by performing qPCR using single-tube TaqMan® miRNA assays
- To identify putative mRNA gene targets of a selected miRNA identified in Aim (i) by using prediction programmes, confirm its potential target by qPCR and western blotting and to perform functional analyses.

# CHAPTER 2: MATERIALS & METHODS

## 2.1 TISSUE CULTURE

### 2.1.1 Cell lines and storage

Two suspension cell lines were used, namely a human B–cell line L1439A, immortalised using EBV which has been derived from a healthy individual (produced at the University of Cape Town by Ms Ingrid Baumgarten, Division of Chemical Pathology, using an adapted protocol by Freshney, 2010), and the well established Burkitt's lymphoma cell line Ramos (an Epstein-Barr virus negative human B-cell line originally established from a Caucasian male diagnosed with Burkitt's lymphoma) purchased from the American Type Culture Collection, (ATCC®, Virgina, USA). Cells were cultured and exposed to aldrithiol – 2.2 dithiopyridine (AT-2) inactivated HIV-1 X4/R5 virus. Cells that were left untreated, as well as treated with matched microvesicles served as controls. Both cell lines were cryopreserved with dimethyl sulfoxide (DMSO)/ glycerol and stored in liquid nitrogen until they were ready to be used.

### 2.1.2 Cell thawing, expansion & freezing

Following the culture conditions recommended by the creator of the cell lines, one vial of cryopreserved cells (Ramos (ATCC®, Virginia, USA)/L1439A (Freshney, 2010)) was removed from the liquid nitrogen stores and was thawed at room temperature. Once the vial was thawed (by hand for Ramos and at 37°C for L1439A) it was cleaned with 70% ethanol (EtOH) (Appendix A) and placed under the Biosafety Level two tissue culture fume hood. Prior to thawing, complete growth media was prepared using Roswell Park Memorial Institute (RPMI) media (Sigma-Aldrich, Missouri, USA) for Ramos cells and Dulbecco's Modified Eagle Medium (DMEM) (Sigma-Aldrich, Missouri, USA) for L1439A cells, fetal bovine serum (FBS) and a penicillin/streptomycin (P/S) solution.

Once all reagents were brought to room temperature, they were sterilised with 70% EtOH and placed under the fume hood. The complete growth media was prepared using RPMI (Ramos) and DMEM (L1439A), FBS (10% for Ramos; 20% for L1439A), and 1% P/S in a 50 mL Falcon tube (Appendix A). Upon completion, 5 mL of the growth media was added to a T25 flask and placed in the $CO_2$ incubator (5% $CO_2$, at 37°C) to warm up and 4 mL of the media

was placed in a 15 mL Falcon tube. The contents of the cryovial were then added to this Falcon tube which was then centrifuged (MSE, London, UK) at 1000 revolutions per minute (rpm) for five minutes to remove the toxic DMSO/glycerol from the cells. Thereafter the supernatant was removed and the pelleted cells were resuspended in 1 mL of the warm media from the T25 flask that was in the incubator. The cells were then transferred to the T25 flask with the remainder of the warm media (4 mL) and placed back in the incubator to expand.

Cells were maintained and expanded by the addition of fresh growth media (1-2 mL) every two to three days upon colour change of the media (Ramos: salmon to yellow; L1439A: red to orange) with depopulation occurring as required. These cells were counted and found to grow best at a density between 2 X $10^5$ and 1 X $10^6$ viable cells/mL and once the volume exceeded 20 mL in the T25 flask, the cells were transferred to a T75 flask.

Cells were transferred to 15 mL Falcon tubes (10 mL in each) for freezing purposes which were centrifuged at 1000 rpm for 10 minutes (MSE, London, UK) with the removal of the supernatant thereafter followed by resuspension in 1 mL of freezing media. The freezing media was prepared in advance using RPMI/DMEM medium (Sigma-Aldrich, Missouri, USA), 10%/20% FBS and 10% DMSO/glycerol (enough to create a cell suspension of 1 X $10^6$ cells/mL) and was left on ice. Upon resuspension the cell suspension was added to each cryovial which were placed in a freezing container at -80°C overnight containing isopropanol to achieve a rate of cooling close to 1°C/minute. The isopropanol allows the process of slowly freezing the cells ensuring that fewer crystals are formed (Thermo Fisher Scientific™, 2010). The cryovials were then placed in liquid nitrogen the following day for long term storage.

### 2.1.3 Mycoplasma testing

Cells were tested for Mycoplasma contamination by plating cells (1 X $10^6$ cells/mL) in P/S free culture medium for a minimum of three days in a 35 mm tissue culture dish to allow for any Mycoplasma present to proliferate to a detectable level (Chen, 1977). Approximately 3 µL of the suspension was placed directly onto a clean microscope slide and air dried until the film of cells were dried, fixed for two minutes by adding enough fixative (Appendix A) to cover the cells, washed with $H_2O$ and then stained with Hoechst 33342 stain (#H1399, Invitrogen, California, USA) (Appendix A) for eight minutes. The stain was then washed off with $H_2O$ and the cover slip placed onto the slide with a drop of mounting fluid (Appendix A). The cells

were then visualised using a fluorescent microscope at a magnification of 40x (Zeiss Axiovert 200M, Carl Zeiss Microimaging, Germany).

The principle behind the Hoechst stain is that it binds to all nuclear material and a positive Mycoplasma result will be indicated as fluorescent dots on the cellular membrane and in the cytoplasm of the cells. A negative result will have only the nucleus of the cell staining positive (Young *et al.,* 2010).

### 2.1.4 Cell treatment

To enter its host cell and replicate effectively, HIV utilises two chemokine receptors, CCR5 and CXCR4 (Moore *et al.,* 1997). For the current project the HIV-$1_{NL4-3}$ and HIV-$1_{BAL}$ dual based CXCR4-tropic (X4) and CCR5 (R5) viruses were utilised since both chemokine receptors are expressed on B-cells (Nie *et al.,* 2004). The mild oxidising agent, AT-2 which has the ability to eliminate the infectivity of HIV, was used to modify the virus so that it was safe to handle in the laboratory. The AT-2 preferentially covalently modifies free sulfhydryl groups of the cysteines of internal virion proteins, particularly the nucleocapsid proteins (Rossio *et al.,* 1998). In conjunction, it maintains the structural and functional integrity of the envelope glycoproteins on the surface of the virus. Therefore, the AT-2 inactivated virions are non-infectious and are able to interact with cell surface receptors. This system was first developed as a promising candidate vaccine, but is also useful and safe for use experimentally in the laboratory. Regardless, the cell treatments were carried out in a certified Biosafety Level two tissue culture facility for optimum safety. Although the virus preparations are highly purified, they do contain some non-virion material in the form of microvesicles (Rossio *et al.,* 1998). These microvesicles which were isolated from the supernatants of uninfected cell cultures in a manner identical to that used for virus preparation from infected cells was used as matched controls. AT-2 inactivated virions (HIV-$1_{NL4-3}$ and HIV-$1_{BAL}$; lot P4244) and matched control microvesicles (SUPT1-CCR5 (MV-CCR5; lot P4287) were kindly donated by Professor Jeff Lifson (and Dr. Wendy Burgers, Medical Virology, UCT) who pioneered the development of this method, through the Biological Products Core of the AIDS and Cancer Virus Program (Leidos Biomedical Research, Inc., Frederick National Laboratory, Frederick, MD, USA).

Once the amount of cells that was required was expanded (40 mL), the cell suspension was placed in 15 mL Falcon tubes (10 mL per tube) and was centrifuged at 1000 rpm (MSE,

London, UK). The supernatant was thereafter removed and resuspended in fresh medium. After the solution was mixed gently by resuspension, 10 µL was used for cell counting using a haemocytometer. A haemocytometer was used to determine the viable cell count number of both miRNA expressing and control cells for HIV-1 AT-2 treatment. Briefly, the cells present in a known volume were counted within four 1 $mm^2$ squares and then the value was converted to a number per mL.

For the treatment, cells (8 x $10^6$/mL) were plated in 35 mm wells approximately 16 hours prior to treatment in low serum medium (0.5% FBS) (Appendix A). Three wells of cells were treated with 500 ng/mL of AT-2 inactivated HIV-1 or with the equivalent amount of microvesicle control or left untreated (Martinson *et al.,* 2007), for a period of three hours (Guo *et al.,* 2014). Each treatment was performed in triplicate and was covered with foil to prevent evaporation and influence by external variables.

### 2.1.5 Viability assay

To verify that the cells would remain viable after the three hour treatment, a viability assay was conducted for both cells using WST-1 (Roche Applied Science, Penzberg, Germany). The WST-1 reagent is designed to quantify cell viability spectrophotometrically. The reagent contains tetrazolium salts which are cleaved to formazan dye in the presence of cellular enzymes produced by metabolically active cells. The more salt that is cleaved, the great the colour change which indirectly indicates the viability of the cells (Riss *et al.,* 2013). Viable cells were counted as above by use of a haemocytometer and plated in a 96 well plate followed by treatment with HIV-1 AT-2 virions in low serum media (Appendix A) for three hours. After exposure was completed, 10 µL of WST-1 reagent was added to the wells, covered with foil and then left to incubate for a further two hours (5% $CO_2$ at 37°C). Upon completion, the absorbance of the samples was measured against a background control as a blank using a Glo-Max®-Multi+ multiplate reader (Promega, Wisconsin, USA) at a wavelength between 420-480 nm.

## 2.2 RNA Extraction & Quantification

### 2.2.1 RNA extraction for miRNA PCR array

Prior to working with RNA, the surface of working areas and reagents were wiped thoroughly with Decon (Thermo Fisher Scientific™, Massachusetts, USA) and 70% EtOH followed by

using plasticware that was treated with 0.1% diethyl pyrocarbonate (DEPC) treated water (Appendix A). These preparations were performed in order to effectively remove any existing RNAses. Following treatment, the cells were harvested from the plate and placed in 15 mL Falcon tubes. Remaining cells were removed by rinsing the wells with cold 1X phosphate-buffered saline (PBS) (Appendix A). The tubes were then centrifuged at 1000 rpm (MSE, London, UK) with the supernatant removed followed by resuspension in 1 mL cold 1X PBS and transfer into 1.5 mL centrifuge tubes. These tubes were thereafter centrifuged at 4°C for 10 minutes at 2000 rpm (Beckman, California, USA).

Extraction was performed using the *mir*Vana™ miRNA Isolation kit (Thermo Fisher Scientific™, Massachusetts, USA) for total RNA isolation as per the protocol. This kit uses a three step procedure involving both organic and solid-phase extraction techniques to isolate high yields of pure RNA. Briefly, the cells were lysed by the addition of 600 µL of lysis/binding solution and was vortexed to obtain a homogenous lysate. Thereafter organic extraction was performed that included the addition of 30 µL of miRNA homogenate additive to the cells. The solution was mixed well by vortexing and left on ice for 10 minutes. A volume of 600 µL of acid-phenol: chloroform was added to the tubes followed by vortexing for 60 seconds to mix. The tubes were then centrifuged for five minutes at 10 000 rpm at room temperature to separate the aqueous and organic phases. On completion, the aqueous phase was transferred to a new 1.5 mL tube with the addition of 100% EtOH before the lysate was passed through a filter cartridge. The mixture was passed through the filter by centrifuging the tubes for 15 seconds at 10 000 rpm (MSE, London, UK). Thereafter the flow-through was discarded and the step repeated until the lysate was passed through the filter. The wash solutions were then added separately to the filter cartridges, centrifuged for 10 seconds each with the flow-through discarded. Finally, the filter cartridges were added to a collection tube, spun for 30 seconds to elute the RNA with 15-18 µL of nuclease-free $H_2O$ (Thermo Fisher Scientific™, Massachusetts, USA). The RNA was then quantified before storage at -80°C.

### 2.2.2 RNA extraction for single-tube TaqMan® PCR assays

The High Pure RNA Isolation Kit (Roche Applied Science, Penzberg, Germany) was used for total RNA extraction of cells, according to the manufacturers protocol. Briefly, cells were placed in a 1.5 mL Falcon tube and washed using 200 µL of 1X cold PBS. Thereafter 400 µL of lysis buffer was added to the cells and the tube was vortexed for 15 seconds. The cells were

then transferred into a High Pure Filter Tube and then placed into the collection tube. These tubes were then centrifuged for 15 seconds again at 8000 x g (Beckman, California, USA) The flow through was discarded and the RNA in the filter was treated with a DNase I treatment provided in the kit for 15 minutes at 25°C. Thereafter the filter was washed with 500 µL of Wash Buffer I. This step was repeated twice, first using 500 µL and then with 200 µL of Wash Buffer II. These were centrifuged for two minutes at 13 000 x g to remove all excess wash buffer (Beckman, California, USA). RNA was then eluted using 100 µL of elution buffer. The RNA was then quantified before storage at -80°C.

### 2.2.3 RNA quantification

Extracted RNA was quantified by two techniques, firstly by using the NanoDrop ND-1000 Spectrophotometer (Thermo Fisher Scientific™, Massachusetts, USA) and secondly by the Qubit™ RNA Assay kit (Invitrogen, California, USA) as recommended by the manufacturer's protocol. NanoDrop™ analyses consists of spectrophotometrically determining the concentration of nucleotides in the samples as well as sample contamination by using 260/280 and 260/230 ratios as a measure of sample purity. Briefly, 1 µL of each sample was analysed on the NanoDrop™ using nuclease-free $H_2O$ (Thermo Fisher Scientific™, Massachusetts, USA) as a blank between sample purity check. The Qubit™ RNA Assays on the other hand is a more specific technique (Invitrogen, 2010) in detecting RNA that consists of a fluorescent dye that intercalates only with RNA present in the samples. Briefly, the Qubit™ working solution was set up by diluting the Qubit™ RNA reagent in a ratio of 1:200 in Qubit™ RNA buffer. The working solution (190 µL) was then added to each of two 0.5 mL PCR tubes for the standards and the same amount for the individual RNA samples. Thereafter 10 µL of each Qubit™ standard was added to the appropriately labelled standard tube and mixed by vortexing for two-three seconds without creating any bubbles. The RNA samples (10 µL) was then added to each individual assay tube and also mixed by vortexing for two-three seconds as before. All tubes were then allowed to incubate at room temperature for two minutes followed by quantification using the Qubit™ 2.0 Fluorometer for RNA as per the manufacturer's protocol.

### 2.2.4 Gel electrophoresis of RNA samples

To verify the integrity of the RNA samples, 1 µg of total RNA for each sample was separated on a 1% agarose gel. Prior to separation, the apparatus was treated with DEPC-treated $H_2O$ and ~10% sodium hypochlorite for three hours preventing RNA degradation. Samples were prepared in DEPC treated RNase free $dH_2O$ with 5 µL of 2X RNA loading buffer (Appendix

A) in a total volume of 15 µL and denatured by heating at 55°C for five minutes. The samples were then briefly centrifuged and loaded onto an agarose gel containing ethidium bromide (EtBr) (0.5 µg/mL) using 1X Tris/Borate/EDTA buffer (Appendix A). The gel was electrophoresed at 100 volts/cm for 35 minutes and then visualised with an ultraviolet (UV) trans-illuminator (Uvitec, UK).

### 2.3 ETHANOL PRECIPITATION USING AMMONIUM ACETATE

The RNA for downstream differential expression of miRNAs using the microarray was concentrated using Ammonium Acetate which reduces the co-precipitation of oligosaccharides (Osterburg *et al.,* 1975) (Figure 2.1). Briefly, 100% EtOH (2.5 volumes) was added to each RNA sample with 2.5M ammonium acetate (0.1 volumes). The samples were then incubated on ice for an hour followed by centrifugation at 12,000 x g for 30 minutes at 4°C (MSE, California, USA). The supernatant was thereafter discarded and the tubes were left to air dry before eluting with 50 µL of nuclease-free $H_2O$ (Thermo Fisher Scientific™, Massachusetts, USA).

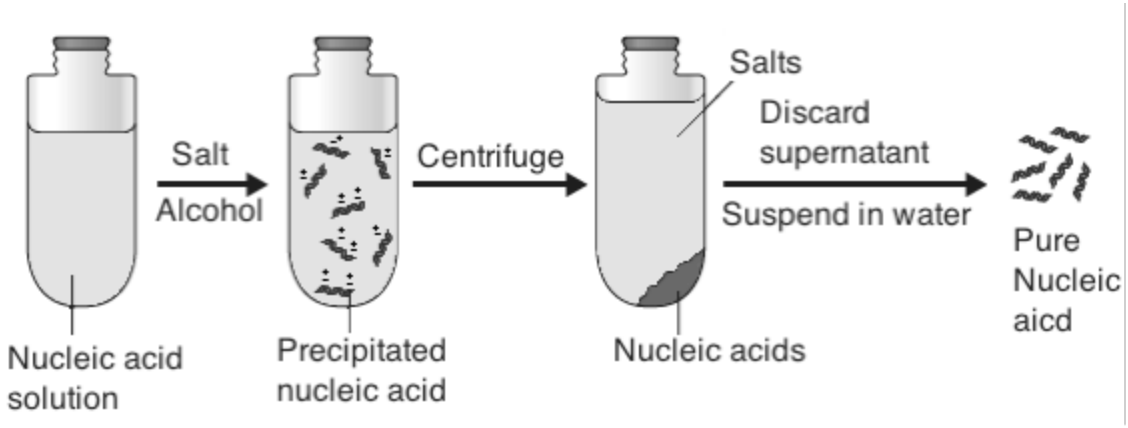


**Figure 2.1: Schematic representation of ethanol precipitation to concentrate RNA** (Reproduced from http://technologyinscience.blogspot.co.za/2014/02/ethanol-precipitation-of-dna-principle.html).

### 2.4 TAQMAN® QUANTITATIVE REAL-TIME PCR LOW DENSITY ARRAY

A comparative and comprehensive profiling analysis of miRNA expression was performed, using the Applied Biosystems™, custom 192a TaqMan® Quantitative real-time PCR low density array (TLDA) card (#4346802). This custom TaqMan® miRNA array platform (Applied Biosystems™, California, USA) was chosen and designed, as it was best suited in establishing a preliminary list of a number of differentially expressed miRNAs of interest for

the study. The 192a-card format was used, with each chosen miRNA target pre-spotted in duplicate on a 384 well plate array.

The miRNAs contained within our customised array were chosen based on extensive literature searches focusing on differential expression studies of miRNAs in B-cell lymphomas (Lawrie *et al.,* 2008; Lenz *et al.,* 2008; Onnis *et al.,* 2010; Robertus *et al.,* 2010; Jima *et al.,* 2010; Bueno *et al.,* 2011; Lenze *et al.,* 2011; Di Lisio *et al.,* 2012). These reviews were then cross referenced with the available TaqMan® Assay Inventory pre-designed assays which are available for spotting onto the array card from Life Technologies, Applied Biosystems™. Additionally, online database resources such as miRBase *(http://www.mirbase.org)* and current literature were used to verify the number of mature miRNA sequences for an individual miRNA, as well as their target sequences. This comprehensive analysis resulted in 191 mature miRNAs including controls (RNU6B, RNU48, RNU44) (Malumbres *et al.,* 2009; Linda *et al.,* 2010; Forte *et al.,* 2012) (Appendix B –Table B1) which were then populated onto a Microsoft Excel spreadsheet for the array to be designed by the company. The custom TaqMan® miRNA array is a uniquely designed microfluidic card with 192 targeted miRNAs fitted with a reservoir of eight ports for loading. It employs a novel target-specific stem loop reverse transcription primer that extends the 3' end of the target to produce a template that can be used for quantification using real time PCR (qPCR) (Figure 2.2). The primer sequences for the endogenous controls are presented in Table 2.1.

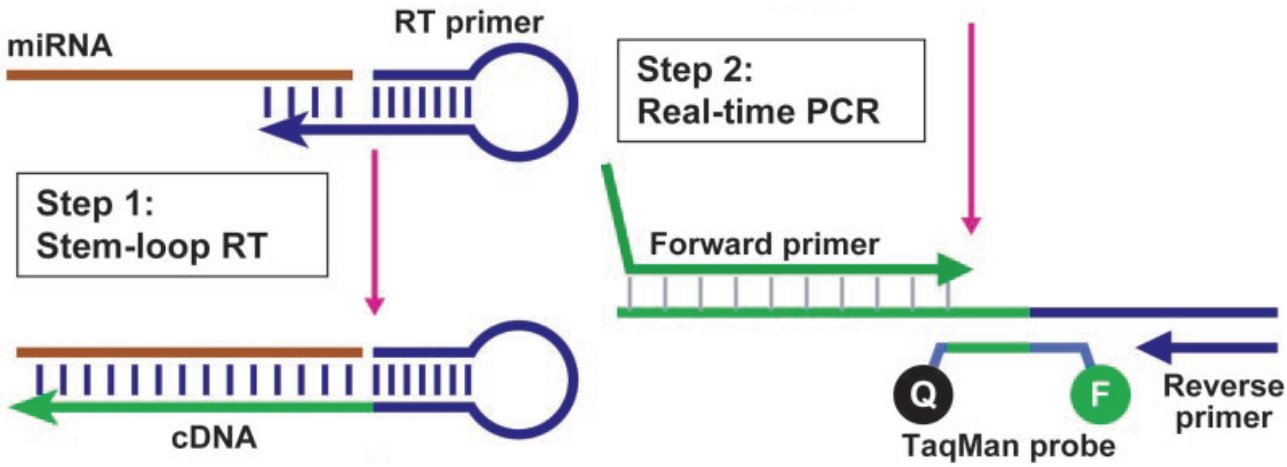


**Figure 2.2: Schematic overview of cDNA conversion from miRNA employing the unique stem-loop primer design** (Reproduced from Chen *et al.,* 2005).

**Table 2.1: Primer sequences for endogenous controls**

| Controls | Primer sequence |
|---|---|
| U6 snRNA | 5'-GUGCUCGCUUCGGCAGCACAUAUACUAAAAUUGGAACGAUACAGAGAAGAUUAG CAUGGCCCCUGCGCAAGGAUGACACGCAAAUUCGUGAAGCGUUCCAUAUUUU-3' |
| U48 | 5'-GAUGACCCCAGGUAACUCUGAGUGUGUCGCUGAUGCCAUCACCGCAGCGCUCUG ACC-3' |
| U44 | 5'-CCUGGAUGAUGAUAGCAAAUGCUGACUGAACAUGAAGGUCUUAAUUAGCUCU AACUGACU-3' |

snRNA – small nucleolar RNA

### 2.4.1 Reverse transcription using custom multiplex stem-loop primers

The first step involved in using the custom 192a TaqMan® miRNA array is to convert RNA into cDNA by reverse transcription (RT) using a custom pool of multiplex stem-loop primers (Appendix B – Table B2). These primers enable specific, efficient and simultaneous synthesis of single stranded cDNA for mature miRNAs from total RNA samples together with the TaqMan® miRNA Reverse Transcription kit (Applied Biosystems$^{TM}$, California, USA). The Ramos cell line was cultured and treated followed by RNA isolation. Briefly, the RT master mix was set-up (without preamplification) as stated in Table 2.2 in RNase free 1.5 mL centrifuge tubes. Prior to combination of solutions, the reagents were thawed on ice followed by set-up and thereafter centrifuged briefly (Beckman, London, UK). This mixture was then pipetted (4.5 µL) into DEPC treated PCR tubes with the addition of 3 µL of total RNA (350 ng/µL). The samples were thereafter spun down and then incubated on ice for five minutes.

**Table 2.2: Components for the TaqMan® miRNA reverse transcription kit**

| Reagent | Volume (µL) |
|---|---|
| Megaplex RT primers (10X) | 0.80 |
| dNTPs with dTTP (100 mM) | 0.20 |
| MultiScribe Reverse transcriptase (50 U/ µL) | 1.50 |
| 10X RT Buffer | 0.80 |
| $MgCl_2$ (25 mM) | 0.90 |
| RNase Inhibitor (20 U/ µL) | 0.10 |
| Nuclease-free water | 0.20 |
| **Total Volume** | **4.50** |

The RT reaction was then run on the Applied Biosystems™ 7900HT Real Time PCR (Applied Biosystems™, California, USA) with the following thermal cycling conditions outlined in Table 2.3 below (as per manufacturer's protocol). Reaction tubes with cDNA were thereafter stored at -20°C until used for qPCR.

**Table 2.3: Cycling conditions for reverse transcription using custom multiplex stem-loop primers**

| Stage | Temp | Time |
|---|---|---|
| 40 cycles | 16.0°C | 2 min |
| | 42.0°C | 1 min |
| | 50.0°C | 1 sec |
| Hold | 85.0°C | 5 min |
| Hold | 4.0°C | ∞ |

### 2.4.2 Quantitative real-time PCR

The second step involved in comparative miRNA analysis by microarray includes quantifying the RT product by qPCR. In this step the DNA polymerase from the TaqMan® Universal PCR Master Mix kit (No AmpErase®, UNG 2X) (Applied Biosystems™, California, USA) amplified the target cDNA using specific sequenced primers and probes on the TaqMan® miRNA microarray. The presence of this target is detected in real time through cleavage of the TaqMan® probe by the polymerase 5' to 3' exonuclease activity (Figure 2.3). Briefly, the qPCR reaction mix was set-up as stated in Table 2.4 in a 1.5 mL centrifuge tube for one array. A total of 100 µL was loaded into each port of the array followed by sealing, centrifuged at 1200 rpm for two minutes (Eppendorf 5804, Hamburg, Germany) and then removal of the reservoir ports before loading onto the 7900HT Real-Time PCR System (Applied Biosystems™, California, USA) as per the manufacturer's protocol (Table 2.5). A total of nine arrays was performed which included each treatment (X3) in triplicate.

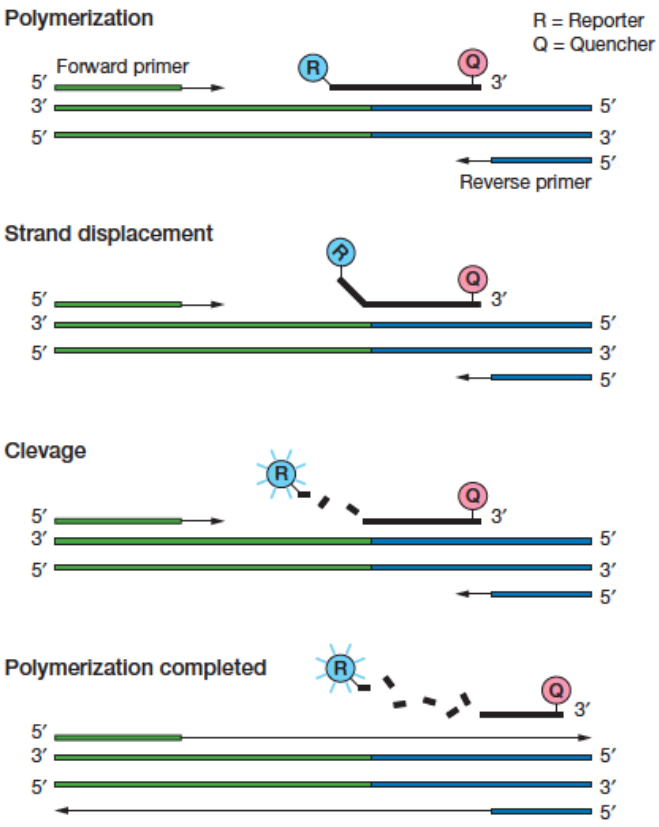


**Figure 2.3: Schematic overview of the TaqMan® probe-based assay chemistry** (Reproduced from http://www.lifetechnologies.com).

**Table 2.4: Components for qPCR in comparative miRNA analysis**

| **Reagent** | **Volume (µL)** |
|---|---|
| TaqMan® Universal PCR Master Mix | 450.00 |
| RT Product | 6.00 |
| Nuclease free water | 444.00 |
| **Total Volume** | **900.00** |

**Table 2.5: Cycling conditions for qPCR in comparative miRNA analysis**

| **Stage** | **Temp** | **Time** | **Cycle** |
|---|---|---|---|
| **Denaturation** | 94.5°C | 10 min | 37 Cycles |
| **Annealing** | 97.9°C | 5 sec | |
| **Extension** | 59.7°C | 45 sec | |

### 2.4.3 Data Analysis

Data and statistical analyses was conducted by a biostatistician, Dr. Wendy Kröger, from the Centre for Proteomic and Genomic Research (CPGR). The Ct values generated from the 384 well plates (one plate per sample) were analysed with Bioconductor's HTqPCR package (Dvinge & Bertone, 2009) in R (R Development Core Team, 2013) to determine differentially expressed miRNAs in the B-cell cancer cell Ramos treated with HIV-1 AT-2 compared to microvesicle treated controls. The quality of the raw data was assessed and normalised. The Ct

values are measured as the cycle number at which point the curve intersects a fluorescence threshold (set to exceed baseline noise). The amount of target template contained within a sample is therefore inversely proportional to the Ct value, i.e. lower Ct values are indicative of a large amount of target present and *vice versa*. In general, Ct values of below 29 are characteristic of strong positive amplifications suggesting abundant target molecule present in the sample. Those Ct values of between 30 and 37 are indicative of positive reactions characterising moderate levels of target molecule present in the sample. Ct values of above 38 are characteristic of weak amplification suggesting minimal amounts or lack of target molecule present within the respective sample.

Statistical analyses was conducted using student t-tests to determine significant differences between the treated samples and microvesicle treated controls. Significance was determined by using the Benjamini-Hochberg false discovery rate corrected for multiple testing (Benjamini & Hochberg, 1995) that was adjusted to $p \leq 0.06$. Given the limitation of the software mentioned above in being unable to eliminate failed replicates and samples with high Ct values, data was manually analysed. Each amplification plot was viewed using RQ Manager (Applied Biosystems™, California, USA) whereby the baseline and threshold values were set (account for noise) and failed replicates or replicates with high Ct values noted above were excluded. The data was then exported into the DataAssist™ software (version 3.01) (Applied Biosystems™, California, USA) to generate the Ct values for each replicate. miRNAs that exhibited a fold change of two or more were selected for further analysis.

### 2.5 miRNA SINGLE-TUBE TAQMAN® PCR ASSAYS

To validate the differentially expressed miRNAs obtained from the miRNA microarray, qPCR using single-tube TaqMan® assays (Applied Biosystems™, California, USA) were performed. These included six assays for miR-200c-3p, miR-222-3p, miR-575, miR-363-3p and RNU48 and RNU6B as endogenous control assays (Malumbres *et al.,* 2009; Linda *et al.,* 2010).

These single-tube assays are more specific and sensitive at detecting miRNAs that have a one nucleotide difference than microarrays which are used mainly as a screening tool for further investigation. The TaqMan® assays contains two tubes, one containing specific stem loop primers for RT and the second tube containing the forward and reverse primers for qPCR and the miRNA specific MGB probe.

### 2.5.1 Reverse transcription using stem-loop primers

The stem-loop primers of the miRNA assays are designed specifically for the mature miRNA sequences of the selected miRNAs. Briefly, after isolation, total RNA was diluted to 10 ng/µL, where after 1 µL was added to each reaction tube. Each RT conversion was performed for the six assays in DEPC treated PCR tubes for both cell lines. Briefly, a master mix reaction was set-up in a 1.5 mL centrifuge tube as per protocol (Table 2.6) using the TaqMan® miRNA Reverse Transcription kit (Applied Biosystems™, California, USA). The RT primers were added respectively to each tube for each sample (3 µL), followed by 7 µL of the master mix reaction, 1 µL of the RNA template and topped up to a total volume of 15 µL with nuclease-free $H_2O$ (Thermo Fisher Scientific™, Massachusetts, USA).

**Table 2.6: Components for the reverse transcription using stem-loop primers**

| Reagent | Volume (µL) |
|---|---|
| 10X RT Buffer | 1.50 |
| RNase Inhibitor (20 U/µL) | 0.19 |
| dNTPs with dTTP (100 mM) | 0.15 |
| MultiScribe Reverse transcriptase (50 U/ µL) | 1.00 |
| Nuclease-free water | 4.16 |
| **Total Volume** | **7.00** |

The cycling conditions were set-up as per the protocol on the MultiGene™ Gradient PCR Thermal Cycler (Labnet International, California, USA) (Table 2.7). Reaction tubes containing cDNA were thereafter stored at -20°C until they were used for qPCR.

**Table 2.7: Cycling conditions for reverse transcription using stem-loop primers**

| Stage | Temp | Time |
|---|---|---|
| Hold | 16.0°C | 30 min |
| Hold | 42.0°C | 30 min |
| Hold | 85.0°C | 5 min |
| Hold | 4.0°C | ∞ |

### 2.5.2 Quantitative real-time PCR

A master mix reaction was prepared using the TaqMan® Universal PCR Master Mix kit (No AmpErase®, UNG 2X) (Applied Biosystems™, California, USA) for each miRNA in duplicate, a negative control (no-template) and two endogenous controls (RNU6B and RNU48). Briefly, reagents in Table 2.8 was added to 0.1 mL reaction tubes supplied by the

manufacturer (Qiagen, Hilden, Germany) in a total volume of 20 µL. The reaction tubes were then loaded onto the Rotor Gene-Q machine (Qiagen, Hilden, Germany) following the cycling conditions outlined in Table 2.9 as per the manufacturers protocol.

**Table 2.8: Components for single tube TaqMan® miRNA assays**

| Reagent | Volume (µL) |
|---|---|
| TaqMan® miRNA Assay | 0.50 |
| TaqMan® Universal Master Mix X2 | 5.00 |
| Nuclease-free water | 3.90 |
| cDNA product | 0.60 |
| **Total Volume** | **10.00** |

**Table 2.9: Cycling conditions for single tube TaqMan® miRNA assays**

| Stage | Temp | Time |
|---|---|---|
| Hold | 95.0°C | 10 min |
| 40 Cycles | 95.0°C | 15 sec |
| | 60.0°C | 45 sec |

### 2.5.3 Data Analysis

The quantification data for all experiments were analysed using the comparative critical threshold (ΔΔCt) method to calculate the fold change expression of the miRNAs. Before this could be performed, each amplification plot was viewed using RQ Manager (Applied Biosystems™, California, USA) whereby the baseline and threshold values were set. The data were exported into the DataAssist™ software (version 3.01) (Applied Biosystems™, California, USA) to generate the Ct values for each replicate and to determine which endogenous control was consistent amongst the data. The Ct values are then used to calculate the fold change by first excluding any outliers in the data set (Ct >35; Change in Ct >1 amongst technical replicates) then the miRNA of interest was normalised to the endogenous control relative to the microvesicle treated control samples. The fold induction was thereafter calculated using the equation $2^{-\Delta\Delta Ct}$. Finally, the average fold changes were represented as means and standard deviations relative to the microvesicle treated control normalised to 1. Student t-tests were performed using Microsoft® Excel for Mac (version 15.2.3) to determine any significant differences between the treated samples relative to the microvesicle treated control. Significance level was set at $p \leq 0.05$.

## 2.6 BIOINFORMATICS ANALYSIS AND TARGET SELECTION

Once the data were analysed, one miRNA was selected for further characterisation. Bioinformatic databases such as miRBase *(http://www.mirbase.org)*, miRNADB *(http://www.mirdb.org)*, microRNA.org *(http://www.microrna.org)* and miRTarBase *(http://mirtarbase.mbc.nctu.edu.tw/index.php)* was used to identify putative gene targets. Target selection was determined by similar search results across all databases (Kuhn *et al.,* 2008). In addition, literature was consulted to identify validated targets in other cancers. These target prediction tools employ complementarity binding of the seed region (6-8 nucleotides in length within the structure of the 5' miRNA end) and its target mRNA (Kuhn *et al.,* 2008). They also employ partial complementarity to the 5' miRNA end compensated by additional base pairings in the 3' end (Liu *et al.,* 2012).

## 2.7 DNASE I TREATMENT OF RNA SAMPLES

RNA samples were DNase treated prior to qPCR of selected gene targets to eliminate any genomic DNA (gDNA) contamination that would affect downstream qPCR experiments. Total RNA that had been previously isolated (Section 2.2.1) (used *mir*Vana kit that lacked a DNase treatment step) were treated with DNase I and concentrated using the RNA Clean & Concentrator™ -5 Kit (Zymo Research, California, USA). Briefly, 10 µL of RNA from each sample was treated with nuclease-free $H_2O$, 5 µL of DNase I in 5 µL of DNA digestion buffer in a total volume of 50 µL. The reactions were incubated at 25°C for 15 minutes and thereafter RNA binding buffer and 100% EtOH was added. Consequent steps of washing with the RNA prep and wash buffers was then performed in corresponding column tubes. After each wash, the flow-through was discarded until the final step, whereby the columns were transferred to DEPC treated 1.5 mL centrifuge tubes. The RNA was eluted in 8-10 µL of RNase free $H_2O$ (Zymo Research, California, USA) followed by quantification by NanoDrop™ (Thermo Fisher Scientific™, Massachusetts, USA) analysis, Qubit™ RNA Assays and visualised by agarose gel electrophoresis.

## 2.8 REVERSE TRANSCRIPTION AND PCR OF SELECTED GENE TARGETS

### 2.8.1 Primer design

Primers specific for qPCR were designed for target genes using the Primer3Plus programme *(http://www.bioinformatics.nl/cgi-bin/primer3plus.cgi)* (Thornton & Basu, 2011). Two primers were designed, (forward and reverse) according to specific parameters. These parameters included the primer length of 18-25 base pairs (bp), melting temperature ($T_m$) of 48-55°C, primer GC% of 40-60%. A potential primer pair was selected after the formation of secondary structures such as homodimers and heterodimers were analysed using OligoAnalyzer (Integrated DNA Technologies, Iowa, USA). Primers were avoided if the ΔG was more than 3 kcal/mole and the $T_m$ of the hairpins exceeded 30°C. The primer pair was analysed to determine whether they would amplify other gDNA regions besides the target region using the Basic Local Alignment Search Tool (BLAST) *(http://blast.ncbi.nlm.nih.gov/Blast.cgi)*. Primer pairs were included if they yielded 100% complementarity to the gene target and less than 75% to non-specific genes (Table 2.10).

**Table 2.10: Primer pairs for gene target analysis**

| Primer | Sequence | Melting temperature ($T_m$) ($^0$C) | Amplicon Size (bp) |
|---|---|---|---|
| BLIDF | 5'-CAGAGACCTTCCTATTTAACC-3' | 52.4 | 91 |
| BLIDR | 5'-CATCTGTCCTAACTCACTCC-3' | 52.0 | |
| GAPDHF | 5'-GAAGGCTGGGGCTCATTT-3' | 55.4 | 133 |
| GAPDHR | 5'-CAGGAGGCATTGCTGATGAT-3' | 55.2 | |
| RPL27F | 5'-ATCGCCAAGAGATCAAAGATAA-3' | 51.7 | 123 |
| RPL27R | 5'-TCTGAAGACATCCTTATTGACG-3' | 52.1 | |

bp – base pairs; *BLID* – BH3-like motif containing cell death inducer; F – forward; *GAPDH* – Glyceraldehyde-3-Phosphate Dehydrogenase; R – reverse; *RPL27* – 60S ribosomal protein 27; $T_m$ – melting temperature

### 2.8.2 Reverse transcription using oligoDT and random hexamer primers

A master mix reaction was set-up by adding 4 µL of 5X iScript Reaction Mix and 1 µL of Reverse Transcriptase in a 1.5 mL centrifuge tube using the iScript cDNA Synthesis Kit (Bio Rad, California, USA). PCR reaction tubes were aliquotted with 5 µL of master mix, RNA template (500 ng/µL) and filled up to a total volume of 20 µL with nuclease-free $H_2O$ (Thermo Fisher Scientific™, Massachusetts, USA). The reaction was run on the MultiGene™ Gradient PCR Thermal Cycling System (Labnet International, California, USA) with the below cycling conditions (Table 2.11). Reaction tubes containing cDNA were stored at -20°C until used.

**Table 2.11: Cycling Conditions for Reverse Transcription using oligoDT & Random Hexamer Primers**

| Stage | Temp | Time |
|---|---|---|
| Hold | 25.0°C | 5 min |
| Hold | 42.0°C | 30 min |
| Hold | 85.0°C | 5 min |
| Hold | 4.0°C | ∞ |

### 2.8.3 PCR of selected gene targets

To confirm the specificity of the qPCR primers, a conventional PCR was first performed for all primer pairs. The reaction was performed using the MyTaq™ DNA polymerase (Bioline, Tennessee, USA) in a total volume of 25 µL (Table 2.12) in a 1.5 mL centrifuge tube. Glyceraldehyde-3-Phosphate Dehydrogenase (*GAPDH*) was used as an internal control (housekeeping gene) followed by a no-template control (NTC). The reaction was run on the MultiGene™ Gradient PCR Thermal Cycling System (Labnet International, California, USA) as per cycling conditions in Table 2.13.

**Table 2.12: Components for Standard PCR using MyTaq™ DNA Polymerase**

| Reagent | Volume (µL) |
|---|---|
| 5X MyTaq™ Buffer | 5.00 |
| MyTaq™ DNA polymerase (50 U/µL) | 0.25 |
| Forward Primer (10 µM) | 1.00 |
| Reverse Primer (10 µM) | 1.00 |
| cDNA template | 1.00 |
| Nuclease-free water | 16.75 |
| **Total Volume** | **25.00** |

**Table 2.13: Cycling Conditions for Standard PCR**

| Stage | Temp | Time | Cycle |
|---|---|---|---|
| Initial Denaturation | 95.0°C | 1 min | 1 Cycle |
| Denaturation | 95.0°C | 15 sec | 30 Cycles |
| Annealing | 48.0°C | 5 sec | |
| Extension | 72.0°C | 10 sec | |
| Hold | 4.0°C | ∞ | |

### 2.8.4 Gel electrophoresis of PCR products

The PCR products were visualised by agarose gel electrophoresis. A 1.5% agarose gel was prepared with 1X TBE buffer (Appendix A) and EtBr (0.5 mg/mL). The samples were prepared

using 15 µL of PCR product and 2 µL of 5X DNA loading dye. Products were electrophoresed at 100 volts/cm for 35 minutes using 1X TBE as running buffer and 1kb DNA ladder (Appendix B – Figure B1). The gel was visualised under a UV trans-illuminator (Uvitec, UK).

### 2.8.5 Quantitative real time PCR of miRNA gene targets

Upon confirmation of the specificity of qPCR primers, qPCR was performed using the KAPA SYBR® FAST qPCR Kit (Kapa Biosystems, Cape Town, SA). Reactions were carried out in triplicate with *GAPDH* and 60S ribosomal protein L27 (*RPL27*) used as validated housekeeping genes. A master mix reaction (Table 2.14) was set-up in 0.1 mL reaction tubes in a total volume of 20 µL and was run on a Rotor Gene-Q (Qiagen, Hilden, Germany) machine (Table 2.15). Quantified data was exported and statistically analysed using the comparative ΔΔCt method and student t-test as described in Section 2.5.3.

**Table 2.14: Components for qPCR for expression of gene targets**

| Reagent | Volume (µL) |
|---|---|
| SYBR Green qPCR Reaction Mix | 5.00 |
| Forward Primer (10 µM) | 0.20 |
| Reverse Primer (10 µM) | 0.20 |
| cDNA template | 1.00 |
| Nuclease-free water | 3.60 |
| **Total Volume** | **10.00** |

**Table 2.15: Cycling Conditions for qPCR for expression of gene targets**

| Stage | Temp | Time | Cycle |
|---|---|---|---|
| Pre-Incubation | 95.0°C | 3 min | 1 Cycle |
| Amplification | 95.0°C | 10 sec | 40 Cycles |
| | 48.0°C | 20 sec | |
| | 72.0°C | 1 sec | |
| Hold | 4.0°C | ∞ | |

## 2.9 Functional Analysis & Characterisation of miRNA

### 2.9.1 Protein extraction using RIPA buffer

Protein were extracted using the Radio-Immunoprecipitation Assay (RIPA) buffer which utilises three non–ionic and ionic detergents to efficiently lyse and permeabilise the cells. The RIPA buffer was prepared (Appendix A) and combined with 7X cOmplete™, Mini, EDTA-

free, Protease Inhibitor (Appendix A) (Roche Applied Science, Penzberg, Germany). The protease inhibitor protects the extracted protein sample from degradation by proteases present in the cell lysate. The above principle applies to both the suspension (L1439A) and adhesion cell lines. The breast cancer adhesion cell lines T47D (ATCC®, Virginia, USA) and MDA-MB231 (ATCC®, Virginia, USA) were used as positive controls since the cell lines have been reported to express endogenous *BLID*. These were not cultured (kindly donated by the Sharon Prince Lab) and protein was received for MDA-MB231 whilst protein was extracted for T47D cells.

#### *2.9.1.1 Suspension Cells*

Fresh RIPA solution was made (Appendix A) and kept on ice under the hood. The cell suspension was transferred into 15 mL Falcon tubes and was centrifuged for five minutes at 2000 rpm (MSE, California, USA). The supernatant was removed and the pellet was washed three times in ice cold 1X PBS (Appendix A) followed by repeating the above centrifugation and removal of the supernatant. Sufficient RIPA solution was added (200-500 µL depending on pellet size) to the cells until it became viscous and was stored overnight at -80°C for optimum lysis. The cells were then thawed on ice and then centrifuged at 4°C at 12 000 rpm for 20 minutes to remove cell debris (Beckman, London, UK). The supernatant was aliquotted and stored at -80°C.

#### *2.9.1.2 Adherent Cells*

As before, fresh RIPA solution was made and kept on ice under the hood. The culture plate containing the cells were placed on ice and the medium was removed and cells were washed three times with ice cold 1X PBS (Appendix A). RIPA solution (500 µL) was added to the culture plate and the cells were scraped using a 1 mL syringe plunger as a cell scraper, transferred into a 1.5 mL Eppendorf tube and stored at -80°C overnight. The procedure thereafter was the same as noted above.

### 2.9.2 Protein quantification using the BCA reagent

The bicinchoninic acid (BCA) reagent was used to determine the protein concentrations, using the Pierce™ BCA Assay kit (Thermo Fisher Scientific™, Massachusetts, USA). The assay uses a sensitive and selective colourimetric detection system where a unique reagent containing BCA detects the reduction of $Cu^{2+}$ to $Cu^{1+}$ (biuret reaction) in an alkaline medium. The color produced from this reaction is stable and increases in a proportional pattern over a broad range

of increasing protein concentrations. A standard curve is generated using bovine serum albumin (BSA) at a range of concentrations (2000 µg/mL, 1000 µg/mL, 500 µg/mL, 125 µg/mL and 0 µg/mL) (Smith *et al.,* 1985). Briefly protein is thawed on ice and then is diluted (1:5; 1:2) in the RIPA buffer in a total volume of a minimum of 25 µL. The BCA standards are prepared as per the manufacturers protocol by combining Reagent A and B in a ration of 50:1 to produce the working reagent. In a 96-well plate, 10 µL of the protein sample (diluted with RIPA buffer) is added to each well with 200 µL of working reagent in duplicate. The plate is then incubated at 37°C for 30 minutes and the colour change is measured using the Glo-Max®-Multi+ multiplate reader (Promega, Wisconsin, USA) at a wavelength of 560 nm. The concentration of the protein is extrapolated from the generated standard curve.

### 2.9.3 SDS-PAGE & Western blotting to determine protein expression

#### *2.9.3.1 SDS-PAGE*

To visualise proteins, a polyacrylamide gel electrophoresis (PAGE) was performed using an anionic detergent, sodium dodecyl sulphate (SDS), to linearise and negatively charge proteins. A 7.5 mL 15% resolving gel and a 5% stacking gel (Appendix A) as per the manufacturers protocol was made using the Mini-PROTEAN 3 casting apparatus (Bio-Rad, California, USA) (Table 2.16). The dithiothreitol (DTT) was used as a small redox reagent to reduce the disulphide bridges present in the proteins.

**Table 2.16: Components for protein sample preparation for SDS-PAGE**

| Reagent | Volume (µL) |
|---|---|
| Protein sample (14-20 µg)* | x |
| 100 mM DTT | 1,00 |
| 1X RIPA Buffer | 30 – x |
| 5X SDS loading dye | 4.00 |
| **Total Volume** | **30.00** |

*Protein concentration varied in order to determine the optimal detection of the protein for western blotting

Prior to loading, samples were denatured at 95°C for five minutes, spun down and kept on ice. The polyacrylamide gel was assembled in the electrophoresis apparatus (Bio-Rad, California, USA) and 1X running buffer was added until it was overflowing (Appendix A). The comb was then removed and was washed with the buffer. Samples were added (30 µL) with 5 µL of the BenchMark™ Pre-Stained Protein Ladder (Appendix B – Figure B2) and 1 µL of 5X SDS loading dye to the empty wells (Appendix A) to ensure the proteins electrophorese vertically.

The apparatus was connected to the Bio-Rad power pack and electrophoresed for two hours, five minutes at 100 volts.

### *2.9.3.2 Protein Transfer*

After the proteins were separated by SDS-PAGE, they were then transferred to a nitrocellulose membrane (Bio-Rad, California, USA). The transfer was set-up in a cassette by placing the gel, filter paper and membrane in a specific order as illustrated in Figure 2.3. This cassette was then placed back into the Mini-PROTEAN 3 casting apparatus (Bio-Rad, California, USA) and cold 1X transfer buffer (Appendix A) was added along with an ice pack. The transfer was conducted using the Bio-Rad power pack at 100 volts for one hour.

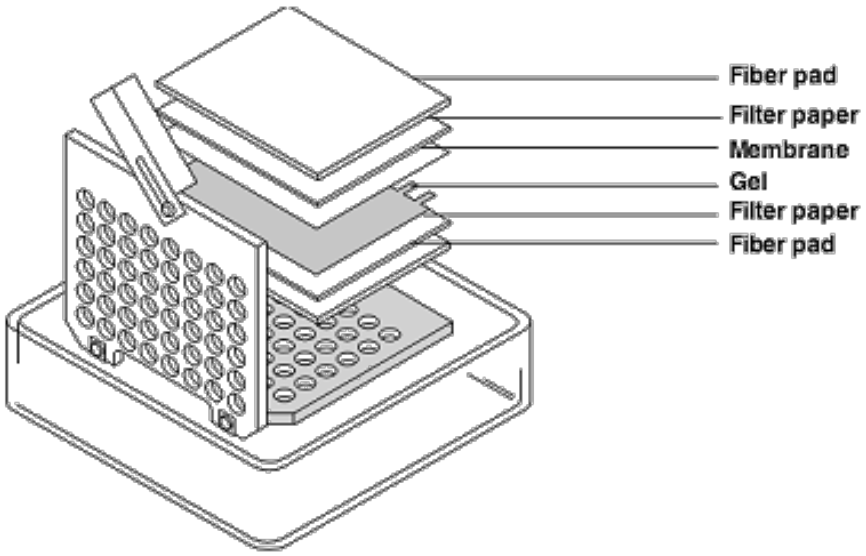


**Figure 2.4: The western blot cassette orientation for transfer of proteins** (Reproduced from http://www.radio.cuci.udg.mx/bch/EN/Western.html).

### *2.9.3.3 Antibody incubation & visualisation*

Upon completion of the transfer, the membrane was stained with Ponceau S (Sigma Aldrich, Missouri, USA) to visualise the protein bands (Appendix A) and confirm a successful transfer. Thereafter the membrane was washed with deionized water followed by PBS/Tween (Appendix A) and then blocked in PBS/Tween containing 5% of fat-free milk powder for one hour (Appendix A) with gentle shaking at room temperature. After blocking was completed, the membrane was incubated with primary antibody diluted to the desired concentration (*BLID* (Novus Technologies, Singapore, Malaysia); p38 (Bio-Rad, California, USA)) (Table 2.17) and was incubated overnight at 4°C in blocking solution with gentle shaking. The membrane was then washed with PBS/Tween (2X quick washes; 2X five minutes; 2X ten minutes) with

gentle shaking. The membrane was then incubated with the appropriate HRP-conjugated secondary antibody diluted in blocking solution for one hour at room temperature with gentle shaking (Table 2.17). Thereafter the membrane was washed as before and then visualised by enhanced chemiluminescence using the Clarity™ Western ECL Substrate (Bio-Rad, California, USA) as per the manufacturers protocol. The membrane was exposed to X-ray film and the resulting signal was captured by developing and fixing the film.

**Table 2.17: Primary and secondary antibody concentrations used for western blot analyses**

| Protein | Primary antibody | Secondary antibody |
|---|---|---|
| BLID | 1:500 | 1:5000 (goat anti-mouse) |
| p38 | 1:5000 | 1:5000 (goat anti-rabbit) |

BH3-like motif containing cell death inducer

### *2.9.3.4 Membrane stripping*

Antibodies were removed from the blot by incubating in 55°C pre-warmed stripping buffer (Appendix A) at 55°C for one hour, with brief agitation every ten minutes. The membrane was then washed twice for ten minutes with PBS/Tween and the blot was reused from the blocking stages noted above to detect the internal loading control p38.

# CHAPTER 3: IDENTIFICATION OF DIFFERENTIALLY EXPRESSED MIRNAS IN B-CELLS EXPOSED TO HIV USING MICROARRAY ANALYSIS

## 3.1 INTRODUCTION

miRNA microarray analysis has gained momentum as a discovery tool for identifying miRNA signatures especially for different cancers (Wang & Xi, 2013). Given the dearth of evidence linking HIV, miRNAs and NHLs, we aimed firstly to identify miRNAs that are differentially expressed in B-cells when they are exposed to HIV. To do this we designed a custom miRNA microarray to profile the expression of miRNAs which are either linked to the development of BL and DLBCL, as well as those which have been described as miRNA signatures for these cancers. This extensive search also expanded towards the addition of deregulated miRNAs that are involved in known cancer pathways. The results of the search for the chosen miRNAs and the microarray analysis are presented below followed by a discussion of these results.

## 3.2 RESULTS

### 3.2.1 Extensive literature searches to identify a panel of miRNAs for the design of a customised PCR array

As mentioned in Section 2.4, an extensive literature search was conducted to identify and select miRNAs for inclusion in the customised microarray card to be used for profiling. Search engines, Google™ Scholar (*http://scholar.google.com*) and PubMed (*http://www.ncbi.nlm.nih.gov/pubmed/*) were used to search for relevant literature with the keywords Diffuse Large B-cell lymphoma, Burkitt's lymphoma and microRNAs. Secondly, to select suitable miRNAs, published miRNA signatures for DLBCL and BL were reviewed and used to select the panel (Table 3.1 and Table 3.2). In addition, commercially available arrays (from SABiosciences *http://www.sabiosciences.com/mirna_pcr_product/HTML/MIHS-102Z.html*) were consulted that featured miRNAs that are implicated in cancer pathways or differentially expressed in other cancers (Human Cancer PathwayFinder miRNA PCR Array: MIHS-102Z) were also selected.

The selected miRNAs were then cross referenced with the TaqMan® Inventory database available from Applied Biosystems™ (California, USA) which are based on the miRBase platform (*https://www.thermofisher.com/za/en/home/life-science/pcr/real-time-pcr/real-time-pcr-assays/mirna-ncrna-taqman-assays/taqman-microrna-assays-educational-resources.html*). In conjunction, controls (RNU44, RNU48, RNU6B) were chosen based on literature and also cross referenced with the list to check on their availability (Malumbres *et al.,* 2009; Linda *et al.,* 2010; Forte *et al.,* 2012). The selected miRNAs were then finalised (n = 188) (Table 3.3) to fit onto a 192a array format assay in duplicate with controls in quadruplicate and two wells unspotted as negative controls (blank).

**Table 3.1: A summary of miRNAs reported to be deregulated in Diffuse Large B-cell lymphoma**

| Subtype | Upregulated miRNAs | Downregulated miRNAs | Reference |
|---|---|---|---|
| **Germinal Centre B-cell like** | miR-10398-3p, NOVEL00260M, NOVELM00010M, miR-10b-5p, miR-423-3p, miR-301a-5p, miR-598, miR-181a-5p, miR-30e-3p, miR-744-5p, miR-4746-5p, miR-1270, miR-3074-5p, miR-589-3p, miR-151a-3p, miR-331-3p, miR-3934-3p, miR-589-5p, miR-210, miR-138-1-3p, miR-28-5p, miR-339-3p, miR-196b-5p, miR-151b, miR-129-2-3p, miR-664a-3p, miR-28-3p, miR-582-3p, miR-3681-5p, miR-129-1-3p, miR-582-5p, miR-138-5p, miR-129-5p, miR-3150b-3p | * | Lim *et al.,* 2015 |
| | * | miR-28 | Schneider *et al.,* 2014 |
| | miR-18a | * | Alencar *et al.,* 2011 |
| | miR-17, miR-18a, miR-19a, miR-20a, miR-19b, miR-92a | * | Fassina *et al.,* 2012 |
| | miR-17-5p, miR-150, miR-145, miR-328 | * | Roehle *et al.,* 2008 |
| | miR-17/92, miR-181a, miR-221 | * | Lawrie *et al.,* 2008 |
| | miR-17, miR-19b, miR-20a | * | Culpin *et al.,* 2010 |
| | miR-28-3p, miR-28-5p, miR-129-3p, miR-589, miR-331-5p, miR-597 | * | Iqbal *et al.,* 2015 |
| **Non-Germinal Centre B-cell like** | miR-10397-5p, NOVELM00288M, miR-155-3p, miR-222-5p, miR-148a-5p, miR-222-3p, miR-625-3p, miR-363-3p, miR-30d-3p, miR-30b-3p, miR-221-3p, miR-92a-1-5p, miR-21-3p, miR155-5p, miR625-5p, miR-29b-1-5p, miR-20a-5p, miR-17-5p, miR-106a-5p, miR-503-5p, miR-424-5p, miR-302a, miR-10b-5p | * | Lim *et al.,* 2015 |
| | miR-181, miR-222 | * | Alencar *et al.,* 2011 |
| | * | miR-34a | Craig *et al.,* 2012 |
| | miR-155, miR-29b, miR-146a, miR-365, miR-30b, miR-26b, miR-374, let-7f, miR-9, miR-9-3p, miR-34b | * | Di Lisio *et al.,* 2012 |
| | miR-23a, miR-24-2, miR-27a | * | Kong *et al.,* 2010 |
| | miR-150, miR-145, miR-328 | * | Roehle *et al.,* 2008 |
| | miR-155, miR-21, miR-210, miR-221 | * | Lenz *et al.,* 2008 |
| | miR-155, miR-21, miR-22, miR-146a, miR-146b, miR-500, miR-363, miR-574-3p, miR-547-5p, miR-222 | * | Malumbres *et al.,* 2009 |
| | miR-29a, miR-92a, miR-106a, miR-720, miR-1260, miR-1280 | * | Culpin *et al.,* 2010 |
| | miR-155, miR-542-3p | * | Iqbal *et al.,* 2015 |

* no miRNAs were reported as downregulated/upregulated in this study (miR-microRNA)

**Table 3.2: A summary of miRNAs as reported to be deregulated in Burkitt's lymphoma**

| Upregulated miRNAs | Downregulated miRNAs | Reference |
|---|---|---|
| miR-371, miR-185, miR-93, miR-326, miR-339, miR-485, miR-193a, miR-448, miR-202, miR-483, miR-26a, miR-328, miR-192, miR-429, miR-324, miR-340, miR-105, miR-124 | miR-221, miR-30a, miR-146a, miR-146b, miR-26b, miR-23a, miR-30d, miR-107, miR-103, miR-222, miR-26a, miR-30a, miR-142, miR-23b, miR-342, miR-29b, miR-34b, miR-9 | Lenze *et al.,* 2011 |
| miR-19a, miR-18a, miR-19b, miR-20a, miR-17-3p, miR-17-5p, miR-92, miR-106a, miR-130b, miR-128b, miR-7, miR-206, miR-370, miR-494, miR-148a, miR- 20b | miR- 210, let-7e, miR-215, miR-144, miR-451, miR-101, miR-125b, miR-139, miR-140, miR-142-3p, miR-146a, miR15a, miR-150, miR-16, miR-195, miR-22, miR-223, miR-23a, miR-23b, miR-24, miR-26a, miR-26b, miR-29a, miR-29b, miR-29c, miR-30c, miR-30e-3p, miR-30e-5p, miR-34a, miR-99b, let-7a, miR-155, miR-196a, miR-342 | Robertus *et al.,* 2010 |
| miR-17-5p, miR-20a, miR-9-3p | * | Onnis *et al.,* 2010 |
| miR-210, miR-494, miR-575, miR-202, miR-801, miR-370, miR-765, miR-188, miR-296, miR-560, miR-663, miR-181, miR-574, miR-197, miR-92, miR-20b, miR-20a, miR-17-5p, miR-106, miR-93, miR- 422, miR-17-3p, miR-18a, miR-130, miR-19b, miR-19a | miR-29b, let-7d, miR-155, miR-15a, let-7e, miR-23b, miR-768-5p, miR-148a, miR-331, miR-27b, miR-28, miR-363, miR-98, let-7a, let-7f, let-7g, miR-29a | Bueno *et al.,* 2011 |

* no miRNAs were reported as downregulated in this study
miR - microRNA

**Table 3.3: Finalised miRNAs (n = 188; 192a format) for microarray profiling, spotted in duplicate with four controls as reported from the literature**

| | | | | | | | | | | | | | | | | | | | | | | |
|---|---|---|---|---|---|---|---|---|---|---|---|---|---|---|---|---|---|---|---|---|---|---|
| let-7a-2-3p | let-7a-1-3p | let-7a-5p | let-7b-5p | let-7b-3p | let-7c-5p | let-7d-5p | let-7e-5p | let-7e-3p | let-7f-5p | U6 | let-7f-1-3p | let-7g-5p | let-7i-5p | miR-100-5p | miR-100-3p | miR-101-3p | miR-103a-3p | miR-105-5p | miR-105-3p | miR-106a-5p | miR-106a-3p | miR-106b-5p | miR-106b-3p |
| let-7a-2-3p | let-7a-1-3p | let-7a-5p | let-7b-5p | let-7b-3p | let-7c-5p | let-7d-5p | let-7e-5p | let-7e-3p | let-7f-5p | U6 | let-7f-1-3p | let-7g-5p | let-7i-5p | miR-100-5p | miR-100-3p | miR-101-3p | miR-103a-3p | miR-105-5p | miR-105-3p | miR-106a-5p | miR-106a-3p | miR-106b-5p | miR-106b-3p |
| miR-107 | miR-124-5p | miR-125b-5p | miR-126-3p | miR-126-5p | miR-127-3p | miR-130b-3p | miR-132-3p | miR-133a-3p | miR-138-5p | miR-140-3p | miR-141-3p | miR-142-3p | U44 | miR-143-3p | miR-143-5p | miR-145-3p | miR-145-5p | miR-146a-3p | miR-146b-3p | miR-146b-5p | miR-148a-3p | miR-148a-5p | miR-149-5p |
| miR-107 | miR-124-5p | miR-125b-5p | miR-126-3p | miR-126-5p | miR-127-3p | miR-130b-3p | miR-132-3p | miR-133a-3p | miR-138-5p | miR-140-3p | miR-141-3p | miR-142-3p | U44 | miR-143-3p | miR-143-5p | miR-145-3p | miR-145-5p | miR-146a-3p | miR-146b-3p | miR-146b-5p | miR-148a-3p | miR-148a-5p | miR-149-5p |
| miR-150-5p | miR-150-3p | miR-151a-3p | miR-155-5p | miR-155-3p | miR-15a-3p | miR-15b-5p | U48 | miR-17-5p | miR-17-3p | miR-18a-5p | miR-18b-5p | miR-185-5p | miR-188-5p | miR-191-5p | miR-192-5p | miR-193a-5p | miR-194-5p | miR-194-3p | miR-195-5p | miR-195-3p | miR-196a-5p | miR-196a-3p | miR-196b-5p |
| miR-150-5p | miR-150-3p | miR-151a-3p | miR-155-5p | miR-155-3p | miR-15a-3p | miR-15b-5p | U48 | miR-17-5p | miR-17-3p | miR-18a-5p | miR-18b-5p | miR-185-5p | miR-188-5p | miR-191-5p | miR-192-5p | miR-193a-5p | miR-194-5p | miR-194-3p | miR-195-5p | miR-195-3p | miR-196a-5p | miR-196a-3p | miR-196b-5p |
| miR-197 | miR-199a-3p | miR-19a-3p | miR-19b-3p | U6 | miR-20b-5p | miR-200c-3p | miR-202-5p | miR-205-5p | miR-21-5p | miR-210-3p | miR-214-3p | miR-215-5p | miR-218-5p | miR-22-3p | miR-221-3p | miR-222-3p | miR-223-5p | miR-224-5p | miR-23a-3p | miR-23b-3p | miR-24-3p | miR-25-3p | miR-26a-5p |
| miR-197 | miR-199a-3p | miR-19a-3p | miR-19b-3p | U6 | miR-20b-5p | miR-200c-3p | miR-202-5p | miR-205-5p | miR-21-5p | miR-210-3p | miR-214-3p | miR-215-5p | miR-218-5p | miR-22-3p | miR-221-3p | miR-222-3p | miR-223-5p | miR-224-5p | miR-23a-3p | miR-23b-3p | miR-24-3p | miR-25-3p | miR-26a-5p |
| miR-26a-1-3p | miR-26b-5p | miR-26b-3p | miR-27a-3p | miR-27b-3p | miR-28-3p | miR-29a-3p | miR-29b-3p | miR-29c-3p | miR-296-3p | miR-30a-3p | miR-30a-5p | miR-30b-3p | miR-30c-5p | miR-30d-5p | miR-30e-3p | U44 | miR-301a-3p | miR-31-5p | miR-32-5p | miR-320a | miR-324-3p | miR-324-5p | miR-326 |
| miR-26a-1-3p | miR-26b-5p | miR-26b-3p | miR-27a-3p | miR-27b-3p | miR-28-3p | miR-29a-3p | miR-29b-3p | miR-29c-3p | miR-296-3p | miR-30a-3p | miR-30a-5p | miR-30b-3p | miR-30c-5p | miR-30d-5p | miR-30e-3p | U44 | miR-301a-3p | miR-31-5p | miR-32-5p | miR-320a | miR-324-3p | miR-324-5p | miR-326 |
| miR-328-3p | miR-331-3p | miR-339-3p | miR-339-5p | miR-340-5p | miR-342-5p | miR-342-3p | miR-345-5p | miR-34a-5p | miR-34b-5p | miR-361-5p | miR-363-3p | miR-365a-3p | miR-370-3p | miR-374a-5p | miR-422a | miR-423-5p | miR-425-5p | miR-429 | miR-448 | miR-454-3p | miR-455-3p | miR-483-3p | miR-484-3p |
| miR-328-3p | miR-331-3p | miR-339-3p | miR-339-5p | miR-340-5p | miR-342-5p | miR-342-3p | miR-345-5p | miR-34a-5p | miR-34b-5p | miR-361-5p | miR-363-3p | miR-365a-3p | miR-370-3p | miR-374a-5p | miR-422a | miR-423-5p | miR-425-5p | miR-429 | miR-448 | miR-454-3p | miR-455-3p | miR-483-3p | miR-484-3p |
| miR-485-3p | U48 | miR-494-3p | miR-497-5p | miR-513a-3p | miR-516b-3p | miR-520d-3p | miR-520d-5p | miR-520f-5p | miR-520f-3p | miR-532-5p | miR-563 | miR-573 | miR-574-3p | miR-575 | miR-582-3p | miR-582-5p | miR-590-3p | miR-595 | miR-624-5p | miR-624-3p | miR-627-3p | miR-627-5p | miR-628-5p |
| miR-485-3p | U48 | miR-494-3p | miR-497-5p | miR-513a-3p | miR-516b-3p | miR-520d-3p | miR-520d-5p | miR-520f-5p | miR-520f-3p | miR-532-5p | miR-563 | miR-573 | miR-574-3p | miR-575 | miR-582-3p | miR-582-5p | miR-590-3p | miR-595 | miR-624-5p | miR-624-3p | miR-627-3p | miR-627-5p | miR-628-5p |
| miR-629-5p | miR-634 | miR-650 | miR-660-5p | miR-7-2-3p | miR-765 | miR-766-3p | miR-769-5p | miR-9-3p | miR-9-5p | miR-92a-3p | miR-92a-1-5p | miR-92a-2-5p | miR-93-3p | miR-95-3p | miR-96-3p | miR-98-5p | miR-99a-5p | miR-16-5p | miR-142-5p | miR-20a-5p | miR-30e-3p | miR-486-5p | BLANK |
| miR-629-5p | miR-634 | miR-650 | miR-660-5p | miR-7-2-3p | miR-765 | miR-766-3p | miR-769-5p | miR-9-3p | miR-9-5p | miR-92a-3p | miR-92a-1-5p | miR-92a-2-5p | miR-93-3p | miR-95-3p | miR-96-3p | miR-98-5p | miR-99a-5p | miR-16-5p | miR-142-5p | miR-20a-5p | miR-30e-3p | miR-486-5p | BLANK |

POSITIVE CONTROLS | NEGATIVE CONTROL | UPREGULATED | DOWNREGULATED | BOTH UP & DOWN | NO RESULT*

*No reported differential expression in B-cell lymphomas and/or cancer (added onto array for miRNA family involvement)

References: See Bueno *et al.,* (2011); Chang *et al.,* (2008); Chiang *et al.,* (2013); Di Lisio *et al.,* (2012); Forte *et al.,* (2012); Imig *et al*., (2010); Jima *et al.,* (2010); Leucci *et al.,* (2008); Linda *et al.,* (2010); Malumbres *et al.,* (2009); Robertus *et al.,* (2010); Sampson *et al.,* (2007) (Appendix B)

### 3.2.2 Cells remained viable after the selected treatment period

Following expansion of the two B-cell lines namely a lymphoblastoid cell line derived from a healthy donor (L1439A), and the commercially available BL cell line Ramos, a sample from each culture was tested for Mycoplasma infection (Section 2.1.3) and was found to be free of the contaminant (data not shown). The length of time chosen to expose the cells to HIV, as well as the amount of virions, were chosen based on what has been reported in the literature for various cell types such as dendritic cells and monocytes (Lapenta *et al.,* 2003; Martinson *et al.,* 2007; Moir *et al.,* 2000; Mureth *et al.,* 2010; Perise-Barrios *et al.,* 2012; Nicholas *et al.,* 2013; Guo *et al.,* 2014; Mdletshe, 2015). Based on these studies, as well as consultation with colleagues working with HIV virions (Dr. Andrea Soares, Dr. Wendy Burgers – Department of Virology, UCT) a treatment time of three hours was selected, using a concentration of 500 ng/mL.

It was important to verify that the cells remained viable after the three hour treatment, and therefore a viability assay was conducted for both cells using WST-1 (Section 2.1.5). No significant differences in cell viability was observed between microvesicle-treated and HIV-1 AT-2 treated cells (Figure 3.1).

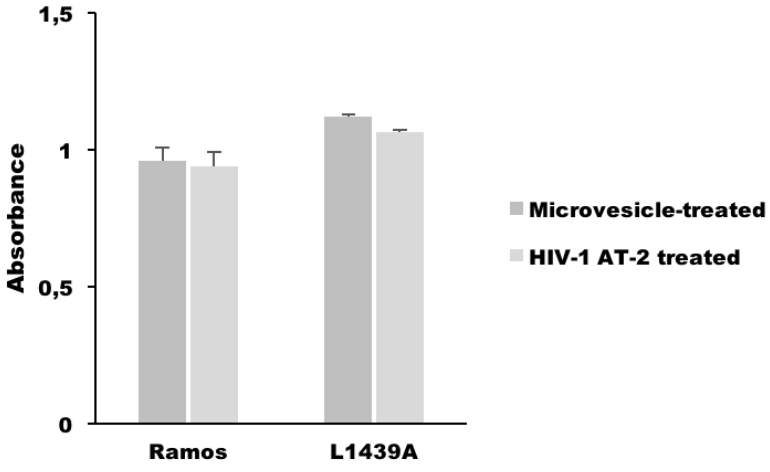


**Figure 3.1: WST-1 assay assessing cell viability after HIV-1 AT-2 treatment in the Ramos and L1439A cell lines.** No significant differences were observed between HIV-1 treated cells and microvesicle-treated controls for both cell lines. The assay was performed in triplicate for both cell lines with the means displayed for each treatment relative to the untreated samples. Absorbance was read at a wavelength between 420-480nm. The error bars represent the standard deviation (Prism 7, Graphpad, USA).

Due to the extremely slow growth of the lymphoblastoid cell line L1439A, the Ramos cell line was chosen for the microarray screening with the intention to perform downstream validity studies in both cell lines.

### 3.2.3 RNA for miRNA profiling was contaminated with genomic DNA

Following treatment which is described in Section 2.1.4 of Chapter two, total RNA was extracted using the *mir*Vana system (Section 2.2.1). Thereafter, an aliquot of RNA from each dish was separated using gel electrophoresis (Section 2.7.5) to analyse integrity (Figure 3.2). The RNA was found to be contaminated with genomic DNA (gDNA) indicated by the bands at the top of the gel picture (indicated as gDNA in Figure 3.2 below). Importantly, the ribosomal RNA (rRNA) bands 18S and 28S were intact.

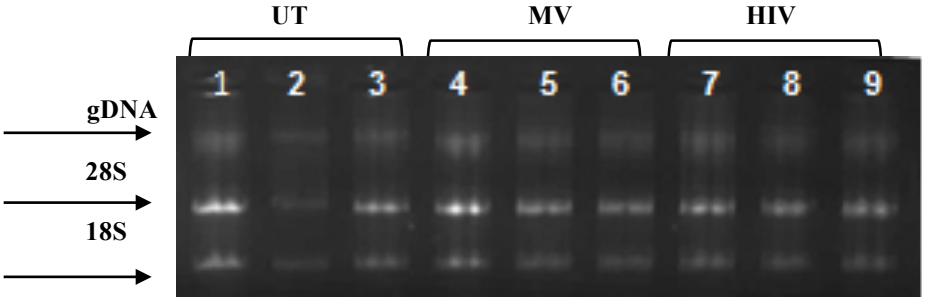


**Figure 3.2: RNA integrity gel displaying RNA extracted from Ramos cells for miRNA profiling.** A 1.5% agarose gel visualised with 6 µL/100 mL EtBr, was used to separate (electrophoresed for 35 minutes at 100 volts/cm) 10 µL of RNA mixed with 5 µL of 5X RNA loading dye and heat denatured at 55°C for 5 minutes in a total volume of 15 µL. Lanes 1-3 represents the untreated (UT) cells; Lanes 4-6 represents the HIV-1 (HIV) treated cells and Lanes 7-9 represents the microvesicle treated (MV) control cells. Two bands were identified for ribosomal RNA, 28S and 18S whilst genomic DNA contamination was also present at the top of the gel image (gDNA).

Following gel electrophoresis, the RNA was quantified (Table 3.4) spectrophotometrically using the NanoDrop™. The concentrations varied from 91.47 to 211.23 ng/µL. The purity of the RNA as denoted by the 260/280 ratio was of high purity as it was close to 2.00. The secondary measurement, the 260/230 ratio which indicates the presence of contaminants was found to be within acceptable range (2.0-2.2) except for samples, UT3 and HIV3 which are flagged in the table (Table 3.4) (Thermo Fisher Scientific™, 2008).

Since we required RNA of good quality and to ensure the correct concentration for downsteam experiments, it was decided that a second and more sensitive method of quantification was necessary. This was done using the Qubit™ RNA assay as described in Section 2.2.3 of Chapter two. The assay revealed extremely low RNA levels which were less than the recommended amount required (per total volume allocated i.e., 120 ng/µL in a total volume of 15 µL) in order to perform the array. Therefore we attempted to concentrate the RNA by ethanol precipitation (Section 2.3). The Qubit™ RNA assay was then performed again and

showed a five-fold increase in RNA concentrations (Table 3.5). However, upon communication with technicians from Life Technologies™ we were subsequently advised that concentrating the RNA in this way may have favoured the precipitation of some miRNAs over others (size dependent). We then performed single-tube miScript SYBR green assays (Qiagen, Hilden, Germany) (Appendix A) to determine whether the experiment would be successful using the lower than recommended amount of RNA. We found the Ct values to be within acceptable range (20-25) and comparable to the result obtained when a higher concentration of RNA is used (Figure 3.3) and we therefore proceeded with the experiment using un-precipitated (non-concentrated) RNA. We used the Qubit™ readings to calculate the concentration of RNA required since this method is a more sensitive approach which can quantify RNA or DNA only in the sample whilst the Nanodrop™ quantifies all nucleic acids in the sample and cannot distinguish between the two acids (O'Neill *et al.,* 2011).

**Table 3.4: RNA quantification using the NanoDrop™ analysis**

| Sample[#] | Concentration (ng/ µL) | 260/280 ratio | 260/230 ratio |
|---|---|---|---|
| **UT1** | 211.23 | 1.98 | 2.20 |
| **UT2** | 91.47 | 1.97 | 2.13 |
| **UT3** | 141.20 | 1.95 | 2.26* |
| **MV1** | 176.70 | 1.98 | 2.19 |
| **MV2** | 157.77 | 1.96 | 2.12 |
| **MV3** | 142.02 | 1.98 | 2.11 |
| **HIV1** | 199.14 | 1.96 | 2.15 |
| **HIV2** | 141.72 | 2.00 | 2.03 |
| **HIV3** | 194.76 | 1.97 | 2.26* |

HIV – HIV-1 Aldriothiol-2.2 treated cells; MV – microvesicle treated control; UT – untreated cells
*Out of acceptable range; [#]eluted in a volume of 15-18 µL

**Table 3.5: RNA quantification as analysed by Qubit™ RNA assay before and after ethanol precipitation**

| Sample | Concentration (ng/ µL) | |
|---|---|---|
| | **BEFORE** | **AFTER** |
| **UT1** | 34.50 | 142.00 |
| **UT2** | 32.00 | 124.00 |
| **UT3** | 37.50 | 148.00 |
| **MV1** | 42.50 | 126.00 |
| **MV2** | 27.00 | 122.00 |

| | | |
|---|---|---|
| **MV3** | 41.00 | 162.00 |
| **HIV1** | 31.50 | 122.00 |
| **HIV2** | 35.50 | 172.00 |
| **HIV3** | 34.00 | 163.00 |

HIV – HIV-1 Aldriothiol-2.2 treated cells; MV – microvesicle treated control; UT – untreated cells

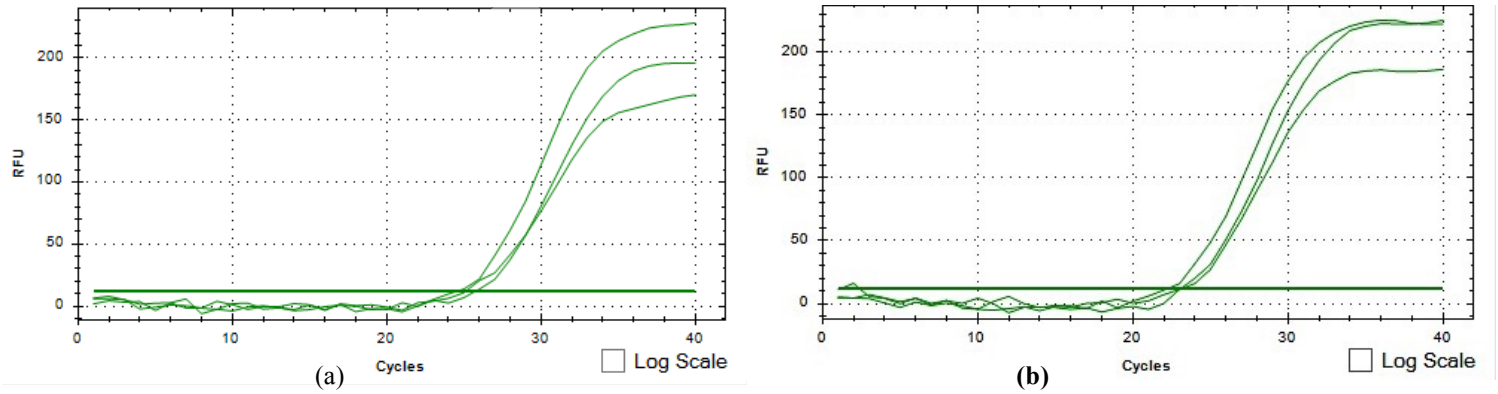


**Figure 3.3: Amplification plots (in log scale) of single tube qPCR using a low RNA sample compared to higher amount of RNA.** Single-tube SYBR Green PCR experiments were performed in triplicate using the lowest RNA sample from our studies and a higher concentration of RNA sample as a control for the RNU6B assay. (a) The cycle threshold value of the lowest RNA sample (91.47 ng/µL) was found at 25 whilst (b) at 23 for the control RNA sample (500 ng/µL).

### 3.2.4 Expression profiling reveals 16 upregulated & 16 downregulated miRNAs in Burkitt's lymphoma cells

Preliminary statistics and data analysis was conducted by the Centre for Proteomic & Genomic Research (CPGR) (Section 2.4.3). Their report revealed no significant differential expression of miRNAs for HIV-1 AT-2 treated samples when compared to microvesicle treated controls, but they recommended two miRNAs (miR-532 (p=0.0584; FC = 0.432) and miR-342-3p (p=0.0584; FC = 1.630) for further analysis (The complete report is included in Appendix C) (Heat map in Appendix B – Table B6). This finding was surprising, however upon interrogation of the methodology they used, it was revealed that a crucial limitation existed. The limitation resided in the software package they used, provided by Thermo Fisher Scientific™ (Massachusetts, USA) for the miRNA microarray, which did not allow for exclusion of failed replicates, or those which were obviously out of range and showed a large variation between samples (Figure 3.4).

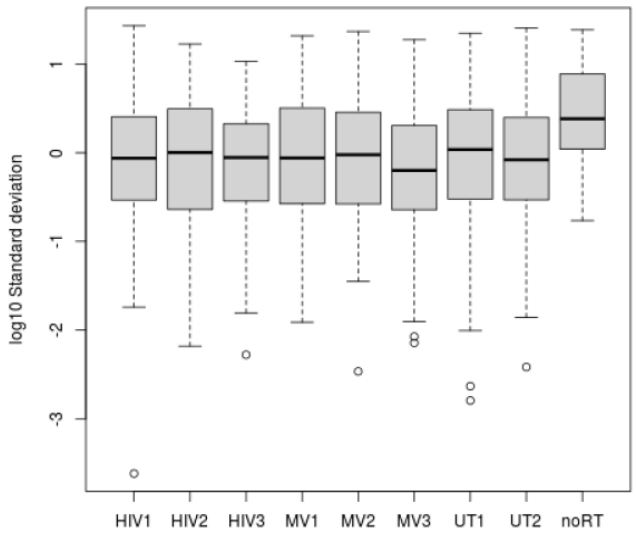


**Figure 3.4: Boxplot comparisons of standard deviation between raw replicated features within samples from the miRNA microarray experiment.** A number of feature replicates indicated large variation between replicates with more than 30% difference from their means. (Full report in Appendix C).

Therefore, an in depth manual analysis of each amplification plot for 192 miRNAs was performed, then the DataAssist™ software (version 3.01) (Applied Biosystems™, California, USA) was used so that we could exclude failed replicates (Section 2.4.3). After this more comprehensive and intensive analysis, the result revealed that 32 miRNAs were either upregulated or downregulated by two or more fold changes. This is summarised below (Table 3.6).

**Table 3.6: miRNAs differentially expressed in Ramos cells exposed to HIV-1 AT-2 compared to microvesicle treated controls**

| miRNAs | p.value | FC |
|---|---|---|
| **UPREGULATED** | | |
| miR-520d-3p | 0.030 | 13.268 |
| miR-342-5p | 0.223 | 9.523 |
| miR-513-3p | 0.074 | 7.907 |
| miR-222-3p | 0.042 | 6.735 |
| let-7a-2-3p | 0.180 | 5.546 |
| miR-575 | 0.211 | 4.519 |
| miR-520f-3p | 0.378 | 4.268 |
| miR-30b-5p | 0.420 | 3.566 |
| miR-363-3p | 0.248 | 3.496 |
| miR-100-5p | 0.328 | 3.308 |
| let7c-5p | 0.532 | 3.247 |
| miR-485-3p | 0.110 | 3.006 |
| miR-132-3p | 0.282 | 2.807 |
| miR-563 | 0.273 | 2.790 |
| miR-101-3p | 0.408 | 2.604 |
| miR-365-3p | 0.250 | 2.046 |
| **DOWN-REGULATED** | | |
| miR-27a-3p | 0.132 | 0.171 |

| | | |
|---|---|---|
| miR-200c-3p | 0.367 | 0.151 |
| miR-769-5p | 0.071 | 0.084 |
| miR-29c-3p | 0.567 | 0.144 |
| miR-628-5p | 0.210 | 0.224 |
| let-7b-5p | 0.151 | 0.297 |
| miR-199a-3p | 0.468 | 0.272 |
| miR-188-5p | 0.102 | 0.263 |
| miR-27b-3p | 0.487 | 0.204 |
| miR-30e-3p | 0.173 | 0.201 |
| let-7b-3p | 0.203 | 0.197 |
| miR-324-3p | 0.320 | 0.194 |
| let-7f-1-3p | 0.100 | 0.185 |
| miR-30e-5p | 0.119 | 0.171 |
| miR-9-3p | 0.378 | 0.030 |
| miR-9-5p | 0.315 | 0.020 |

FC – fold change; miRNAs – microRNA

### 3.3 DISCUSSION

We report the first study on the investigation of differentially expressed miRNAs in B-cells exposed to HIV. B-cells are the cell of origin of two highly aggressive cancers namely DLBCL and BL, which preferentially affect HIV positive people (Abayomi *et al.,* 2011). It has become clear that HIV does not merely promote cancer development through a compromised immune system, but more directly through the alteration of host cellular pathways (Seddiki *et al.,* 2013; Guha *et al.,* 2016). Thus far, this has been mostly demonstrated in HIV-associated Karposi Sarcoma (Zhou *et al.,* 2013b; Xue *et al.,* 2014; Yan *et al.,* 2014). In this study, B-cells were exposed to an attenuated form of HIV, and changes in miRNA expression was assessed.

Firstly, the viability of our cells under our treatment conditions were assessed. This is important because HIV has been shown to promote apoptosis (Moir & Fauci, 2009; Perise-Barrios *et al.,* 2012) and our aim was to use treatment conditions which are physiologically relevant, and able to affect cell functions, but at the same time not kill the cells. We found no significant changes in cell viability (Figure 3.1) when exposing cells to 500 ng/mL of HIV-1 AT-2 for 3 hours. Previously, Perise-Barrios *et al.,* (2012) exposed B-cells to 125 ng/mL of HIV-1 and significant changes in cell surface markers was only seen upon day four of treatment. In contrast, Nazli *et al.,* (2010), was able to show no viability change in primary genital epithelial and intestinal cells after 24 hours exposure to HIV-1 (49-773 ng/mL). It would seem that HIV exposure and viability depends on the tissue type however for our experiments, our conditions were adequate as they did not result in significant viability changes in the cells during treatment.

Microarray analysis (DNA, protein, antibody or for tissue application) is a powerful high throughput tool for standardised genome-wide assays since it can monitor the expression of thousands of targets in an organism at the same time (Ekins & Chu, 1999; Git *et al.,* 2010; Hernandez *et al.,* 2012). Though initially used for gene expression analysis it has become increasingly utilised for investigating complex molecular interactions involving miRNAs. Like any other platform in biomedical research, array profiling has its disadvantages which include acquiring and analysing data, sample preparation, hybridisation of the probes (basis for determining relative abundance of miRNAs) and equipment errors (Benes & Castoldi, 2010; reviewed by Wang & Xi, 2013). We opted to use a TLDA platform from Life Technologies™ for various reasons. Firstly, the system is well cited in the literature, and furthermore a colleague at Stellenbosch University (Lani Thiart, personal communication) had used the same platform and had associated technical expertise and attested to a satisfactory overall outcome for her experiment. She used a readily available miRNA array, as opposed to a custom array. Secondly, the equipment needed for the array (setting up of plate, qPCR machine and data analyses expertise) was available at CPGR, which provided the service at no cost as long as their platform was used. This array also allowed us to customise the miRNAs that we were interested in and previous literature reported no significant differences for intra-platform reproducibility when the TaqMan® Low Density Array was compared to Locked Nucleic Acid or beads array and was an effective solution for miRNA profiling (Wang *et al.,* 2011) whilst Baker, (2010) reported various platforms can provide different answers.

The challenges however with miRNA microarray analysis is that variability can occur in both biological and technical procedures which makes experimental design essential to minimise irregularities (Chuaqui *et al.,* 2002; Wang & Xi, 2013). We ensured that adequate time was spent on the design by consulting other array platforms since strengths of others should be referred to when performing these experiments (Mestdagh *et al.,* 2009). In addition, we had several positive controls and a negative control (Git *et al.,* 2010) since normalisation is an essential step in this process that helps reduce non-biological errors and converts the raw data into valid results (Wang & Xi, 2013). The use of different controls and their expression varies from tissue samples and it is challenging to find controls that are stable in different cell lines but they should have properties similar to miRNAs in size, biogenesis and stability (Wang *et al.,* 2010). We could not however validate these controls since we did not have spare array cards to do so but relied on literature to make our choice (Wang *et al.,* 2011).

Our microarray experiments were performed at the CPGR to ensure efficiency of sample preparation. Good quality RNA is required for efficient miRNA microarray analysis (Baker, 2010; Becker *et al.,* 2010) especially when it comes to the design of the Taqman® microarray cards (Figure 3.4). Though it eliminates the need to aliquot and track large numbers of assays, it has eight ports in which the recommended RNA concentration (350 ng/μL) must disperse evenly to 384 wells. Our RNA levels were below this range but previous literature reported using less than the recommended amount and the experiments were successful (Chen *et al.,* 2005) and our experiments using single-tube SYBR green PCR assays were also successful (Figure 3.3). In addition, the use of the stem-loop primers enables accurate detection of larger number of miRNAs with small amounts of RNA sample (Hurley *et al.,* 2011). Nevertheless an important step is validating this RNA yield with an initial array card which we unfortunately did not have. However, this was not a necessity and we proceeded with the experiment.

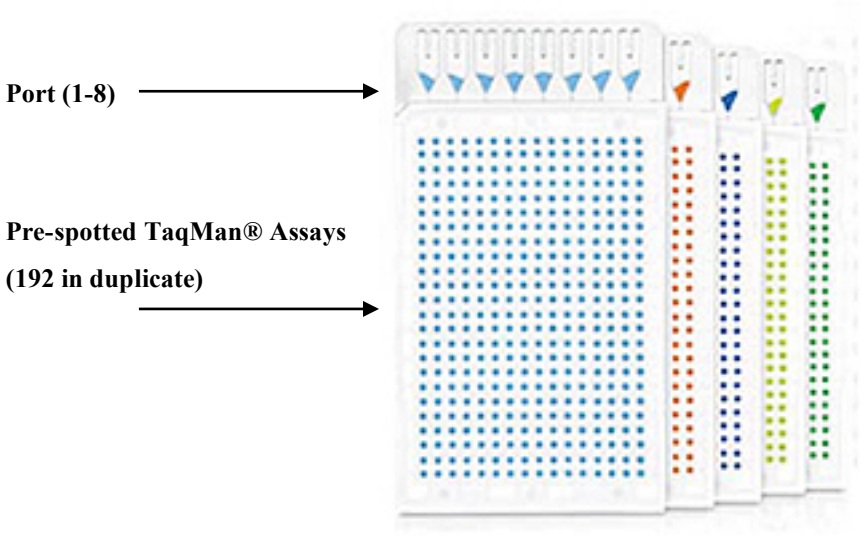


**Figure 3.5: Schematic of TaqMan® Array Card from Life Technologies™.** TaqMan® Array Card is a 384-well microfluidic card, designed for performing 384 simultaneous real-time PCR reactions without the need for expensive liquid-handling automation. TaqMan® Array Cards are preloaded with dried-down, high-quality TaqMan® Assays (TaqMan® probes and PCR primer sets), ready for 1 to 8 samples to be run in parallel against 12 to 384 TaqMan® Gene Assay targets. (Reproduced from https://www.thermofisher.com).

Analysis of microarray data is another challenge that arises after profiling and this is well documented in the literature (Reviewed by Pritchard *et al.,* 2012; reviewed by Chugh & Dittmer, 2012; reviewed by Wang & Xi, 2013; Backes *et al.,* 2016). Our data analysis revealed high Ct values with large variation (Pearson correlation clustering) between technical replicates with 18.75% flagged as unreliable data (Appendix C). Specific normalisation methods for miRNA profiling analysis are relatively few (Wang *et al.,* 2010) but proper normalisation methods can improve the sensitivity and specificity of determining differentially expressed

miRNAs (Wang *et al.,* 2011). For our data (treated samples (HIV-1 AT-2) were normalised with the matched microvesicle treated control samples) we used three different methods, geometric mean (Mestdagh *et al.,* 2009), delta Ct, and quantile methods (Bolstad *et al.,* 2003). Each method has its own advantages and disadvantages but it is better to use more than one method to observe how the data best fits a normalisation algorithm (Meyer *et al.,* 2010; Wang & Xi, 2013). In addition, these methods worked well for our larger Ct values with the geometric mean and delta Ct methods displaying the most similar patterns to the raw data for all Ct values. Though the quantile method is reported as one of the best performed normalisation methods for miRNA data (Hua *et al.,* 2008), the method showed large deviations suggesting a possible over-normalisation so we omitted this method when determining differential expression. However the geometric mean normalisation has some advantages over others particularly for miRNA studies (Dvinge & Bertone, 2009; Mestdagh *et al.,* 2009) which is the method we particularly focused on.

The focus for miRNA profiling data is on 'differentially expressed' miRNAs between two cell populations, but this term is not well-defined. The fold change (FC) is the main means for assessing a difference but it is also not clear on what the difference should be to regard treated samples as differentially expressed (FC = 1< upregulation; =1 no change; 1>downregulation). For gene expression analyses it is widely accepted that a difference can be regarded as significant when there is a FC of two or more (Rays *et al.,* 1996) however for miRNA studies this is not clear. When adhering strictly to the software analysis, we observed no significant differences in our samples. Wang & Xi, (2013) recommend both the FC and the basal level of the miRNA to be taken into consideration since a miRNA can be highly expressed with a practical meaning whilst another miRNA can be weakly expressed and lack a measurable biological phenotype (Chugh & Dittmer, 2012). The FC needs to be used cautiously and should be used only for miRNAs that are expressed in both samples. In practice, many laboratories do not repeat array experiments and lack replicates. After the preliminary analysis by CPGR, no miRNAs were found to be significantly differentially expressed due to the software limitation and being unable to eliminate replicates with large deviation amongst samples which may have introduced significant bias to the detection of differentially expressed miRNAs (Wang & Xi, 2013). Raw data was therefore comprehensively consulted by manual analysis before we made a final decision on the list of 32 (Table 3.6) since the importance of low abundance miRNAs may still serve as specific biomarkers and should not be omitted from determining differential expression (Chugh & Dittmer, 2012; Wang & Xi, 2013).

As noted above, proper normalisation methods (Hua *et al.,* 2008; reviewed by Meyer *et al.,* 2010) are crucial to determining differentially expressed miRNAs but validation is also a critical factor when it comes to profiling (Wang *et al.,* 2011). Validation by qPCR is favoured (Meyer *et al.,* 2010) and future work should validate the above results by efficient and accurate methods. Since miRNAs are often clustered in families (such as let-7; miR-17-92) that can differ by only one nucleotide; validation by qPCR allows one to quantify these precise changes (Roush & Slack, 2008).

# CHAPTER 4: MIRNA VALIDATION BY SINGLE-TUBE TAQMAN® QPCR ASSAYS

## 4.1 INTRODUCTION

Studying miRNAs *in situ* and validation are two important steps for miRNA investigation (Baker, 2010). The standard method for validation of results is by using an efficient method (such as qPCR) in order to either confirm or reject the result as observed from the microarray analysis (Wang & Xi, 2013). It is a more reliable and accurate method since it focuses on quantifying one miRNA per assay and can detect low amounts of miRNA (Chugh & Dittmer, 2012). The aim of this part of the study was to validate selected miRNAs identified in the microarray in Chapter three. Following a comprehensive analysis of the miRNA microarray results, 32 differentially expressed miRNAs were selected for further investigation. In this chapter, we describe the validation of four miRNAs namely miR-200c-3p, miR-363-3p, miR-222-3p and miR-575. The chapter starts with a summary of relevant literature on each of these miRNAs followed by the results of the validation using single-tube miRNA Taqman® qPCR assays. Thereafter the results are discussed.

## 4.2 RESULTS

### 4.2.1 Selection of miRNAs for validation

The four miRNAs that were selected for further analysis from the 32 were based on existing literature reporting their involvement in cancer, particularly in B-cell lymphomas (Figure 4.1). Furthermore, reports on any gene targets (whether identified or validated) was also searched for and were summarised in the table below (Table 4.1).

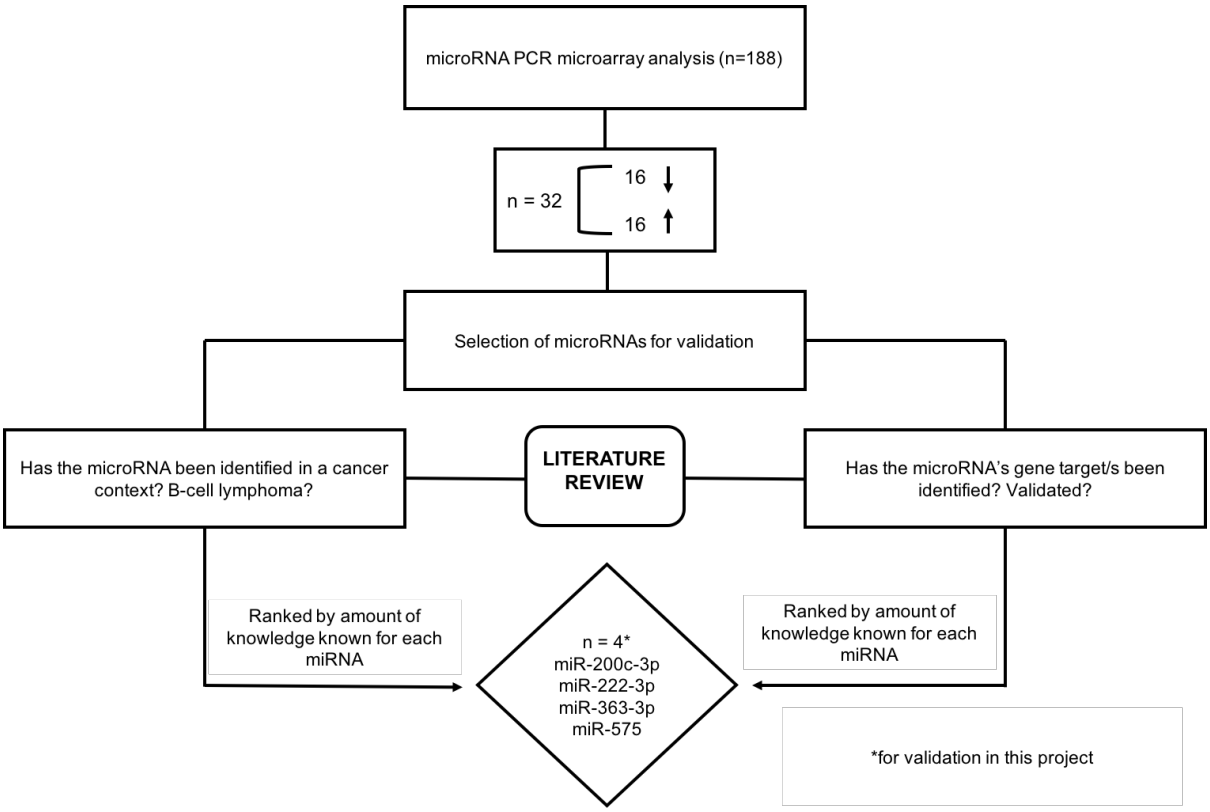


**Figure 4.1: Flow diagram illustrating the selection process of four miRNAs for validation in this part of the study.** microRNA – miRNA; Mature microRNA – miR; up arrow indicates upregulation and down arrow indicates downregulation

**Table 4.1: Literature on miRNAs selected for validation**

| miRNA | B-cell lymphoma | Other cancers | References |
|---|---|---|---|
| miR-200c-3p | Survival marker for DLBCL (downregulation results in more aggressive cancer through de-repression of *ZEB1*)<br><br>Downregulated in BL when compared to CLL (profiling data) | Tumour suppressor miR in breast, ovarian and endometrial cancers (*ZEB1/2* -promotes epithelial to mesenchymal transition) | Cochrane *et al.,* 2010<br>Ibrahim *et al.,* 2015<br><br>Lim *et al.,* 2015<br>Robertus *et al.,* 2010 |
| miR-222-3p | Upregulated in DLBCL ($p \leq 0.05$)<br><br>Long term prognostic value for DLBCL<br><br>Downregulated in BL compared to DLBCL (profiling data) | Tumour suppressor miR in breast cancer (*TRPS1* - promotes epithelial to mesenchymal transition), squamous cell carcinoma, thyroid papillary carcinomas<br><br>OncomiR in glioblastoma (*p27* - cell cycle inhibitor & tumour suppressor; *PUMA* - induces cell survival) | Le Sage *et al.,* 2007<br>Zhang *et al.,* 2010<br>Stinson *et al.,* 2011<br><br>Malumbres *et al.,* 2009<br>Lenze *et al.,* 2011 |

| | | | |
|---|---|---|---|
| miR-363-3p | Diagnostic marker for DLBCL (downregulated; $p \leq 0.05$)<br><br>Downregulated in BL compared to lymph nodes ($p \leq 0.05$) | Tumour suppressor miR in head and neck cancer (HNSCC) (*PDPN* (podoplannin) – contributes towards invasion and metastasis) and neuroblastoma<br><br>OncomiR in colorectal cancer *GATA6* (suppresses tumourigenecity) | Tsuji *et al.,* 2014<br>Qiao *et al.,* 2013<br>Sun *et al.,* 2013<br><br>Jorgensen *et al.,* 2014<br>Bueno *et al.,* 2011 |
| miR-575 | Upregulated in BL compared to lymph nodes ($p \leq 0.05$) | OncomiR in non small cell lung cancer (NSCLC) (*BLID* - promotes growth and invasion)<br><br>Downregulated in bladder cancer (profiling data)<br><br>Upregulated in gastric cancer ($p \leq 0.05$) | Wang *et al.,* 2015<br>Tatarano *et al.,* 2011<br><br>Bueno *et al.,* 2011<br><br>Yao *et al.,* 2009 |

BL – Burkitt's lymphoma; *BLID* – BH3-like motif containing cell death inducer; CLL – chronic lymphocytic leukaemia; DLBCL – Diffuse large B-cell lymphoma; *GATA6* - GATA Binding Protein 6; HNSCC – head and neck cancer; miR- microRNA; NSCLC – non small cell lung cancer; *PDPN* – podoplannin; *TRPS1* – Transcriptional Repressor GATA Binding 1

### 4.2.2 RNA for miRNA validation was of good quality

Cells were plated and treated as before with attenuated HIV and microvesicle treated controls (Section 2.1.4). This time, in addition to the Ramos cells, the B-lymphoblastoid cell line L1439A, derived from a healthy individual, was also treated. Following RNA extraction, the samples were separated on an agarose gel to analyse integrity (Figure 4.1 and Figure 4.2). The RNA was found to be of good quality indicated by the clear intact rRNA bands, 18S and 28S. Furthermore, contrary to previous extraction, there was no evidence of genomic DNA contamination. This is because the kit used for extraction (Roche Applied Science, Germany) has a gDNA elimination step (Section 2.2.2).

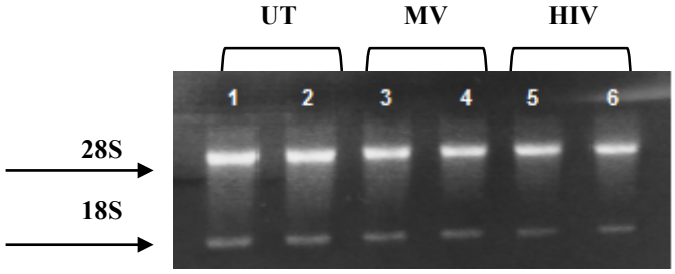


**Figure 4.2: RNA integrity gel of L1439A cells for miRNA validation.** A 1% agarose gel visualised with 6 µL/100 mL EtBr, was electrophoresed for 45 minutes at 100 volts/cm and used to analyse the integrity of 10 µL of extracted

RNA combined with 5 µL of 5X RNA loading dye heat denatured at 55°C for 5 minutes in a total volume of 15 µL. Lanes 1-2 represents the untreated (UT) cells; Lanes 3-4 represents microvesicle treated (MV) control cells and Lanes 5-6 represents the the HIV-1 (HIV) treated cells. Two bands were identified for ribosomal RNA, 28S and 18S.

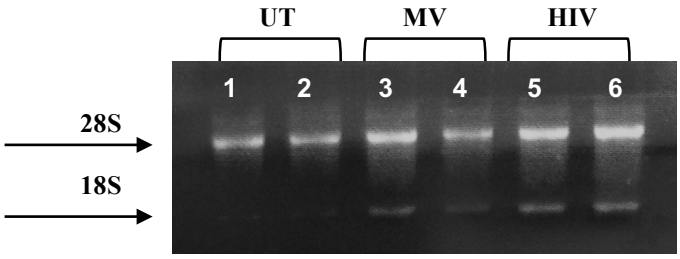


**Figure 4.3: RNA integrity gel of Ramos cells for miRNA validation.** A 1% agarose gel visualised with 6 µL/100 mL EtBr, was electrophoresed for 45 minutes at 100 volts/cm and used to analyse the integrity of 10 µL of RNA and 5 µL of 5X RNA loading dye heat denatured at 55°C for 5 minutes in a total volume of 15 µL. Lanes 1-2 represents the untreated (UT) cells; Lanes 3-4 represents microvesicle treated (MV) control cells and Lanes 5-6 represents the the HIV-1 (HIV) treated cells. Two bands were identified for ribosomal RNA, 28S and 18S.

Quantification by spectrophotometry using the NanoDrop™ and Qubit™ assay revealed much higher RNA yields than obtained previously using the *mir*Vana kit (Table 4.2 and 4.3) for both cell lines. The 260/280 ratio revealed that the RNA contained a small amount of contaminants (>2,0) whilst the 260/230 ratios further confirmed this as the levels were slightly below normal range (0.90-1.97) (Thermo Fisher Scientific™, 2008). Since there is no consensus on the lower range of the latter ratio, we continued with downstream validation (Von Ahlfen & Schlumpberger, 2010).

**Table 4.2: RNA quantification by NanoDrop™ analysis & Qubit™ assay for L1439A**

| Sample* | NanoDrop™ | | | Qubit™ |
|---|---|---|---|---|
| | Concentration (ng/ µL) | 260/280 ratio | 260/230 ratio | Concentration (ng/ µL) |
| **UT1** | 253.29 | 2.05 | 1.75 | 712.00 |
| **UT2** | 371.71 | 2.06 | 1.96 | 716.00 |
| **MV1** | 377.64 | 2.05 | 1.48 | 724.00 |
| **MV2** | 251.16 | 2.10 | 1.85 | 648.00 |
| **HIV1** | 463.45 | 2.04 | 1.74 | 682.00 |
| **HIV2** | 317.21 | 2.07 | 1.45 | 480.00 |

HIV – HIV-1 Aldriothiol-2.2 treated cells; MV – microvesicle treated control; UT – untreated cells
*eluted in volume of 100 µL

**Table 4.3: RNA quantification by NanoDrop™ analysis & Qubit™ assay for Ramos cells**

| Sample* | NanoDrop™ | | | Qubit™ |
|---|---|---|---|---|
| | Concentration (ng/µL) | 260/280 ratio | 260/230 ratio | Concentration (ng/µL) |
| **UT1** | 235.50 | 2.06 | 0.90 | 504.00 |
| **UT2** | 211.26 | 2.10 | 1.71 | 400.00 |
| **MV1** | 244.54 | 2.08 | 1.80 | 732.00 |
| **MV2** | 285.66 | 2.10 | 1.77 | 608.00 |
| **HIV1** | 206.10 | 2.12 | 1.97 | 656.00 |
| **HIV2** | 269.40 | 2.11 | 1.84 | 610.00 |

HIV – HIV-1 Aldriothiol-2.2 treated cells; MV – microvesicle treated control; UT – untreated cells

* eluted in a volume of 100 µL

### 4.2.3 miRNA-575 is significantly downregulated in Ramos cells

To ensure that the results obtained are true for qPCR, two endogenous controls were used namely the small nucleolar RNAs, RNU48 and RNU6B (Section 2.5). It was found that RNU48 produced the most consistent result amongst replicates and across experiments and was therefore used to report on expression of the miRNAs of interest (Data for RNU6B presented in Appendix B – Table B3). The expression of miR-575 was found to be significantly downregulated (p=0.001) in the Ramos cells when treated with HIV-1 AT-2, relative to microvesicle treated control cells (Figure 4.3). A significant fold change was observed with the highest found at 0.781 and the lowest at 0.509.

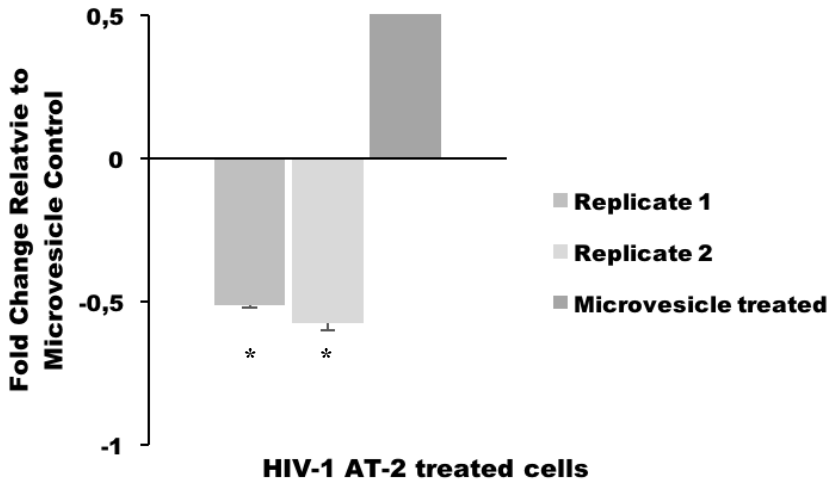


**Figure 4.4: miR-575 is downregulated after HIV-1 AT-2 treatment in Ramos cells relative to microvesicle treated control cells.** Downregulated expression of miR-575 expressed as the average fold change in HIV-treated cells relative to microvesicle-treated control cells, which has been normalised to one. The small RNA molecule RNU48 was used as the endogenous control. Two independent experiments were performed with each sampe performed in

triplicate. Error bars represent the standard deviation. A consistent and significant downregulated expression was observed ranging from 0.509-0.781. $p \leq 0.05$* when compared to microvesicle treated control cells (Prism 7, Graphpad, USA).

The results for miR-363-3p, miR-200c-3p and miR-222-3p were inconsistent (Data presented in Appendix B – Table B4), and were not repeated. Since at this stage the validation and characterisation of those miRNAs in the Ramos cells became part of a separate project, the role of the miRNAs in the normal lymphoblastoid cell line, L1439A became the focus in this study.

### 4.2.4 miRNA-575 is significantly upregulated in normal B-cells L1439A whilst miR-363-3p, miR-200c-3p and miR-222-3p are significantly downregulated

Validation for miR-575 showed a consistent and significant upregulation (p=0.003) in the normal B-cells when treated with HIV-1 AT-2, relative to microvesicle treated control cells (Figure 4.4). A significant fold change was observed with the highest found at 3.31 and the lowest at 1.54.

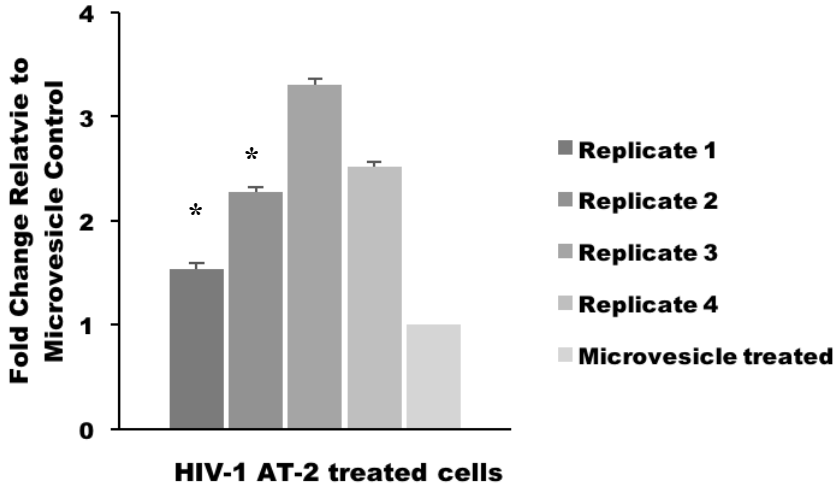


**Figure 4.5: miR-575 is consistently upregulated after HIV-1 AT-2 treatment in normal B-cells relative to microvesicle treated control cells.** Upregulation of miR-575 expressed as fold changes in two independent experiments in HIV-treated cells relative to microvesicle treated control cells, which has been normalised to one. The small RNA molecule RNU48 was used as the endogenous control. Two independent experiments was performed with samples performed in triplicate. Error bars represent the standard deviation. An upregulated fold change was observed ranging from 1.54-3.31. $p \leq 0.05$* when compared to microvesicle treated control cells (Prism 7, Graphpad, USA).

The expression of miR-363-3p, miR-200c-3p and miR-222-3p were all found to be significantly downregulated (p=0.003; p=0.001; p=0.027 respectively) in normal B-cells when treated with HIV-1 AT-2 relative to microvesicle treated cells (Figure 4.5a) (Data for RNU6B presented in Appendix B – Table B5). The highest downregulated average fold change for

miR-363-3p was 0,837 and the lowest fold change was for miR-222-3p (0.551) whilst the average fold change for miR-575 was 2.410 (Figure 4.5b).

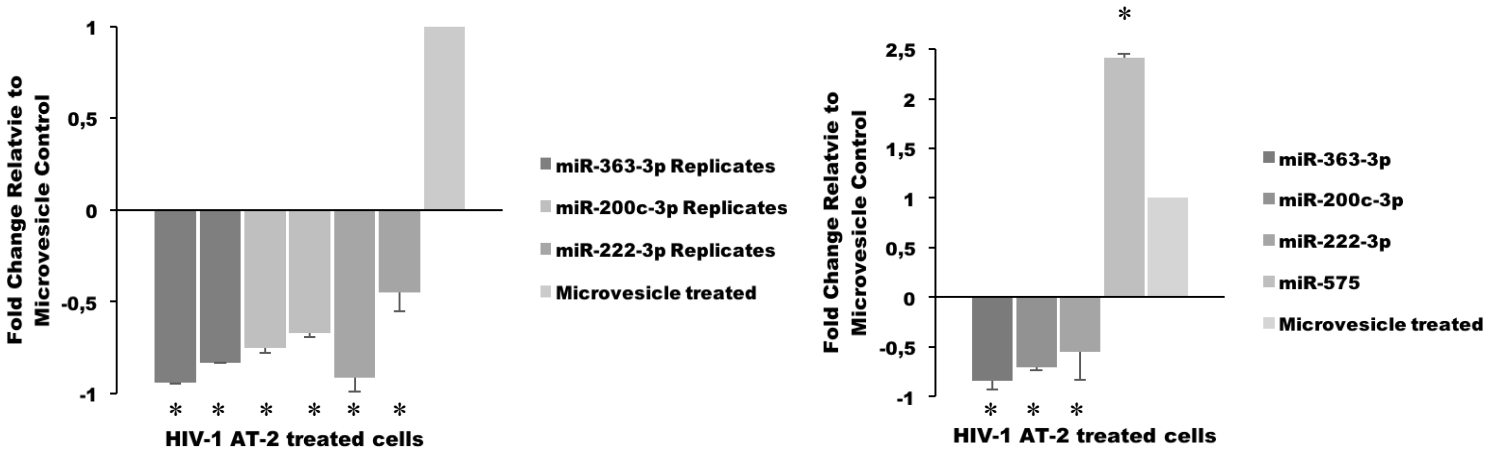


**(a)** **(b)**

**Figure 4.6: Downregulation of miR-363-3p, miR-222-3p and miR-200c-3p after HIV-1 AT-2 treatment in the normal B-cell line L1439A relative to microvesicle treated control cells (a) Average fold change of all miRNAs chosen for validation (b).** (a) miR-363-3p, miR-200c-3p and miR-222-3p are significantly downregulated. Fold changes displayed in HIV-treated cells relative to microvesicle treated cells, which has been normalised to one. The small nucleolar RNA molecule RNU48 was used as the endogenous control. Two independent experiments were performed with each sample performed in triplicate. A significant downregulation was observed for miR-363-3p ranging from 0.830- 0.939; miR-200c-3p ranging from 0.669-0.754 and for miR-222-3p ranging from 0.448-0.912. (b) Average fold change displayed in HIV treated cells relative to microvesicle treated cells for miR-363-3p, miR-200c-3p, miR-222-3p and miR-575. The average downregulated fold changes for miR-363-3p, miR-200c-3p and miR-222-3p was 0.837; 0.707 and 0.551 respectively. Error bars represent the standard deviation. $p \leq 0.05$* when compared to microvesicle treated control cells (Prism 7, Graphpad, USA).

### 4.2.5 Comparison of array results with validation studies

The findings from the validation experiments were compared with results from the miRNA array. We found consistent results with two of the miRNAs namely miR-200c-3p (downregulated) and miR-575 (upregulated) when compared with the array data whilst the opposite trend was found for the rest of the miRNAs (Table 4.4).

**Table 4.4: Differential expression of miRNAs: comparison between the miRNA array and miRNA validation assays**

| miRNA | Array FC | Assay (L1439A) FC |
|---|---|---|
| miR-363-3p | 3.496 | 0.837* |
| miR-200c-3p | 0.151* | 0.707* |
| miR-222-3p | 6.735 | 0.551* |
| miR-575 | 4.519 | 2.410 |

FC – fold change; miR – microRNA; *downregulation

## 4.3 DISCUSSION

As mentioned in the previous chapter, validation is a critical component of microarray profiling (Wang *et al.,* 2010) since profiling is limited in terms of sensitivity and specificity and is used as a screening tool (Krichevsky, *et al.,* 2003). Currently, no standard definition of validation exists however it can be described as either confirming or rejecting a result so that the result can be considered genuine or not (Chen *et al.,* 2005; Morey *et al.,* 2006). As such we chose four miRNAs to validate in this study by single-tube TaqMan® qPCR assays which is a sensitive and accurate technique to validate profiling data (Meyer *et al.,* 2010). This is necessary in order to attach biological plausibility and significance to a profiling result presented in the previous chapter (Chugh & Dittmer, 2012).

Traditionally, northern blot analysis was used for validation of miRNAs but given their small nature, they escape by this method (Lagos-Quintana *et al.,* 2001) and so the gold standard currently in use for gene expression is real time qPCR but a novel scheme was thereafter developed that accurately detects miRNAs. This system, the TaqMan® PCR assay contains stem loop primers which is widely accepted to specifically quantify miRNA expression levels with superior performance over existing conventional detection methods (Hurley *et al.,* 2011). In addition, these assays are much more efficient at detecting a one nucleotide difference between family members of miRNAs (Chen *et al.,* 2005). It also has a dynamic range and can detect as low as seven copies in the PCR reaction. It was also found that this novel assay has a high precision and specificity to mature miRNAs with the stem-loop primers being as much as 100 times more efficient than conventional primers (Chen *et al.,* 2005). We therefore chose this platform in which to validate our microarray data for the four chosen miRNAs. Choosing miRNAs for validation are primarily based on the FC however we based our selection on the context of our investigation namely, potential involvement in B-cell lymphomas but also cancers (Table 4.1).

High quality RNA is essential for single-tube TaqMan® assays and though a small amount of genomic DNA maybe present in the sample (this is dependent on the kit used) it has been found that it does not readily affect the reaction suggesting that the assays are highly specific for RNA targets (Chen *et al.,* 2005). In our study, we used two kits for total RNA isolation,

the *mir*Vana™ miRNA Isolation kit (Thermo Fisher Scientific™, Massachusetts, USA), which lacks a gDNA elimination step (Section 2.2.1), and revealed the presence of gDNA in the sample (Figure 3.2); as well as the Roche kit (Roche Applied Science, Penzberg, Germany) that contains a gDNA removal step (Section 2.2.2) which resulted in the absence of gDNA (Figure 4.1 and 4.2). The *mir*Vana™ miRNA Isolation kit (Thermo Fisher Scientific™, Massachusetts, USA) was used when extracting RNA for use in the miRNA microarray, as it is the recommended kit for that purpose. For single-tube validation, we shifted to the use of the Roche kit since the isolated RNA was to be used for investigating both changes in miRNA expression, as well as miRNA gene target expression. For the latter purpose, it was important that genomic DNA is not present in the sample.

We could not draw conclusions on the differential expression of miR-363-3p, miR-200c-3p and miR-222-3p in the Ramos cell line (Appendix B – Table B3). Reasons for this include large variation between technical replicates as well as high Ct values (>35). These particular experiments were subsequently repeated by another Masters student in the laboratory and will therefore not be reported here. Instead, the focus is on validation in the B-lymphoblastoid cell line L1439A, which was derived from a healthy individual. It is important to make a distinction between the two, as previous work in the laboratory has shown that a normal B-cell line, and a Burkitt's lymphoma cell line respond differently to exposure to HIV particles (Mdletshe, 2015). This wil be discussed in more detail in the sections below. However, before shifting our focus entirely to responses in L1439A, it is worth reporting that the single-tube assays revealed that miR-575 is downregulated in Ramos cells (Figure 4.3) which is contrary to the result obtained in the microarray (Table 4.4). Since validation experiments hold more credibility, this result is taken as being more reliable than the microarray result for miR-575. Yet again, this highlights the importance of validation of microarray data (Allison *et al.,* 2006). Often in microarrays, the cost involved limits the number of times the experiment can be performed, and therefore relies on validation studies for confirmation (Kerr, 2003).

As mentioned above, previous work in the laboratory has revealed that 'normal' B-cells respond differently to the same treatment conditions compared to cancer cells, such as the Burkitt's lymphoma cell line Ramos (Mdletshe, 2015). In the latter study, opposite effects were found on changes in the expression of two genes involved in BL development, when cells were exposed to HIV. This is the same as what has been found in the current study with regards to the expression of miR-575. This is likely due to the fact that there is a difference in

genomic integrity and signalling pathways in the two cell lines. Cancer cells tend to have more compromised stress response pathways than normal cells (reviewed by Hanahan & Weinberg, 2011), and are more able to mitigate the negative effects of stress agents, such as exposure to HIV, by bypassing cell death mechanisms. It is therefore important to investigate both scenarios i.e., effect on 'normal' and cancer cells. This is because, *in vivo,* the former represents an HIV infected individual who has not yet developed NHL, and the latter represents an HIV infected individual who has developed NHL and continues to harbour the virus.

The role of miR-222-3p has been studied as a survival marker of prognostic value for DLBCL with high tissue expression associated with progression free survival (Malumbres *et al.,* 2009; Montes-Moreno *et al.,* 2011; Alencar *et al.,* 2011) however this could not be significantly distinguished between patient cohorts in a later study by Shepshelovitch *et al.,* (2015). In addition, the evidence from these studies above have been from profiling array data and while Lenze *et al.,* (2011) attempted validation of this downregulated miRNA from their BL/DLBCL array data, the sample demonstrated reproducible signals in the NTC and was therefore omitted. In our study, we found the expression of miR-222-3p to be significantly downregulated when normal B-cells were treated with HIV-1 relative to microvesicle treated cells (Figure 4.5a). The literature indicates that mRNA targets for this miRNA include *Era, MYC, CDKN1B/p27, c-KIT, p57, PUMA* and *TRPS1* (Poliseno *et al.,* 2006; Visione *et al.,* 2007; Le Sage *et al.,* 2007; Zhao *et al.,* 2008; Sun *et al.,* 2008; Miller *et al.,* 2008; Felicetti *et al.,* 2008; Medina *et al.,* 2008; Zhang *et al.,* 2010; Stinson *et al.,* 2011) (Table 4.1). Research characterising the precise role of miR-222-3p in cancer is still emerging.

The expression of miR-200c-3p was also found to be downregulated in L1439A cells, when exposed to attenuated HIV-1 (Figure 4.5a). This not only confirmed what was observed in our microarray (using Ramos cells) (Table 4.4), but other studies that profiled miRNAs for DLBCL and BL also support this finding (Lim *et al.,* 2015). Furthermore, miR-200c-3p levels in BL tissues were found to be downregulated when compared to chronic lymphocytic leukaemia (CLL) and mantle cell lymphoma (MCL) tissues (Robertus *et al.,* 2010). However, the prognostic value in DLBCL is unclear (Malumbres *et al.,* 2009) since Berglund *et al.,* (2013) found the miRNA expression to be upregulated with an association with poor overall survival but Yamagishi *et al.,* (2015) found the opposite conclusion associated with overall survival. In serous ovarian cancer however, profiling data revealed that the expression was

upregulated (Ibrahim *et al.,* 2015). There is strong evidence supporting the fact that the two transcription factors *ZEB1/ZEB2* are targets of miR-200c-3p. These ZEB proteins are involved in epithelial to mesenchymal transition in breast, ovarian and endometrial cancers (Cochrane *et al.,* 2010; Hill *et al.,* 2013) as well as *ZEB1* characterised for gastric DLBCL (Huang *et al.,* 2014). Furthermore, using miRNA-seq to profile DLBCL patient samples, a significant decreased expression was observed when compared to other cancers (Lim *et al.,* 2015) resulting in a more aggressive DLBCL through the de-repression of *ZEB1* (Huang *et al.,* 2014). Other targets have been validated for other cancers such as *E-cadherin* (Hurteau *et al.,* 2007) and *TGFβ2* (Bai *et al.,* 2014).

The expression of miR-363-3p on the other hand is one that has been quite controversial in our laboratory since several independent experiments have yielded inconclusive results suggesting that the basal levels may be too low to be detected. Validation in the normal B-cell line however revealed a downregulation (Figure 4.5a) which is consistent with the findings by Bueno and colleagues (2011). In a study investigating the expression of miRNAs, miR-363-3p was found to be significantly downregulated in BL when compared to lymph nodes (Bueno *et al.,* 2011) and when compared to MCL (Robertus *et al.,* 2010). In DLBCL, its downregulation ($p \leq 0.05$) has been reported as a diagnostic marker predicting B-cell lymphoma up to 12 months before diagnosis (Jorgensen *et al.,* 2014). Therefore the experiment should be repeated in other BL cell lines as well as in the context of DLBCL to elucidate its expression.

As stated earlier, the expression of miR-575 was found to be downregulated in Ramos cells; whilst we found that in the normal B-cell, miR-575 was found to be significantly upregulated (Figure 4.4). The result obtained in the normal B-cell line is consistent to what was observed in our PCR array, although the cell line is different (Table 4.4). It has been found by microarray analysis to be significantly upregulated in BL by Bueno *et al.,* (2011) and our finding is also supported by other studies focusing on other cancers such as gastric cancer ($p \leq 0.05$) (Yao *et al.,* 2009), breast cancer (Fisher *et al.,* 2015), oesophageal adenocarcinoma (Drahos *et al.,* 2015) and recurrent serous ovarian carcinoma ($p \leq 0.05$) (Nam *et al.,* 2016). The finding is however in contrast to other cancers such as leukaemia, (downregulation) (Pizzimenti *et al.,* 2009) and lymphoblastic cancer (downregulation) (Lee *et al.,* 2012) whilst it has also been identified as a biomarker for the prediction of colorectal cancer responses to chemotherapy (Zhu *et al.,* 2017). The miR has however been comprehensively studied in bladder cancer.

Using cell lines and tissues samples, miR-575 was reported as downregulated and validated upon using TaqMan® assays as well as conducting gain of function studies. It was interesting to note that they determined differential expression by a FC of >0.01 and their results ranged consistently between 0.01-0.09 for miR-575 expression (Tatarano *et al.,* 2011). Recently Wang *et al.,* (2015) investigated the role of miR-575 and found that it promotes growth and invasion of non small cell lung cancer by functioning as an oncogene by directly targeting BH3-like motif containing inducer of cell death (*BLID*). A significant inverse correlation was found between miR-575 (upregulation) and *BLID* mRNA (downregulation) and lower levels of protein was found by western blotting. In the next chapter, experiments are performed in order to further validate the role of miR-575 in our context.

# CHAPTER 5: THE CHARACTERISATION OF MIR-575 IN THE PATHOGENESIS OF HIV-ASSOCIATED NHL

## 5.1 INTRODUCTION

In this chapter, we report on further characterisation of miR-575, which was found to be significantly upregulated during the validation studies (Figure 4.4). A literature search revealed that, although miR-575 has been found to be deregulated in cancer, its role is not well described. Therefore the aim of this part of the study was to conduct functional analyses to characterise the role of miR-575 in the pathogenesis of HIV-associated NHLs. We first used bioinformatic tools to predict its mRNA gene targets of which the BH3-like motif containing inducer of cell death (*BLID*) was chosen for expression analysis at the mRNA level (by qPCR) and at the protein level (by western blotting). These results are presented below followed by a discussion.

### 5.1.1 The role of the BH3-like motif containing inducer of cell death (*BLID*)

A tumour suppressor function for *BLID* also known as breast cancer cell type 2 (*BRCC2*) has been proposed by a Yu & Li (2015) for breast cancer but it is unclear for other cancers. Previous literature does however elude *BLID*, a member of the Bcl-2 family of cell death controllers to a possible interaction or function in B-cell NHLs. *BLID* can control gene transcription in cancer and overexpression has been shown to significantly inhibit the phosphorylation of the AKT pathway (Li *et al.,* 2013), and shown to induce apoptosis by correlation with the activation of caspase-3 and caspase-9 (Broustas *et al.,* 2004) both of which play an important role in the proliferation, migration and invasion of cancer. In addition, Broustas *et al.,* (2010) identified BLID as a new binding partner of BCL-$X_L$ and showed that *BLID*-induced apoptosis was associated with the activation of BAX and an increase in cytosolic cytochrome c. Furthermore, MMP-2 and MMP-9 that degrade type I and IV collagen and breakdown of the extracellular matrix contributing to cancer metastasis, was found to be significantly decreased when *BLID* was overexpressed (Li *et al.,* 2013). Despite the above evidence, the mechanism by which *BLID* is deregulated remains unknown and this is also currently largely unknown for its role in HIV-associated NHLs. However, unlike other tumour suppressor genes of its family, it is unique in that it is emerging as a prognostic and therapeutic target especially for breast cancer (Cavalli *et al.,* 2011; Li *et al.,* 2014).

## 5.2 RESULTS

### 5.2.1 An assessment of the role of miR-575 in cancer

The table below is a summary of the current published literature (as of March 2017) on the involvement of miR-575 in cancer.

**Table 5.1: Summary of existing literature on the role of miR-575**

| Findings | Reference |
|---|---|
| Significantly upregulated in gastric cancer ($p \leq 0.05$)<br>No mRNA target identified | Yao *et al.,* (2009) |
| Upregulated in B-cell lymphoma<br>No mRNA target validated | Bueno *et al.,* (2011) |
| Upregulation promotes increased cell proliferation, migration and invasion in non-small cellular lung cancer cells.<br>*BLID* identified and verified as a direct mRNA target | Wang *et al.,* (2015) |
| Upregulation in breast cancer<br>PLCXD1 identified as novel target | Fisher *et al.,* (2015) |
| Upregulated in oesophageal adenocarcinoma<br>No mRNA target identified | Drahos *et al.,* (2015) |
| Significantly upregulated in recurrent ovarian carcinoma ($p \leq 0.05$)<br>No mRNA target identified | Nam *et al.,* (2016) |
| Upregulated by administration of the human cathelicidin AMP, LL-37, and its analogue peptide, FF/CAP18, in the colon cancer cell line HCT116<br>No mRNA target identified | Kuroda *et al.,* (2017) |
| Upregulated in HT-29 cells as candidate biomarker for colorectal cancer response to chemoradiotherapy<br>No mRNA target identified | Zhu *et al.,* (2017) |

*BLID* – BH3-like motif containing inducer of cell death; miRNA – microRNA; mRNA – messenger RNA; *PLCXD1* - Phosphatidylinositol Specific Phospholipase C X Domain Containing 1

Using recommended miRNA prediction tools (Witkos *et al.,* 2011; Thomson *et al.,* 2011; Ekimler & Sahin, 2014), hundreds of putative mRNA targets for miR-575 were identified with each respective programme. Recommendations from the literature suggests the use of three or more prediction programmes and that at least two methods must predict the same miRNA binding site before additional validation experiments can be conducted (Witkos *et al.,* 2011; Ekimler & Sahin, 2014). To narrow down the search we combined the output of all the

programmes and selected the overlapped mRNA targets (Barbato *et al.,* 2009; Thomson *et al.,* 2011) since they are largely build upon the same assumptions (Table 5.2). Due to the nature of these programmes providing possible interactions against a scoring method, we also searched the literature for reported and/or validated mRNA targets for miR-575. The only report of a validated target for miR-575 is by Wang and colleagues (2015), who showed, using luciferase reporter assays, that miR-575 directly targets sites in the 3'-UTR of the *BLID* gene (Wang *et al.,* 2015). This was shown in the context of non small cell lung cancer where miR-575 was found to be upregulated, as we have shown in our studies.

**Table 5.2: Predicted mRNA targets for miR-575**

| Online software | Predicted targets | Function | Cancer |
|---|---|---|---|
| miRanda | *CDK1*<br><br>*DENND5A* | Cell cycle regulator<br><br>GTPase signalling pathway | NSCLC (Chang *et al.,* 2015),<br><br>Epithelial ovarian cancer (Xi *et al.,* 2015) |
| DIANA microT | *DENND5A* | GTPase signalling pathway | X |
| miRTarBase | *ATAD5* | ATPase | Predisposition to cancer (Bell *et al.,* 2011) |
| picTar | Only has known miR families (miR-575 not well studied) | X | X |
| TargetScan | *CSTA*<br><br>*DENND5A* | Cysteine protease inhibitors<br><br>GTPase signalling pathway | Lung cancer (Butler *et al.,* 2011) |

*ATAD5* – ATPase Family, AAA domain containing 5; *CDK1* – cyclin-dependent kinase 1; *CSTA* – cystatin-A *DENND5A* – DENN domain containing 5Al; NSCLC – non small cellular lung cancer; X – no result

As mentioned earlier in Chapter one, classification of miRNA target sites are based on the complementarity within the seed region and 3' UTR of the miRNA. There are different types of sites that can be distinguished and the majority of known targets have complete pairing in the canonical sites. There are three types of canonical sites of which *BLID* forms an 8mer site with miR-575 (Table 5.3) and is also evolutionary conserved with the chimp species (http://www.targetscan.org/cgi-bin/targetscan/vert_71/view_gene.cgi?rs=ENST00000560104.1&taxid=9606&members=miR-575/4676-

5p&showcnc=1&shownc=1&shownc_nc=1&showncf1=1&showncf2=1&subset=1) (Appendix B – Figure B8). Although poorly conserved, it warranted experimental validation of its interaction.

**Table 5.3: *BLID* and miR-575 interaction as predicted by the TargetScan software database**

| mRNA: miRNA | Predicted consequential pairing of target region (top) and miRNA (bottom) | Site type |
|---|---|---|
| Position 196-203 of *BLID* 3' UTR<br>hsa-miR-575 | 5' ...UUUUAAAAAGGAUAAACUGGCUA...<br>3' CGAGGACAGGUUGACCGAG | 8mer |

*BLID* – BH3-like motif containing inducer of cell death; mRNA – messenger RNA; miRNA – microRNA

### 5.2.2 RNA for mRNA target analysis was of good quality

The normal B-lymphoblastoid (L1439A) cells were treated as before (Section 2.1.4) and total RNA was extracted (Section 2.2.2), quantified (Section 2.2.3), separated on an agarose gel (Section 2.2.4) and assessed for integrity (Figure 5.1). The RNA was found to have reasonable purity (Table 5.4) and acceptable integrity as indicated by the intact rRNA bands, 18S and 28S shown in Figure 5.1.

**Table 5.4: RNA quantification by NanoDrop™ analysis for Ramos and L1439A cells**

| Sample* | L1439A | | |
|---|---|---|---|
| | Concentration (ng/µL) | 260/280 ratio | 260/230 ratio |
| **MV1** | 245.36 | 2.05 | 1.17 |
| **MV2** | 208.69 | 1.97 | 1.17 |
| **HIV1** | 228.77 | 2.05 | 1.42 |
| **HIV2** | 191.18 | 2.03 | 1.58 |

HIV – HIV-1 Aldriothiol-2,2 treated cells; MV – microvesicle treated control
* eluted in a volume of 100 µL

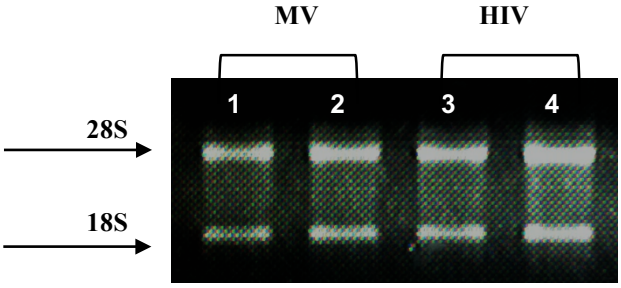

**Figure 5.1: RNA integrity gel of L1439A cells for mRNA gene target analysis.** A 1% agarose gel visualised with 6 µL/100 mL EtBr, was electrophoresed for 45 minutes at 100 volts/cm and used to analyse the integrity of 10 µL of RNA and 5 µL of 5X RNA loading dye of heat denatured at 55°C for 5 minutes in a total volume of 15 µL. Lanes 1-2 represents microvesicle treated (MV) control cells and Lanes 3-4 represented the HIV-1 AT-2 treated cells. Two bands were identified for ribosomal RNA, 28S and 18S.

### 5.2.3 Primer design and validation

Despite validated primers for *BLID* found in the literature (Wang *et al.,* 2015), upon analysis using BLAST *(http://blast.ncbi.nlm.nih.gov/Blast.cgi),* we found that the primers had more than 75% amplification affinity to non-specific genes. We therefore designed our own primers using parameters as described in Section 2.8.1. As housekeeping genes, the validated *GAPDH* primer pair was used (Mowla *et al.,* 2011), as well as the *RPL27* primer pair (de Lima Reboucas *et al.,* 2013) of which primer pairs were not designed for.

#### *5.2.3.1 Genomic DNA contamination affects downstream qPCR*

To verify the specificity of all primer pairs including the housekeeping genes, conventional PCR was performed (Section 2.8.3). As an initial test, the primers were used on cDNA which were generated from RNA isolated using the *mir*Vana kit (Section 2.2.1) and which was used in the microarray. We were interested in investigating the expression of the gene targets present in these samples. As a control for the PCR, RNA was included as a template for one of the samples using primers specific to the control *GAPDH*. As shown in Figure 5.2 below it was found that the sample which included the RNA as template (Lane 1) produced a band of expected size (133 base pairs), indicating the presence of gDNA contamination in the sample which can potentially lead to false positive results. In Lane 2, the *BLID* primers were used, and the template was reverse transcribed using microvesicle treated RNA. As can be seen, the *BLID* primers successfully amplified a band of the expected size (91 base pairs). Lane 3 is a negative control where water was used as a template.

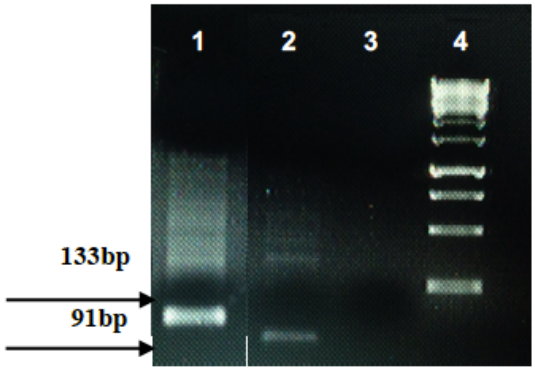

**Figure 5.2: Agarose gel picture of PCR products.** A 1.5% agarose gel visualised with 6 µL/100 mL EtBr, was electrophoresed for 45 minutes at 100 volts/cm and used to visualise 18 µL of PCR product, 2 µL of 10X DNA loading dye in a total volume of 25 µL with 5µL of 2X 1kb ladder. Lane 1 represents the RNA template control using *GAPDH* primers (133bp); Lane 2 represents the PCR products for BLID target gene (91bp); Lane 3 represents the no template (water) control whilst Lane 4 represents the 1kb DNA ladder. A single band was amplified for the *BLID* gene using the microvesicle treated control (MV) sample used for the microarray analysis however, a *GADPH* product was amplified for the RNA template control sample as noted in Lane 1.

We proceeded to DNase I treat the RNA samples using the RNA Clean & Concentrator$^{TM}$ -5 Kit (Zymo Research, USA) (Section 2.7) before downstream qPCR since the *mir*Vana$^{TM}$ Isolation Kit used for RNA extraction for the microarray does not contain a gDNA elimination step (Section 2.2.1). The DNase treatment led to a significant decrease in yield of RNA (Figure 5.3a), but succeeded in eliminating genomic DNA from the sample as found when the qPCR was repeated. When the DNase-treated RNA was used as template, no amplification took place (Figure 5.3b). A single amplified product was successfully observed for *GAPDH* in Lane 1 with no band in the water template control lane.

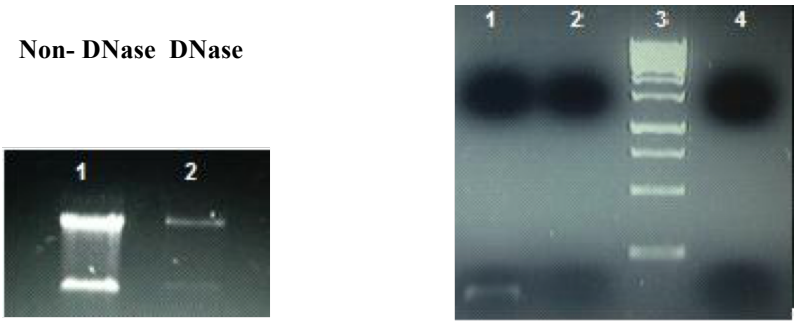


**(a)** **(b)**

**Figure 5.3: Agarose gel picture comparing PCR products before and after DNase treatment (a) and PCR products for target gene expression (b).**
(a) A 1% agarose gel visualised with 3 µL/50 mL EtBr, was electrophoresed for 45 minutes at 100 volts/cm and used to visualise 5 µL of RNA, 5 µL of 5X RNA loading dye heat denatured at 55°C for five minutes in a total volume of 10 µL. Lane 1 represents the non-DNase treated sample (microvesicle treated control sample) and Lane 2 represents the DNase treated sample. (b) A 1,5% agarose gel visualised with 3 µL/50 mL EtBr, was electrophoresed for 45 minutes at 100 volts/cm and used to visualise 18 µL of PCR product, 2 µL of 10X DNA loading dye in a total volume of 25 µL. Lane 1 represents the PCR product using *GAPDH* primers; Lane 2 represents the RNA template control; Lane 3 represents the 1kb DNA ladder and Lane 4 represents the no template (water) control. A single band was amplified for *GADPH* using the microvesicle treated control sample.

While the removal of gDNA was successful, it significantly reduced the concentration of the RNA to such an extent that there were insufficient amounts to be used for reverse transcription. Therefore our efforts for qPCR of the *BLID* target gene was focused on RNA extracted using the Roche kit (Penzberg, Germany) (Section 2.2.2).

### 5.2.4 *BLID* mRNA is downregulated upon HIV-1 AT-2 treatment in B-cells

Once the primer pairs were successful in amplifying the BLID gene by conventional PCR, qPCR was performed using the cDNA reverse transcribed from the RNA isolated from the L1439A cells (Section 2.8.2) that were treated with HIV-1 AT-2 (Section 2.1.4). In line with what was observed for miR-575 expression in the L1439A, *BLID* mRNA expression was found to be downregulated (Figure 5.4). An average fold change of 0.588 was reported when normalised with *GAPDH*, the housekeeping gene, and although statistically not significant, the trend was consistent and reproducible. As noted in Chapter four, (Section 4.2.3), two housekeeping genes were used but a more consistent result was obtained using *GAPDH.*

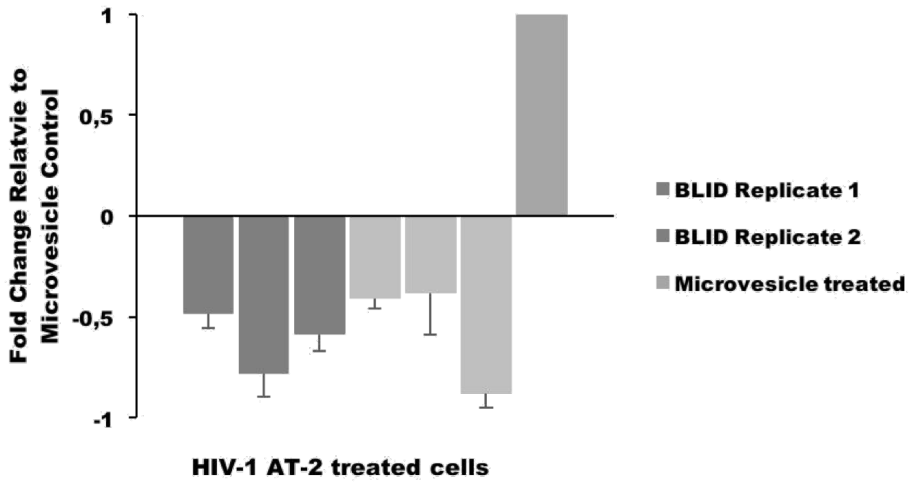


**Figure 5.4: *BLID* mRNA is consistently downregulated after HIV-1 AT-2 treatment in normal B-cells relative to microvesicle treated control cells.** Downregulation of *BLID* mRNA expressed as fold changes in two independent experiments in HIV-treated cells relative to microvesicle-treated control cells, which has been normalised to one. The housekeeping gene, *GAPDH* was used as the endogenous control. Two independent experiments were performed with each sample performed in triplicate. Error bars represent the standard deviation. A downregulated fold change was observed ranging from 0.383-0.878 (Prism 7, Graphpad, USA).

### 5.2.5 BLID protein was undetectable in both treated and untreated cells

The next step was to assess the expression of the BLID protein in the cells. Cells were treated as before (Section 2.1.4) and total protein extracted as described in Section 2.9.1. The initial western blotting result produced unclear results, as a band of the correct size could not be detected (Appendix B – Figure B5). There were several possible explanations for this. To eliminate the possibility that the transfer of proteins onto the nitrocellulose membrane was unsuccessful, a Ponceau S stain (Sigma Aldrich, Missouri, USA) was performed (Section 2.9.3.3). This revealed that the transfer was successful (Appendix B –

Figure B3). A second possibility was that the anti-BLID antibody was not working optimally and/or the amount of protein loaded and transferred was insufficient. However, this problem was not solved even when the amount of protein was doubled (data not shown). We thereafter ran several western blots with the inclusion of a positive control from two different breast cancer cell lines, T47D and MDA-MB231, which have been reported to express endogenous BLID (Section 2.9.1) (Li *et al.,* 2013) as well as making use of two different forms of the antibody from the manufacturer (monoclonal #H00414899-M05 and polyclonal #H00414899-B01; Novus Biologicals, Singapore, Malaysia) at varying concentrations (1:500 and 1:250). A band of the correct size was eventually detected in our positive control sample (Figure 5.5) for one of the analyses but this could not be detected in our L1439A protein samples even at high concentrations of the protein (Appendix B – Figures B7).

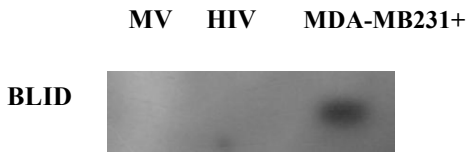


**Figure 5.5: BLID protein expression in normal B-cells relative to microvesicle treated control cells.** Western blot analysis displaying BLID expression (~11.8 kDa) in the L1439A cell line. 5 µL of 5X SDS loading dye and 1 µL of DTT was added to 20 µg of protein (varying volumes) in RIPA buffer and denatured at 95 °C for five minutes before being loaded and separated on a 15 % SDS-PAGE gel at 100 V for two hours in 1X running buffer. The protein was then transferred onto a nitrocellulose membrane (Bio-Rad, USA) for one hour at 100 V in 1X transfer buffer. This was then detected using the Clarity™ Western ECL Blotting Substrate (Bio-Rad, USA). To detect BLID, mouse anti-BLID antibody (Novus Biologicals, Singapore, Malaysia) was used, with a HRP bound goat anti-mouse secondary antibody (Bio-Rad, California, USA). BLID – BH3-like motif containing inducer of cell death; HIV – HIV-1 AT-2 treated L1439A cells; MV – microvesicle treated L1439A cells (control); + - positive control (breast cancer cell line MDA-MB231).

## 5.3 DISCUSSION

For this part of the study, we chose to characterise miR-575 given the minimal research investigating its role in cancer as well as in B-cell lymphomas. The next step for studying differential miRNAs in the context of disease is identifying and validating its potential mRNA target to understand its role in cellular pathways (Hamzeiy, *et al.,* 2014). This is done by using online bioinformatic tools followed by experimental validation of the mRNA target for the miRNA of interest (Kuhn *et al.,* 2008; Ekimler & Sahin, 2014; Palanichamy & Rao, 2014).

The effective prediction of mRNA:miRNA interactions remains a current challenge due to not only the complexity of miRNAs and their regulation of their targets (Reviewed by Pasquinelli, 2012; Vasudevan, 2011) but also to the limited criteria governing the process (Wikos *et al.,* 2011). In addition, it has been shown both experimentally and predicted that a single miRNA can potentially regulate many gene targets (Zhou *et al.,* 2013a) and several miRNAs may compete for the same mRNA (Krek *et al.,* 2005; Wu *et al.,* 2010). Computational methods that use target prediction algorithms have been the main catalyst assisting in finding possible interactions (Witkos *et al.,* 2011) but there is a need for better approaches (Hamzeiy *et al.,* 2014). Most of these prediction algorithms are focused on alignment of the complementary elements in the 3' UTR with the seed sequence of the miRNA as well as the evolutionary conservation of this region amongst species (Hamzeiy, *et al.,* 2014). Perfect complementarity of mRNA to miRNA are seen in plants, however for animals it is a rare phenomenon (Yekta *et al.,* 2004). miRNA complementary elements can also be found sporadically in the 5' UTR or open reading frames (ORF) of their target genes (Lytle *et al.,* 2007). This means that some of the mRNA gene targets that the algorithms predict (that use the above criteria) can be non-functional and unreliable (Kuhn *et al.*, 2008; Ekimler & Sahin, 2014).

Besides sequence based approaches, other computational methods are homology based, and structure based. Many authors have reviewed the strengths and weaknesses of various algorithms and bioinformatic tools (Kuhn *et al.,* 2008; Witkos *et al.,* 2011; Pasquinelli, 2012; Ekimler & Sakin, 2014; Hamzeiy *et al.,* 2014; Peterson *et al.,* 2014), but some recommend four tools that have high precision and sensitivity namely, TargetScan, picTar and Miranda and DIANA-microT (Witkos *et al.,* 2011; Thomson *et al.,* 2011; Ekimler & Sahin, 2014). We searched these online software databases for the gene target of miR-575 (Table 5.2) followed by combining the output of all these programmes and selecting the overlapped mRNA targets (Barbato *et al.,* 2009; Thomson *et al.,* 2011). In our search, the target, *DENND5A* was found in three out of the four recommended methods to use but these tools are used as guides rather than confirmed results (Hamzeiy *et al.,* 2014) as they produce scores based on searches of potential interactions (Witkos *et al.,* 2011). Since there is also no consensus as to what criteria should be followed to determine miRNA targets and to confirm biological efficacy (Ekimler & Sahin, 2014), experimentally validated

mRNA targets are the most suitable approach for identifying mRNA:miRNA interactions (Witkos *et al.,* 2011). Some online software databases store this information such as miRTarBase but the disadvantage is that novel interactions may not yet have been discovered or added on to the database (Hamzeiy *et al.,* 2014) such as for miR-575. The reliance therefore is by manually searching the literature for evidence of interactions between mRNA targets and the miRNA of interest (Witkos *et al.,* 2011).

Recently, BLID was identified as a validated target of miR-575 in non small cell lung cancer (NSCLC) (Wang *et al.,* 2015). This is the only study to date that has identified and validated a target for miR-575. However, *BLID* has been identified as a target for other miRNAs such as miR-125b-1 in childhood B-cell precursor acute lymphoblastic leukemia (Tassano *et al.,* 2010), miR-17-5p (Wang *et al.,* 2016) and miR-603 (Ma *et al.,* 2016) in osteosarcoma. BLID (also known as breast cancer cell 2 (BRCC2)) was first reported in the MDA-MB-231 human breast cancer cell line in 2004 (Broustas *et al.,* 2004) and has been recently identified as a novel tumour suppressor gene (Yu & Li, 2015). It is an intronless gene that has been mapped to chromosome 11q24.1 which is also a region that is characterised by extensive loss of heterozygosity in cancer. These include breast cancer with the loss associated with poor prognoses (Chunder *et al.,* 2004; Climent *et al.,* 2007), in chronic lymphocytic leukaemia (Crowther-Swanepoel *et al.,* 2010) cervical cancer (Zhang *et al.,* 2005) and many other diseaseas (Beneteau *et al.,* 2011). Studies in human cancer cell lines reveal that *BLID* can inhibit cell growth and metastasis in breast cancer cells (Li *et al.,* 2013) whilst overexpression can cause apoptotic cell death in three different cell lines (Broustas *et al.,* 2004).

It is important to experimentally validate the possible interaction of mRNA:miRNA produced by the predictive tools (Kuhn *et al.,* 2008; reviewed by Thomson *et al.,* 2011; Palanichamy & Rao, 2014). To do this we firstly analysed the mRNA level of *BLID* by qPCR. Since qPCR is a sensitive technique that amplifies small amounts of RNA, contaminants such as gDNA can affect the downstream application producing unreliable results (Bustin, 2000; Udvardi *et al.,* 2008). We attempted to convert the RNA to cDNA isolated for use in the PCR array but after successful DNase treatment (Figure 5.3a) our volumes were not enough to conduct qPCR. We then treated our cells again and isolated

RNA using the Roche kit (Section 2.2.2) that contained a gDNA elimination step. Upon downstream qPCR we found that *BLID* mRNA was significantly downregulated in our normal B-cell line L1439A. Our findings are supported by other studies investigating other cancers such as NSCLC (Wang *et al.,* 2015), and osteosarcoma (Ma *et al.,* 2016; Wang *et al.,* 2016). Importantly, we observed an inverse relationship between our validation data (expression of miR-575 in L1439A), and *BLID* mRNA expression in the same cells. If miR-575 targets *BLID* for degradation in our context, then this result supports this. However, this could not be further verified at the protein level as a band could not be detected in our samples (Appendix B – Figures B6 and B7). The longest predicted ORF of *BLID* is 862 base pairs and its mRNA encodes a protein that is 108 amino acids in length (~11.8 kDa) (GenBank accession numbers AF220061 and AF303179) (Li *et al.,* 2013). It is possible that basal levels of the BLID protein may be too low to be detected using western blotting, even in microvesicle treated control cells (Li *et al.,* 2013).

Interestingly, *BLID* mRNA was found to be upregulated in the BL cell line Ramos (Figure B4 in Appendix B) upon treatment with HIV and once again, a reverse relationship between miRNA and its target is demonstrated. *BLID* was found to be upregulated in childhood B-cell precursor acute lymphoblastic leukeamia resulting from a novel IGH translocation which is a common abnormality in mature B-cell neoplasms (Tassano *et al.,* 2010) which is also seen in BL with the translocation of the transcription factor, c-MYC (Dang, 2012; Ott *et al.,* 2013; Spender & Inman, 2014). These contrasting findings between the two cell lines support the notion that mRNA:miRNA interactions are tissue dependent (Palinichamy & Rao, 2014). Future studies should therefore probably focus on a different predicted target for miR-575 (Table 5.2) such as *DENND5A*.

# CHAPTER 6: SUMMARY & CONCLUSION

## 6.1 SUMMARY

Recently, it has emerged that HIV may play a direct role in the development of HIV-associated NHLs. In this study, we propose that one of the mechanisms by which it can do this is via the modulation of miRNAs in B-cells. As such, the aim of our project was to to identify cellular miRNAs whose expressions are altered by HIV and which contribute to the development of HIV-associated NHLs. We sought to achieve this through three main objectives.

In the first part of our study, we conducted a miRNA microarray analysis, using a custom made array plate, to identify miRNAs with altered expression in BL cells treated with HIV-1 AT-2, compared to microvesicle treated control cells. No other study to date has identified expressed miRNAs in B-cells after HIV-1 exposure. Due to limitations in the original statistical analysis software, we conducted a comprehensive analysis and selected 32 differentially expressed miRNAs that were not statistically significant, both upregulated and downregulated, with a fold change of two or more, for further validation. Not all dsyregulated miRNAs discovered by expression profiling are potentially pathogenetic and many do not have a clear mechanism of action in oncogenesis. As such, validation of these results is essential to add biological significance to the findings.

In Chapter four we report on four miRNAs namely miR-363-3p, miR-200c-3p, miR-222-3p and miR-575, which were chosen based on their reported involvement in cancer. For the validation we used single-tube TaqMan® qPCR assays to assess their expression in both normal B-cells and the Ramos BL cell line. Unfortunately, we could not reach a conclusion for miR-222-3p, miR-200c-3p and miR-363-3p in the BL cells due to the large variability in replicates (beyond the scope of this study) but were able to show that miR-575 was significantly upregulated in the normal B-cell line L1439A. Whilst many studies have validated their array results one could question what result can be constituted as validated since the criteria for validation are unclear (Chuaqui *et al.,* 2002; Allison *et al.,* 2006). Correlations of qPCR and microarray data are rarely presented in the literature and non-agreeing data is also rarely explained (Morey *et al.,* 2006).

In the last part of our study we selected miR-575 to characterise in the context of HIV-associated lymphomas. We first used bioinformatic online tools to identify predicted mRNA gene targets for miR-575. Although we followed what literature recommended with regards to prediction target softwares, we chose an experimentally validated target, BLID, that was validated as a target for miR-575 in NSCLC. At the mRNA level, *BLID* was downregulated in normal B-cells. This inverse relationship pointed to a potentially physiologically relevant role of miR-575 in HIV-associated NHLs. However, we could not detect the BLID protein expression in our cells.

*BLID* has already been identified as a novel tumour suppressor gene in breast cancer and is a promising therapeutic agent for diagnosis in this cancer. However, its role in other cancers such as HIV-associated lymphomas remains unclear. We have attempted for the first time a study identifying miRNAs that are differentially expressed upon HIV-1 exposure. Few miRNA have known biological functions and validated experimental targets which is one of the reasons that miRNA studies remain complex (Chugh & Dittmer, 2012). In addition, the complex nature of miRNAs, its complexity of many levels of gene regulation and structure can create intricate patterns of miRNA expression (Palanichamy & Rao, 2014). Differential gene expression may also represent phenotypic variants within the same population (Mukherji *et al.,* 2011) which may also depend on the number of miRNA binding sites in the 3' UTR of the mRNA and miRNA in the cell. An interesting question prompted by Palanichamy & Rao (2014) is whether we should be interpreting the roles of miRNAs in disease states the way in which we evaluate the role of proteins in oncogenesis; and what are the mechanisms that distinguish miRNAs as novel factors in disease causation and progression. Unfortunately, consensus and guidelines for studying miRNA by qPCR (Bustin, 2000) is yet to be determined including what fold change can be considered biologically plausible and relevant but an attempt has been made by Chuquai *et al.,* (2002).

## 6.2 LIMITATIONS

There were several limitations in this study ranging from the selection of miRNAs for profiling to the design of the array. Firstly, not all miRNAs which we identified in the literature to be relevant for our research could be included in the array as we were limited to the ones available for selection by the manufacturer which could have introduced a study bias. This led us to choose different miRNAs and could not investigate the expression of those

such as miR-93, miR-92, miR-801 (Robertus *et al.,* 2010; Bueno *et al.,* 2011). In addition, studies that were consulted for selecting mature miRNAs did not specify which pre-miRNA (3p or 5p arm) they had included in their study which made choosing specific miRNAs challenging since they differ in sequence from the different arms (Pritchard *et al.,* 2012).

A third limitation is that there was a serious time limiting constraint of the manufacturing of the array plate. As mentioned in the previous chapter, the array has a unique design (Section 3.3; Figure 3.4) but another challenge arose when the microfluidic array cards did not disperse evenly after centrifugation as per the manufacturer's protocol (Figure 6.1) (Wong *et al.,* 2015). According to the manufacturer's protocol the results from those arrays should be omitted but fortunately we managed to resolve the distribution through additional centrifugation which redistributed the samples evenly within the reservoirs. Lastly, we could not quantify the amount of miRNA in our RNA samples for microarray analysis due to the expensive cost factor involved in using specific analysers such as the Agilent Bioanalyser (Agilent Technologies, Waldbronn, Germany).

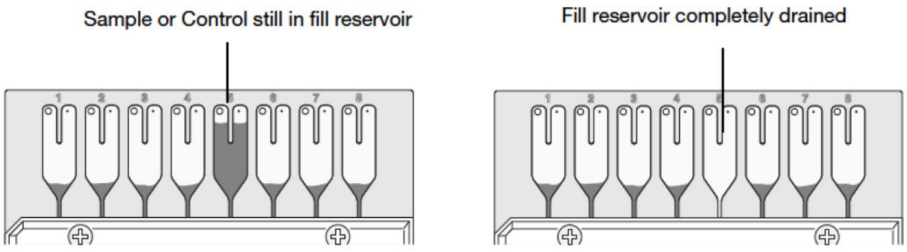


**Figure 6.1: Schematics of TaqMan® Array Cards when loading the sample.** Samples are added through eight ports which are then evenly distributed by centrifugation. Instances can arise whereby samples are not distributed evenly and the sample or control is still present in the fill reservoir or the fill reservoir is completed drained. (Reproduced from https://www.thermofisher.com)

The limitations in the second part of our study focused mainly on technical errors which can occur when pipetting small amounts for sensitive qPCR experiments. The inconsistency amongst replicates may have also occurred due to improper pipetting as well as evaporation of samples prior to sealing tubes. Lastly, in the final part of our study, we had two limitations. Firstly, we had challenges in culturing the slow growing L1439A normal B-cell line as it is a fragile cell line which limited the speed at which experiments were conducted. Although we could not use this cell line for the miRNA microarray analysis, by the time validation of

miRNAs were conducted we had reached a confluency of the cells that were adequate for downstream treatment and experimentation. Secondly, we were unable to detect the BLID protein despite several attempts.

## 6.3 CONCLUSION & FUTURE DIRECTIONS

Our profiling analysis has provided for the first time a starting point for HIV-associated NHLs but detailed studies are required to fully determine and validate the role of the miRNAs that were found as differentially expressed. In line with our aims we have provided evidence for miRNAs that are differentially expressed upon HIV exposure. miR-575 was found to be upregulated whilst *BLID* was found to be downregulated in normal B-cells. Further characterisation is required to understand its mechanism of action in HIV associated NHLs by investigating other mRNA targets of miR-575 and by functional analyses, such as measure of apoptosis, expression of key regulators of the cell cycle, and other cellular events characteristic of cancer. Future studies should also focus on validation and characterisation of the remaining differentially expressed miRNAs upon HIV exposure to fully elucidate and contribute to the emerging role of cellular miRNAs contributing towards HIV-associated NHL development and/or progression.

# REFERENCES


1. Abayomi, E.A., Somers, A., Grewal, R., *et al.* (2011). Impact of the HIV epidemic and Anti-Retroviral Treatment policy on lymphoma incidence and subtypes seen in the Western Cape of South Africa, 2002-2009: Preliminary findings of the Tygerberg Lymphoma Study Group. *Transfusion and Apheresis Science, 44:* 161 – 166.
2. Abudulai, L.N., Fernandez, S., Corscadden, K. *et al*. (2016). Chronic HIV-1 infection induces B-cell dysfunction that is incompletely resolved by long-term antiretroviral therapy. *Journal of Acquired Immune Deficiency Syndrome, 71*(4): 381 – 389.
3. Abdul Mohsen, M., Deng, X., Danesh, A. *et al.* (2014). Role of microRNA modulation in the Interferon- α/Ribavirin suppression of HIV-1 *in vivo. Public Library of Science ONE 9*(1): e109220. doi:10.1371/journal.pone.010920.
4. Aboulafia, D.M., Pantanowitz, L., Dezube, B.J. (2004). AIDS-related non-Hodgkin lymphoma: still a problem in the era of HAART. *AIDS Read, 14:* 605 – 617.
5. Ahluwalia, J., Khan, S., Soni, K., *et al.* (2008). Human cellular miRNA hsa-miR-29a interferes with viral Nef protein expression and HIV-1 replication. *Retrovirology, 5:* 117.
6. Alencar, A.J., Malumbres, R., Kozloski, G.A., *et al.* (2011). MicroRNAs are independent proedictors of outcome in Diffuse Large B-Cell Lymphoma patients treated with R-CHOP. *Clinical Cancer Research, 17* (12): 4125 – 4135.
7. Allison, D.B., Cui, X., Page, G.P., Sabripour, M. (2006). Microarry data analysis: from disarray to consolidation and consensus. *Nature Genetics Reviews, 7:*55 – 65.
8. Ambrosio, M.R., Navari, M., Di Lisio, L., *et al*. (2014). The Epstein Barr-encoded BART-6-3p microRNA affects regulation of cell growth and immuno response in Burkitt Lymphoma. *Infectious Agents & Cancer, 9:*12.
9. Aqil, M., Naqvi, A.R., Mallik, S., *et al*. (2014). The HIV Nef protein modulates cellular and exocsomal miRNA profiles in human monocytic cells. *Journal of Extracellular Vesicles, 3:* 23129.
10. Backes, C., Sedaghat-Hamedani, F., Frese, K., *et al*. (2016). Bias in high-throughput analysis of miRNAs and implications for biomarker studies. *Analytical Chemistry, 88*(4): 2088 – 2095.
11. Bai, X.T., & Nicot, C. (2015). miR-28-3p is a cellular restriction factor that inhibits HTLV-1 replication and virus infection. *The Journal of Biological Chemistry, e19,* doi: 10.1074/jbc.M114.626325.

12. Bai, W.D., Ye, X.M., Zhange, M.Y., *et al.* (2014). miR-200c surpresses TGF-b signaling and counteracts trastuzumab resistance and metastasis by targeting ZNF217 and ZEB1 in breast cancer. *International Journal of Cancer, 135*: 1356 – 1368.
13. Baker, M. (2010). MicroRNA profiling: separating signal from noise. *Nature Methods, 7*(9): 687 – 692.
14. Barbato, C., Arisi, I., Frizzo, M. E., *et al.* (2009). Computational challenges in miRNA target predictions: to be or not to be a true target? *Journal of Biomedicine & Biotechnology,* 803069.
15. Bashir, Z. & A.J. Davies. (2011). New Therapies for Diffuse Large B Cell lymphoma. Current Medical Literature: *Leukemia & Lymphoma, 19*(3): 57.
16. Becker, C., Hammerle-Fickinger, A., Riedmaier, I., Pfaffl, M.W. (2010). mRNA and microRNA quality control for RT-qPCR analysis. *Methods 50*: 237 – 243.
17. Bell, D.W., Sikdar, N., Lee, K.Y., *et al.* (2011). Predisposition to cancer caused by genetic and functional defects of mammalian Atad5. *PLoS Genetics*, *7*(8): e1002245.
18. Benes, V., & Castoldi, M. (2010). Expression profiling of microRNA using real-time quantitative PCR, how to use it and what is available. *Methods, 50:* 244 – 249.
19. Berglund, M., Hedstrom, G., Amini, R.M., Enblad, G., Thunberg, U. (2013). High expression of microRNA-200c predicts poor clinical outcome in diffuse large B-cell lymphoma. *Oncology Reports, 29:* 720 – 724
20. Beneteau, C., Landais, E., Doco-Fenzy, M., *et al.* (2011). Microtriplication of 11q24.1: A highly recognisable phenotype with short stauture, distinctive facial features, keratoconus, overweight and intellectual disability. *Journal of Medical Genetics, 48:* 635 – 639.
21. Bennasser, Y., & Jeang, K.T. (2006). HIV-1 Tat interaction with Dicer: requirement for RNA. *Retrovirology, 3*: 95, doi:10.1186/1742-4680-4-95.
22. Benjamini, Y., & Hochberg, Y. (1995). Controlling the False Discovery Rate: A Practical and Powerful Approach to Multiple Testing. *Journal of the Royal Statistical Society. Series B (Methodological)*, *57*(1): 289 – 300. doi:10.2307/2346101
23. Bennasser, Y., Le, S.Y., Yeung, M.L., *et al.* (2004). HIV-1 encoded candidate micro-RNAs and their cellular targets. *Retrovirology, 43*(1): 1 – 5.
24. Bernard, M.A., Zhao, H., Yue, S.C., *et al.* (2014). Novel HIV-1 miRNAs stimulate TNFα release in human macrophages via TLR8 signalling pathway, *Public Library of Science ONE, 9*(9): e106006, doi:10.1371/journal.pone.0106006.
25. Bernstein, E., Kim, S.Y. Carmell, M.A., *et al.* (2003). Dicer is essential for mouse development. *Nature Genetics, 35:* 215 – 217.

26. Bolstad, B.M., Irizarry, R.A., Astrand, M., Speed, T.P. (2003) A comparison of normalization methods for high density oligonucleotide array data based on variance and bias. *Bioinformatics 19:* 185-193.

27. Bohlius, J., Schmidlin, K., Constagliola *et al.* (2009). Prognosis of HIV-associated non-Hodgkin lymphoma in patients starting combination antiretroviral therapy. *AIDS, 23*(15): 2029 – 2037.

28. Brennecke, J., Hipfner, D.R., Stark, A., *et al.* (2003). *Bantam* encodes a developmentally regulated microRNA that controls cell proliferation and regulates the proapoptotic gene *hid* in Drosophila. *Cell, 113:* 25 – 36.

29. Broustas, C.G., Gokhale, P.C., Rahman, A., Dritschilo, A., Ahmad, I., Kasid, U. (2004). BRCC2, a novel BH3-like domain-containing protein, induces apoptosis in a caspase-dependent manner. *Journal of Biological Chemistry, 279*(25): 26780 – 26788.

30. Broustas, C.G., Ross, J.S., Yang, Q., *et al.* (2010). The proapoptotic molecule BLID interacts with Bcl-XL and its downregulation in breast cancer correlates with poor disease-free and overall survival. *Clinical Cancer Research*, *16*(11): 2939 – 2948.

31. Bueno, M.J., de Cedron, M.G., Gomez-Lopez, G., *et al.* (2011). Combinatorial effects of microRNAs to suppress the Myc oncogenic pathway. *Blood, 117*(23): 6255 – 6266.

32. Burkitt, D. (1958). A sarcoma involving the jaws in African children. *Journal of Surgery, 46:* 218 – 223.

33. Bustin, S.A. (2000). Absolute quantification of mRNA using real-time reverse transcription polymerase chain reaction assays. *Journal of Molecular Endocrinology, 25*:169 –193.

34. Butler, M.W., Fukui, T., Salit, J., *et al.* (2011). Modulation of cystatin A expression in human airway epithelium related to genotype, smoking, COPD, and lung cancer. *Cancer research*, *71*(7): 2572 – 2581.

35. Caccuri, F., Rueckert, C., Giagulli, C., *et al*. (2014). HIV-1 matrix protein p17 promotes lymphangiogenesis and activates the endothelin-1/endothelin B receptor axis. *Arteriosclerosis, Thrombosis, and Vascular Biology, 34:* 846 – 856.

36. Calin, G.A., & Croce, C.M. (2006). MicroRNAs signatures in cancer. *Nature Reviews, 6:* 857–866.

37. Calin, G.A., Sevignani, C., Dumitru, C.D., *et al.* (2004). Human microRNA genes are frequently located at fragile sites and genomic regions are involved in cancers. *Proceedings of the National Academy of Sciences USA, 101* (9): 2999 – 3004.

38. Carbone, A. & Gloghini, A. (2005). AIDS-related lymphomas: From pathogenesis to pathology. *British Journal of Haematology, 130:* 662 – 670.

39. Calin, G.A., Dumitru, C.D., Shimizu, M., *et al.* (2002). Frequent deletions and down-regulation of microRNA genes miR-15 and miR-16 at 13q14 in chronic lymphocytic leukeamia. *Proceedings of the National Academy of Sciences USA, 99:* 15524 – 15529.

40. Campo, E., Swerdlow, S.H., Harris, N.L., *et al*. (2011). WHO classification of tumours of heamatopoetic and lymphoid tissues. *Blood, 117*(19): 5019 – 5032.

41. Capello, D., Scandurra, M., Poretti, G., *et al.* (2009). Genome wide DNA profiling of HIV-related B-cell lymphomas, *British Journal of Haematology, 148:* 245 – 255.

42. Carl, S., Greenough, T.C., Krumbiegel, M., *et al*. (2001). Modulation of different Human Immunodeficiency Virus type 1 Nef functions during progression to AIDS. *Journal of Virology, 75*(8): 3657 – 3665.

43. Cote, T.R., Biggar, R.J., Rosenberg, P.S., et al. (1997). Non-Hodgkin's lymphoma among people with AIDS: incidence, presentation and public health burden. *International Journal of Cancer, 73*(5): 645 – 650.

44. Cavalli, L. R., Noone, A. M., Makambi, K. H., *et al.* (2011). Frequent loss of the BLID gene in early-onset breast cancer. *Cytogenetic and Genome Research*, *135*(1): 19 – 24.

45. Chang, T.S., Yu, D., Lee, Y.S., *et al*. (2008). Widespread microRNA repression by Myc contributes to tumourigenesis. *Nature Genetics, 40*(1): 43 – 50.

46. Chang, L.C., Yu, Y.L., Liu, C.Y., *et al.* (2015). The newly synthesized 2-arylnaphthyridin-4-one, CSC-3436, induces apoptosis of non-small cell lung cancer cells by inhibiting tubulin dynamics and activating CDK1. *Cancer Chemotherapy and Pharmacology*, *75*(6):1303 – 1315.

47. Chang, S.T., Thomas, M.J., Sova, P., *et al.* (2013). Next generation sequencing of small RNAs from HIV-infected cells identifies phased microRNA expression patterns and candidate novel microRNAs differentially expressed upon infection. *mBio, 4*(1): e00549, 12.

48. Chen, C., Rodzon, D.A., Broomer, A.J., *et al.* (2005). Real-time quantification of microRNAs by stem-loop RT-PCR. *Nucleic Acids Research, 33*(20): e179.

49. Chen, T.R. (1977). In situ detection of mycoplasma contamination in cell cultures by fluorescent Hoechst 33258 stain. *Experimental Cell Research, 104*(2): 255 – 262.

50. Chiang, K., Liu, H., Rice, A.P. (2013). MiR-132 enhances HIV-1 replication. *Virology, 438*: 1 – 4.

51. Choi, H.J., & Smithgall, T.E. (2004). HIV-1 Nef promotes survival of TF-1 macrophages by inducing *BCL-$X_L$* expression in an extracellular signal-regulated kinase-dependent manner. *The Journal of Biological Chemistry, 279*(49): 51688 – 51696.

52. Chunder, N., Mandal, S., Roy, A., Roychoudhury, S. and Panda, C.K. (2004). Analysis of different deleted regions in chromosome 11 and their interrelations in early-and late-onset breast tumors: association with cyclin D1 amplification and survival. *Diagnostic Molecular Pathology*, *13*(3): 172 – 182.

53. Christopher, A.F., Kaur, R.P., Kaur, G., Kaur, A., Gupta, V., Bansal, P. (2016). MicroRNA therapeutics: Discovering novel targets and developing specific therapy. *Perspectives in Clinical Research, 7*(2): 68 – 74.

54. Chugh, P., & Dittmer, D.P. (2012). Potential pitfalls in microRNA profiling. *Wiley Interdisciplinary Review RNA, 3*(5): 601 – 616.

55. Clifford, G.M., de Vuyst, H., Tenet, V., Plummer, M., Tully, S., Franceschi, S. (2016). Effect of HIV infection on Human Papillomavirus types causing invasive cervical cancer in Africa. *Journal of Acquired Immune Deficiency Syndrome, 73*(3)*:* 332 – 339.

56. Climent, J., Dimitrow, P., Fridlyand, J., *et al.* (2007). Deletion of chromosome 11q predicts response to anthracycline-based chemotherapy in early breast cancer. *Cancer Research*, *67*(2): 818 – 826.

57. Cochrane, D.R., Howe, E.N., Spoelstra, N.S., Richer, J.K. (2010). Loss of miR-200c: A Marker of aggressiveness and chemoresistance in female reproductive cancers. Journal of Oncology, 1– 12.

58. Corti, M., Villanfane, M.F., Bistmans, A., *et al*. (2013). Burkitt's Lymphoma in AIDS patients: Report of six cases and review of the literature. *Journal of Symptoms and Signs, 2* (4): 198 – 202.

59. Craig, V.J., Tzankov, A., Flori., M., *et al.* (2012). A systemic microRNA-34a delivery induces apoptosis and abrogates growth of diffuse large B-cell lymphoma in vivo. *Leukemia, 26:* 2421– 2426.

60. Chuaqui, R.F., Bonner, R.F., Best, C.J.M., *et al.* (2002). Post-analysis follow-up and validation of microarray experiments. *Nature Genetics, 32*:509 – 514.

61. Crowther-Swanepoel, D., Mansouri, M., Enjuanes, A., *et al.* (2010). Verification that common variation at 2q37. 1, 6p25. 3, 11q24. 1, 15q23, and 19q13. 32 influences chronic lymphocytic leukaemia risk. *British Journal of Haematology*, *150*(4): 473 – 479.

62. Culpin, R.E., Proctor, S.J., Angus, B., *et al.* (2010). A 9 series microRNA signature differentiates between germinal centre and activated B-cell-like diffuse large B-cell lymphoma cell lines. *International Journal of Oncology, 37:* 367 – 376.

63. Curreli, S., Krishnan, S., Reitz, M., *et al.* (2013). B cell lymphoma in HIV transgenic mice. *Retrovirology, 10:* 92.

64. Dang, C.V. (2012). MYC on the path to cancer. *Cell, 149* (1): 22 – 35.

65. de Lima Rebouças, E., do Nascimento Costa, J. J., Passos, M. J., *et al.* (2013). Real time PCR and importance of housekeeping genes for normalization and quantification of mRNA expression in different tissues. *Brazilian Archives of Biology and Technology*, *56*(1): 143 – 154.

66. Del Corno, M., Donninelli, G., Varano, B., *et al.* (2014). HIV-1 gp120 activates the STAT3/interleukin-6 axis in primary human monocyte-derived dendritic cells. Journal of *Virology, 88* (19): 11045 – 11055.

67. Dietrich, U., Grez, M., von Briessen, H., *et al.* (1993). HIV-I strains from India are highly divergent from prototypic African and US/European strains, but are linked to a unique South African isolate. *AIDS, 7:*23 – 27.

68. Di Leva, G., Garofalo, M., Croce, C.M. (2014). MicroRNAs in cancer. Annual Review of Pathology: *Mechanisms of Disease, 9:* 287 – 314.

69. Di Lisio, L., Sanchez-Beato, M., Gomez-Lopez, G., *et al.* (2012). MicroRNA signatures in B-cell lymphomas. *Blood Cancer Journal, 2:* e57, doi: 10.1038/bcj.2012.1.

70. Dvinge, H., & Bertone, P. (2009). HTqPCR: high-throughput analysis and visualization of quantitative real-time PCR data in R. *Bioinformatics, 25*(24): 3325 – 3326.

71. Dolcetti, R., Gloghini, A., Caruso, A., *et al.* (2016). A lymphomagenic role for HIV beyond immune suppression. *Blood,* 1 – 23. Doi:10.1182/blood-2015-11-681411.

72. Donadoni, G., Bruno-Ventre, M., Ferreri, A.J.M. (2013). Treatment of HIV-associated Burkitt's Lymphoma. *European Medical Journal of Haematology, 1:* 38 – 52.

73. Drahos, J., Schwameis, K., Orzolek, L.D., *et al.* (2015). MicroRNA profiles of Barrett's Esophagus and esophageal adenocarcinoma: Differences in glandular non-native epithelium. *Cancer Epidemiology, Biomarkers & Prevention, 25*(3): 429 – 437.

74. Egana-Gorrono, L., Escriba, T., Boulanger, N., *et al.* (2014). Differential microRNA expression profile between stimulated PBMCs from HIV-1 infected elite controllers and viremic progressors. *Public of Library Science ONE, 9*(9): e106360.

75. Egger, M., May, M., Chêne, G., Phillips, A.N., Ledergerber, B., Dabis, F., Costagliola, D., Monforte, A.D.A., De Wolf, F., Reiss, P. and Lundgren, J.D. (2002). Prognosis of HIV-1-infected patients starting highly active antiretroviral therapy: a collaborative analysis of prospective studies. *The Lancet*, *360*(9327): 119 – 129.

76. Ekimler, S. and Sahin, K., (2014). Computational methods for microRNA target prediction. *Genes*, *5*(3): 671 – 683.

77. Ekins, R., & Chu, F.W. (1999). Micorarrays: their origins and applications. *Trends in Biotechnology, 17*(6): 217 – 218.

78. Epeldegui, M., Vendrame, E., Martinez-Maza, O. (2010). HIV-associated immune dysfunction and viral infection: role in the pathogenesis of AIDS-related lymphoma. *Immunology Research, 48:* 72 – 83.

79. Esquela-Kerscher, A., & Slack, F.J. (2006). Oncomirs – microRNAs with a role in cancer. *Nature Reviews Cancer, 6:* 259 – 269.

80. Fabbri, M. (2013). Cancer as a microRNA-driven disease. The heresies of the miRNome direct cancer biology. *Revista de Hematologia, 14* (1): S25 – S28.

81. Farazi, T.A., Hoell, J.I., Morozov, P., *et al*. (2013) in Schmitz, U., *et al.* (eds), MicroRNA cancer regulation: advanced concepts, bioinformatics and systems biology tools, *Advances in Experimental Medicine and Biology, 774,* doi:10.1007/978-94-007-5590-1_1.

82. Farberov, L., Herzig, E., Modai, S.*, et al.* (2015). MicroRNA regulation of p21 and TASK1 cellular restriction factors enhances HIV-1 infection. *Journal of Cell Science, 128:* 1607 – 1616.

83. Fassina, A., Marino, F., Siri, M.*, et al.* (2012). The mir-17-92 microRNA cluster: a novel diagnostic tool in large B-cell malignancies. *Laboratory Investigation, 92:* 1574 – 1582.

84. Felicetti, F., Errico, M.C., Bottero, L., *et al.* (2008). The promyelocytic leukemia zinc finger-microRNA-221/-222 pathway controls melanoma progression through multiple oncogenic mechanisms. *Cancer Research, 68:* 2745 – 2754.

85. Fisher, J.N., Terao, M., Fratelli, M., *et al.* (2015). MicroRNA networks regulated by all-trans retinoic acid and Lapatinib control the growth, survival and motility of breast cancer cells. Oncotarget, 6(15): 13176 – 13200.

86. Flor, T.B., & Blom, B. (2016). Pathogen use: an abuse microRNAs to deceive the immune system. *International Journal of Molecular Sciences, 17:* 538 – 565.

87. Forte, E., Salinas, R.E., Chang, C., *et al.* (2012). The Epstein-Barr Virus (EBV) induced tumour suppressor microRNA miR-34a is growth promoting in EBV infected B cells. *Journal of Virology, 86*(12): 6889 – 6898.

88. Fowler, L., & Saksena, N.K. (2013). Micro-RNA: new players in HIV-pathogenesis, diagnosis, prognosis and antiviral therapy. *AIDS Review, 15:* 3 – 14.

89. Frankel, A.D., & Pabo, C.O. (1988). Cellular uptake of the tat protein from human immunodeficiency virus. *Cell, 55:* 1189–1193

90. Freshney, R. I. (2010). Culture of Animal Cells: A Manual of Basic Technique and Specialized Applications, 6th Edition, Hoboken, New Jersey, Wiley-Blackwell.
91. Gaur, A., Jewell, D.A., Liang, Y., *et al.* (2007). Characterization of microRNA expression levels and their biological correlates in human cancer cell lines. *Cancer Research, 67*(6): 2456 – 2468.
92. Git, A., Dvinge, H., Salmon-Divon, M., *et al.* (2010). Systematic comparison of microarray profiling, real-time PCR, and next-generation sequencing technologies for measuring differential microRNA expression. *RNA, 16*(5): 991-1006.
93. Gloghini, A., Dolcetti, R., Carbone, A. (2013). Lymphomas occurring specifically in HIV-infected patients: From pathogenesis to pathology. *Seminars in Cancer,* 457 – 467.
94. Gregory, R.I., Yan, K.P., Amuthan, G., *et al*. (2004). The microprocessor complex mediates the genesis of microRNAs. *Nature, 432*: 235 – 240.
95. Grewal, R., Cucuianu, A., Swanepoel, C., *et al.* (2015). The role of microRNAs in the pathogenesis of HIV-related lymphomas. *Critical Reviews in Clinical Laboratory Sciences, 52*(5): 232 – 241.
96. Griffith-Jones, S., Grocock, R.J., van Dongen, S., Bateman, A., Enright, A.J. (2006). miRBase: microRNA sequences, targets and gene nomenclature. Nucleic Acids Research, 34: D140 – 144, doi: 10.1093/nar/gkj112.
97. Grundoff, A. & Sullivan, C.S. (2011). Virus-encoded microRNAs. *Virology, 411:* 325 – 343.
98. Guo, H., Gai, J., Taxman, D.J. *et al.* (2014). HIV-1 infection induces interleukin-1B production via TLR8 protein-dependant and NLRP3 inflammasome mechanisms in human monocytes. *Journal of Biological Chemistry, 289:* 21716 – 21726.
99. Guo, Y.E., & Steitz, J.A. (2014). Virus meets host microRNA: the destroyer the booster, the hijacker. *Molecular and Cellular Biology, 34*(20): 3780 – 3787.
100. Guttler, T., & Gorlich, D. (2011). Ran-dependant nuclear export mediators: a structural perspective. *European Molecular Biology Organization Journal, 30:* 3457 – 3474.
101. Guha, D., Mancini, A., Sparks, J., *et al.* (2016). HIV-1 infection dysregulates cell cycle regulatory protein p21 in CD4+ T cells through miR-20a and miR-106b regulation. *Journal of Cellular Biochemistry, 9999:* 1 – 11.
102. Gygi, S.P., Rochon, Y., Franza, B.R., Aebersold, R. (1999). Correlation between protein and mRNA abundance in yeast. *Molecular Cell Biology, 19:*1720 –1730.
103. Haij, N.B., Planes, R., Leghmari, K., *et al.* (2015). HIV-1 Tat protein induces production of pro-inflammatory cytokines by human dendritic cells and monocytes/macrophages through

engagement of TLR4-MD2-CD14 complex and activation of NF-κB pathway. *Public Library of Science ONE, 10*(6): e0129425, doi:10.1371/journal.pone.0129425.

104. Hamzeiy, H., Allmer, J., Yousef, M., (2014). Computational methods for microRNA target prediction. *miRNomics: MicroRNA Biology and Computational Analysis, 1107*: 207 – 221.
105. Hanahan, D., & Weinberg, R.A. (2011). Hallmarks of cancer: The next generation. Cell, 144: 646 – 674.
106. Hariharan, M., Scaria, V., Pillai, B., *et al.* (2005). Targets for human encoded miRNAs in HIV genes. *Biochemical and Biophysical Research Communication, 337*: 1214 – 1218.
107. Hayes, A.M., Qian, S., Yu, L., *et al.* (2011). Tat RNA silencing suppressor activity contributes to perturbation of lymphocyte miRNA by HIV-1. *Retrovirology, 8:* 36 – 49.
108. Hayward, W.S., Neel, B.G., Astrin, S.M. (1981). Activation of a cellular oncogene by promoter insertion in ALV-induced lymphoid leukosis. *Nature, 290:* 475 – 480.
109. Harwig, A., Das, A.T., Berkhout, B. (2014). Retroviral microRNAs. *Current Opinion in Virology, 7:* 47 – 54.
110. Hernandez Bort, J.A., Hackl, M., Hoflmayer, H., *et al.* (2012). Dynamic mRNA and miRNA profiling of CHO-K1 suspension cell cultures. *Biotechnology Journal, 7:* 500 – 515.
111. Hill, L., Browne, G., Tulchinsky, E. (2013). ZEB/miR-200 feedback loop: at the crossroads of signal transduction. *International Journal of Cancer, 132:* 745 – 754.
112. Holland, B., Wong, J., Li, M., *et al.* (2013). Identification of human microRNA-like sequences embedded within the protein-encoding genes of the human immunodeficiency virus. *Public Library of Science, ONE, 8:* 3e58586.
113. Houzet, L., & Jeang, K.T. (2011). MicroRNAs and human retroviruses. *Biochimica et Biophysica Acta, 1809:* 11 – 12, doi:10.1016/j.bbagrm.2011.05.009.
114. Houzet, L., Yeung, M.L., de Lame, V.*, et al.* (2008). MicroRNA profile changes in human immunodeficiency virus type I (HIV-1) seropositive individuals. *Retrovirology, 5:* 118, doi:10.1186/1742-4690-5-118.
115. Hua, Y.J., Tu, K.,Tang, Z.Y., Li, Y.X., Xiao, H.S. (2008). Comparison of normalization methods with microRNA microarray. *Genomics, 92:* 122–128.
116. Huang, W.T., Kuo, S.H., Cheng, A.L., Lin, C.W. (2014). Inhibition of ZEB1 by miR-200 characterizes Helicobacter pylori-positive gastric diffuse large B-cell lymphoma with a less aggressive behavior. *Modern Pathology, 27:* 1116 – 1125.
117. Huang, J., Wang, F., Argyris, E., *et al.* (2007). Cellular microRNAs contribute to HIV-1 latency in resting primary $CD4^+$ T lymphocytes. *Nature Medicine, 13*(10): 1241 – 1247.

118. Huang, H., Gu, J., Yao, S., *et al.* (2015). MicroRNAs are related to rituximab in combination with cyclophosphomide, doxorubicin, vincristine and prednisone resistance in patients with Diffuse Large B-cell Lymphoma. *Cancer Translational Medicine, 1*(1): 6 – 10.
119. Hurley, J., Roberts, D., Bond, A., Keys, D. and Chen, C. (2011). Stem-loop RT-qPCR for microRNA expression profiling. *Methods in molecular biology, 822*: 33 – 52.
120. Hurteau, G.J., Carlson, J.A., Spivack, S.D. and Brock, G.J. (2007). Overexpression of the microRNA hsa-miR-200c leads to reduced expression of transcription factor 8 and increased expression of E-cadherin. *Cancer research*, *67*(17): 7972 – 7976.
121. Huysentruyt, L.C., & McGrath, M.S. (2010). The role of macrophages in the development and progression of AIDS-related non-Hodgkin lymphoma. *Journal of Leukocyte Biology, 87:* 627 – 632.
122. Ibrahim, F.F., Jamal, R., Syafruddin, S.E., *et al.* (2015). microRNA-200c and microRNA-31 regulate proliferation, colony formation, migration and invasion in serous ovarian cancer. *Journal of Ovarian Research, 8*(56): 1 – 14.
123. Iqbal, J., Shen, Y., Huang, X., *et al.* (2015). Global microRNA expression profiling uncovers molecular markers for classification and prognosis in aggressive B-cell lymphoma. *Blood,* doi:10.1182/blood-2014-04-566778.
124. Jacobson, M.A., Khayam-Bashi, H., Martin, J.N., *et al.* (2002) Effect of long-term highly active antiretroviral therapy in restoring HIV-induced abnormal B-lymphocyte function. *Journal of Acquired Immune Deficiency Syndrome, 31:* 472–477.
125. Jima, D.D., Zhang, J., Jacobs, C., *et al.* (2010). Deep Sequencing of the small RNA transcriptome of normal and malignant human B cells identifies hundreds of novel microRNAs. *Blood, 116:* e118 – e127.
126. Johnson, S.M., Grosshans, H., Shingara, J., *et al.* (2005). RAS is regulated by the let-7 microRNA family. *Cell, 120:* 635 – 647.
127. Johnston, R.J., & Hobert, O. (2003). A microRNA controlling left/right neuronal asymmetry in *Caenorhabditis elegans*. *Nature, 426:* 845 – 549.
128. Jopling, C.L., Yi, M., Lancaster, A.M., *et al*. (2005). Modulation of Hepatitis C virus RNA abundance by a liver specific microRNA. *Science, 309:* 1577. Doi:10.1126/science.1113329.
129. Jorgensen, S., Tholstrup, D., Hansen, J.W., *et al.* (2014). Plasma microRNA predicts B-cell lymphoma up to 12 months before diagnosis – data from the Danish blood donor group. *Blood, 124*: 708.
130. Kaul, D., Ahlawat, A., Gupta, S.D. (2009). HIV-1 genome-encoded hiv1-mir-H1 impairs cellular responses to infection. *Molecular Cell Biochemistry, 323:* 143 – 148.

131. Kerr, M. K. (2003). Design considerations for efficient and effective microarray studies. *Biometrics, 59:* 822 – 828.
132. Kincaid, R.P., Burke, J.M., Sullivan, C.S. (2012). RNA virus microRNA that mimics a B-cell oncomiR. *Proceedings of National Academy of Sciences, 109*(8): 3077 - 3082.
133. Klase, Z., Houzet, L., Jeang, K.T. (2012). MicroRNAs and HIV-1: Complex interactions. *The Journal of Biological Chemistry, 287*(49): 40884 – 40890.
134. Klase, Z., Sampey, G., Kashanchi, F. (2013). Retrovirus infected cells contain viral microRNAs. *Retrovirology, 10*(1): 15.
135. Klotman, M.E., Kim, S., Buchbinder, A., *et al*. (1991). Kinetics of expression of multiply spliced RNA in early human immunodeficiency virus type 1 infection lymphocytes and monocytes. *Proceedings of the National Academy of Sciences USA, 88:* 5011 – 5015.
136. Kong, K.Y., Owens, K.S., Rogers, J.H., *et al.* (2010). MiR-23A microRNA cluster inhibits B-cell development. *Experimental Haematology, 38:* 629 – 640.
137. Krek, A., Grun, D., Poy, M.N., *et al.* (2005). Combinatorial microRNA target predictions. *Nature Genetics, 37*(5): 495 – 500.
138. Krichevsky, A.M., King, K.S., Donahue, C.P., Khrapko, K. and Kosik, K.S. (2003). A microRNA array reveals extensive regulation of microRNAs during brain development [Erratum (2004) RNA, 10, 551.]. RNA, 9: 1274–1281.
139. Kuhn, D.E., Martin, M.M., Feldman, D.S., Terry, A.V., Nuovo, G.J. and Elton, T.S., (2008). Experimental validation of miRNA targets. *Methods*, *44*(1): 47 – 54.
140. Kumar, M.S., Lu, J., Mercer, K.L., *et al.* (2007). Impaired microRNA processing enhances cellular transformation and tumorigenesis. *Nature Genetics, 39* (5): 673 – 677.
141. Kuroda, K., Fukuda, T., Krstic-Demonacos, M., *et al.* (2017). miR-663a regulates growth of colon cancer cells, after administration of antimicrobial peptides, by targeting CXCR4-p21 pathway. *BMC Cancer, 17:*33, DOI 10.1186/s12885-016-3003-9.
142. Lagos-Quintana, M., Rauhut, R., Lendeckel, W., Tuschl, T. (2001). Identification of novel genes coding for small expressed RNAs. *Science, 294*(5543): 853 – 858.
143. Lai, X., Wolkenhauer, O., Vera, J. (2016). Understanding microRNA-mediated gene regulatory networks through mathematical modelling. *Nucleic Acids Research, 44*(13): 6019 – 6035.
144. Lamers, S.L., Fogel, G.B., Huysentruyt, L.C., *et al.* (2010). HIV-Nef protein visits B-cell via macrophage nanotubes: a mechanism for AIDS-related lymphoma pathogenesis? *Current HIV Research, 8* (8): 638 – 640.

145. Lane, H.C., Masur, H., Edgar, L.C., *et al.* (1983). Abnormalities of B-cell activation and immunoregulation in patients with the acquired immunodeficiency syndrome. *New England Journal of Medicine, 309:* 453–458.
146. Lapenta, C., Santini, S.M., Logozzi, M., *et al.* (2003). Potent immune response against HIV-1 and protection from virus challenge in hu-PBL-SCID mice immunized with inactivated virus-pulsed dendritic cells generated in the presence of IFN-α. *Journal of Experimental Medicine, 198*(2): 361 – 367.
147. Lawrie, C.H. (2012). MicroRNAs and lymphomagenesis: a functional review. *British Journal of Haematology*, doi: 10.1111/bjh.12157.
148. Lawrie, C.H., Gal, S., Dunlop, H.M., *et al.* (2008). Detection of elevated level of tumour-associated microRNAs in serum of patients with diffuse large B-cell lymphoma. *British Journal of Haematology, 141:* 672 – 675.
149. Lecellier, C.H., Dunoyer, P., Arar, K., *et al.* (2005). A cellular microRNA mediates antiviral defence in human cells. *Science, 308:* 557 – 560.
150. Lee, Y., Joen, K., Lee, J.T., *et al.* (2002). MicroRNA maturation: stepwise processing and subcellular localization. *European Molecular Biology Organization Journal, 21:* 4663 – 4670.
151. Lee, J.E., Hong, E.J., Nam, H.Y., Hwang, M., Kim, J.H., Han, B.G. and Jeon, J.P. (2012). Molecular signatures in response to Isoliquiritigenin in lymphoblastoid cell lines. *Biochemistry and Biophysical Research Communications, 427:* 392–397.
152. Lee, R.C., Feinbaum, R.L., Ambros, V. (1993). The C. elegans heterochronic gene *lin-4* encodes small RNAs with antisense complementarity to *lin-14*. *Cell, 75:* 843 – 854.
153. Lehmann, M.H., Walter, S., Ylisastigui, L., *et al.* (2006). Extracellular HIV-1 Nef increases migration of monocytes. *Experimental Cell Research, 312:* 3659 – 3668.
154. Lenz, G., Wright, G.W., Tolga Emre, N.C., *et al.* (2008). Molecular subtypes of diffuse large B-cell lymphoma arise by distinct genetic pathways. *Proceedings of the National Academy* of *Science, 15* (36): 13520 – 13525.
155. Lenze, D., Leonicini, L., Hummel, M., *et al.* (2011). The different epidemiologic subtypes of Burkitt's Lymphoma share a homogenous microRNA profile distinct from diffuse large B-cell lymphoma. *Leukemia, 25*(12): 1869 – 1876.
156. Leucci, E., Cocco, M., Onnis, A., *et al.* (2008). MYC translocation-negative classical Burkitt lymphoma cases: an alternative pathogenetic mechanism involving miRNA deregulation. *Journal of Pathology, 216*(4): 440–450.

157. Leucci, E., Onnis, A., Cocco, M., *et al.* (2010). B-cell differentiation in EBV-positive Burkitt lymphoma is impaired at posttranscriptional level by miRNA-altered expression. *International Journal of Cancer, 126*(6): 1316–1326.
158. Le Sage, C., Nagel, R., Egan, D.A., *et al.* (2007). Regulation of the p27(Kip1) tumor suppressor by miR-221 and miR-222 promotes cancer cell proliferation. *The EMBO Journal, 26*(15): 3699 – 3708.
159. Li, X., Kong, X., Wang, Y., & Yang, Q. (2013). BRCC2 inhibits breast cancer cell growth and metastasis in vitro and in vivo via downregulating AKT pathway. *Cell Death & Disease*, *4*(8): e757.
160. Li, X., Su, P., Liu, X. *et al.* (2014). Aberrant BLID expression is associated with breast cancer progression. Tumor Biology, 35: 5449.
161. Li, S., Bozzo, L., Wu, Z*., et al.* (2010). The HIV-1 matric protein p17 activates the transcription factors c-Myc and CREB in human B cells. *New Microbiologica, 33:* 13 – 24.
162. Lim, E.L. & Marra, M.A. (2013). MicroRNA dysregulation in B-cell non-Hodgkin lymphoma. *Blood and Lymphatic Cancer: Targets and Therapy, 3:* 25 – 40.
163. Lim, S.T., Karim, R., Nathwani, B.N., *et al*. (2005). AIDS-related Burkitt's lymphoma versus Diffuse Large B-cell lymphoma in the pre-highly active antiretroviral therapy (HAART) and HAART eras: Significant differences in survival with standard chemotherapy. *Journal of Clinical Oncology, 23* (19): 4430 – 4438.
164. Lim, E.L., Tring, D.L., Scott, D.W., *et al.* (2015). Comprehensive miRNA sequence analysis reveals survival differences in diffuse large B-cell lymphoma patients. *Genome Biology, 16:* 18, doi:10.1186/s13059-014-0568-y.
165. Linda, W., Lee, K., Russell, I., Chen, C. (2010). Endogenous controls for real-time quantitation of miRNA using Taqman microRNA assays. Applied Biosystems, Application Note. Available from http://tools.thermofisher.com/content/sfs/brochures/cms_044972.pdf
166. Liu, B., Li, J., Cairns, M.J. (2012). Identifying miRNAs, targets and functions. *Briefings in Bioinformatics, 15* (1): 1 – 19.
167. Livak, K.J. and Schmittgen, T.D. (2001) Analysis of relative gene expression data using real-time quantitative PCR and the $2^{-\Delta\Delta Ct}$ method. *Methods, 25:* 402–408.
168. Lu, J., Getz, G., Miska, E.A., *et al.* (2005). MicroRNA expression profiles classify human cancers. *Nature, 435* (9): 834 – 838.

169. Luzzi, A., Morettini, F., Gazaneo, S., *et al.* (2014). HIV-1 Tat induces DNMT over-expression through microRNA dysregulation in HIV-related non Hodgkin lymphomas. *Infectious Agents and Cancer, 9:* 41.

170. Lytle, J.R., Yario, T.A., Steitz, J.A. (2007). Target mRNAs are repressed as efficiently by microRNA-binding sites in the 5' UTR as in the 3' UTR. *Proceedings of National Academy of Science USA, 104*(23): 9667 – 9672.

171. Ma, L., Shen, C.J., Cohen, E.A., *et al.* (2014). miRNA-1236 inhibits HIV-1 infection of monocytes by repressing translation of cellular factor VprBP. *Public Library of Science ONE, 9* (6): e99535, doi:10.1371/journal.pone.0099535.

172. Ma, C., Zhan, C., Yuan, H., Cui, Y., & Zhang, Z. (2016). MicroRNA-603 functions as an oncogene by suppressing BRCC2 protein translation in osteosarcoma. *Oncology Reports, 35:* 3257 – 3264.

173. Malumbres, R., Sarosiek, K.A., Cubedo, E., *et al.* (2009). Differentiation stage-specific expression of microRNAs in B lymphocytes and diffuse large B-cell lymphomas. *Blood, 113:* 3754 – 3764.

174. Mangani, D., Roberti, A., Rizzolio, F., Giordano, A. (2013). Emerging molecular networks in Burkitt's lymphoma. *Journal of Cellular Biochemistry, 114:* 35 – 38.

175. Martelli, M., Fererri, A.J.M., Agostinelli, C., *et al.* (2013). *Critical Reviews in Oncology/Haematology*, http://dx.doi.org/10.1016/j.critrevonc.2012.12.009.

176. Manterola, L., Fernandez-Mercado, M., Larrea, E., *et al.* (2015). MicroRNAs as B-cell lymphoma biomarkers. Blood and Lymphatic Cancer: *Targets and Therapy. 5:* 25 – 34.

177. Mazan-Mamczarz, K. & Gartenhaus, R.B. (2013). Role of microRNA deregualtion in the pathogenesis of diffuse large B-cell lymphoma (DLBCL). *Leukemia Research, 37:* 1420 – 1428.

178. Martinson, J.A., Roman-Gonzalez, A., Tenoria, A.R. *et al.* (2007). Dendritic cells from HIV-1 infected individuals are less responsive to toll-like receptor (TLR) ligands. *Cellular Immunology, 250:* 75 – 84.

179. Masotti, A., Donninelli, G., Da Sacco, L., *et al.* (2015). HIV-1 gp120 influences the expression of microRNAs in human monocyte-derived dendritic cells via STAT3 activation. *BMC Genomics, 16:* 480, doi:10.1186/s12864-015-1673-3.

180. Mdletshe, N. (2015). The role of HIV proteins Tat and Nef in HIV/AIDS-related lymphoma: effects on *c-MYC* and *AID* expression. Masters Thesis, University of Cape Town, South Africa.

181. Medina, R., Zaidi, S.K., Liu, C.G., *et al.* (2008). MicroRNAs 221 and 222 bypass quiescence and compromise cell survival. *Cancer Research, 68:* 2773 – 2780.

182. Mestdagh, P., Van Vlierberghe, P., De Weer, A., *et al.* (2009). A novel and universal method for microRNA RT-qPCR data normalization. *Genome Biology*, *10*(6): R64.

183. Meyer, S.U., Pfaffl, M.W., Ulbrich, S.E. (2010). Normalisation strategies for microRNA profiling experiments: a 'normal' way to a hidden layer of complexity? *Biotechnology Letters, 32(*12): 1777 – 1788.

184. Miller, T.E., Ghoshal, K., Ramaswamy, B., *et al.* (2008). MicroRNA-221/222 confers tamoxifen resistance in breast cancer by targeting p27Kip1. *Journal of Biological Chemistry, 283:* 29897 – 298903.

185. Monteleone, K., Selvaggi, C., Cacciotti, G., *et al.* (2015). MicroRNA-29 family expression and its relation to antiviral immune response and viro-immunological markers in HIV-1 infected patients. *BMC Infectious Diseases, 15:* 51.

186. Moir, S., Malaspina, A., Li, Y., Chun, T.W., Lowe, T., *et al.* (2000) B cells of HIV-1-infected patients bind virions through CD21-complement interactions and transmit infectious virus to activated T cells. *Journal of Experimental Medicine, 192:* 637–646.

187. Moir, S., & Fauci, A.S. (2009). B cells in HIV infection and disease. *Nature Review Immunology, 9* (4): 235 – 245. Doi:10.1038/nri2524.

188. Montes-Moreno, S., Martinez, N., Sanchez-Espiridion, B., Diaz-Uriarte, R., *et al.* (2011). miRNA expression in diffuse large B-cell lymphoma treated with chemoimmunotherapy. *Blood, 118*: 1034 – 1040.

189. Moore, J.P., Trkola, A., Dragic, T. (1997). Co-receptors for HIV-1 entry. *Current Opinion on Immunology, 9:* 551 – 562.

190. Morey, J.S., Ryan, J.C., Van Dolah, F.M. (2006). Microarray validation: factors influencing correlation between oligonucleotide microarrays and real-time PCR. *Biological Procedures online, 8:*175 – 193.

191. Mowla, S., Pinnock, R., Leaner, V. D., Goding, C. R. and Prince, S. (2011). PMA-induced up-regulation of TBX3 is mediated by AP-1 and contributes to breast cancer cell migration. *The Biochemical Journal*, *433*(1):145 – 153.

192. Müller, A.M., Ihorst, G., Mertelsmann, R. and Engelhardt, M. (2005). Epidemiology of non-Hodgkin's lymphoma (NHL): trends, geographic distribution, and etiology. *Annals of Haematology*, *84*(1): 1 – 12.

193. Munshi, S.U., Panda, H., Holla, P., *et al*. (2014). MicroRNA-150 is a potential biomarker of HIV/AIDS disease progression and therapy. *Public Library of Science ONE, 9*(5): e95920, doi:10.1371/journal.pone.0095920.

194. Mureith, M.W., Chang, J.J., Lifson, J.D., Ndung'u, T. and Altfeld, M. (2010). Exposure to HIV-1 encoded TLR8 ligands enhances monocytes response to microbial encoded TLR2/4 ligands. *AIDS*, *24*(12): 1841.

195. Nam, E.J., Kim, S., Lee, T.S., *et al.* (2016). Primary and recurrent ovarian high-grade serous carcinomas display similar microRNA expression patterns relative to those of normal ovarian tissue. *Oncotarget, 7*(43): 70524 – 70535.

196. Nathans, R., Chu, C., Serquina, A.K., *et al.* (2009). Cellular microRNA and P bodies modulate host HIV-1 interactions. *Molecular Cell, 34:* 696 – 709.

197. Nazli, A., Chan, O., Dobson-Belaire, W.N., Ouellet, M., Tremblay, M.J., Gray-Owen, S.D., *et al.* (2010) Exposure to HIV-1 Directly Impairs Mucosal Epithelial Barrier Integrity Allowing Microbial Translocation. *PLoS Pathog 6*(4): e1000852.

198. Ni, H., Tong, R., Zou, L., *et al.* (2016). MicroRNAs in diffuse large B-cell lymphoma (Review). *Oncology Letter, 11:* 1271 – 1280.

199. Nicholas, K.J., Zern, E.K., Barnett, L., *et al.* (2013). B cell responses to HIV antigen are a potent correlate of viremia in HIV-1 infection and improve with PD-1 blockade. *PloS one*, *8*(12): e84185.

200. Nie, Y., Waite, J., Brewer F., *et al.* (2004). The Role of CXCR4 in Maintaining Peripheral B-Cell Compartments and Humoral Immunity. *The Journal of Experimental Medicine, 200* (9), 1145 – 1156.

201. Nossal, G, J.V. (2003). The double helix and immunology. *Nature, 421:* 440 – 444.

202. O' Neill, M., McPartlin, J., Arthure, K., Riedel, S. and McMillan, N.D., (2011). Comparison of the TLDA with the Nanodrop and the reference Qubit system. In *Journal of Physics: Conference series* (Vol. 307, No. 1, p. 012047). IOP Publishing.

203. Omoto, S., Ito, M., Tsutsumi, Y., *et al.* (2004). HIV-1 nef suppression by virally encoded microRNA. *Retrovirology 1* (1): 44.

204. Omoto, S. & Fujii, Y.R. (2005). Regulation of human immunodeficiency virus 1 transcription by nef microRNA. *Journal of General Virology, 86:* 751 – 751.

205. Onnis, A., De Falco, G., Antonicelli, G., *et al.* (2010). Alteration of microRNAs regulated by c-Myc in Burkitt's lymphoma. *Public Library of Science, 5* (9): e12960.

206. Orecchini, E., Doria, M., Michienzi, A., *et al.* (2014). The HIV-1 Tat protein modulates CD4 expression in human T cells through the induction of miR-222. *RNA Biology, 11* (4): 1 – 5.

207. Osterburg, H.H., Allen, J.K., Finch, C.E. (1975). The use of ammonium acetate in the precipitation of ribonucleic acid. *Biochemistry Journal, 147:* 367 – 368.
208. Ott, G., Rosenwald, A., Campo, E. (2013). Understanding MYC-driven aggressive B cell lymphomas: pathogenesis and classification. *Blood, 122:* 3884 – 3891.
209. Palanichamy, J.K. and Rao, D.S. (2014). miRNA dysregulation in cancer: towards a mechanistic understanding. *Frontiers in Genetics*, *5*: 54.
210. Pasquinelli, A.E. (2012). MicroRNAs and their targes: recognition, regulation and an emerging reciprocal relationship. *Nature Genetics Review, 13:* 271 – 282.
211. Patel, M., Philip, V., Omar, T., *et al.* (2015). The impact of human immunodeficiency virus infection (HIV) on lymphoma in South Africa. *Journal of Cancer Therapy, 6:* 527 – 535.
212. Pasquinelli, A.E., Reinhart, B.J., Slack, F.J., *et al.* (2000). Conservation of the sequence and temporal expression of let-7 heterochronic regulatory RNA. *Nature, 408:* 86 – 89.
213. Perise´-Barrios, A.J., Mun˜oz-Fernandez, M.A., Pion, M. (2012). Direct Phenotypical and Functional Dysregulation of Primary Human B Cells by Human Immunodeficiency Virus (HIV) Type 1 *In Vitro*. *Public Library of Science, ONE 7* (7): e39472. doi:10.1371/journal.pone.0039472.
214. Peterson, S.M., Thompson, J.A., Ufkin, M.L., *et al.* (2014). Common features of microRNA target prediction tools. *Frontiers in Genetics*, *5*: 23.
215. Pfeffer, S., Sewer, A., Lagos-Quintana, M., *et al.* (2005). Identification of microRNAs of the herpesvirus family. *Nature Methods,* doi:10.1038/NMETH746.
216. Pizzimenti, S., Ferracin, M., Sabbioni, S., *et al.* (2009). MicroRNA expression changes during human leukemic HL-60 cell differentiation induced by 4-hydroxynonenal, a product of lipid peroxidation. *Free Radical Biology Medicine, 46:* 282–288.
217. Poliseno, L., Tuccoli, A., Mariani, L., *et al.* (2006). MicroRNAs modulate the angiogenic properties of HUVECs. *Blood, 108:* 3068 – 3071.
218. Pritchard, C.C., Cheng, H.H., Tewari, M. (2012). MicroRNA profiling: approaches and considerations. *Nature Review Genetics, 13*(5): 358 – 369.
219. Puvvada, S., Kendrick, S., Rimsza, L. (2013). Molecular classification, pathway addiction, and therapeutic targeting in diffuse large B-cell lymphoma. *Cancer Genetics, 206*: 257 – 265.
220. Qiao, J., Lee, S., Paul, P., Theiss, L., Tiao, J., Qiao, L., *et al.* (2013). miR-335 and miR-363 regulation of neuroblastoma tumorigenesis and metastasis. *Surgery, 154*(2): 226 – 233.
221. Rana, T.M., & Jeang, K.T. (1999). Biochemical and functional interactions between HIV-1 Tat protein and TAR RNA. *Archives of Biochemistry & Biophysiology, 365:* 175–185.

222. Rays, M., Chen, Y., Su, Y.A. (1996). Use of a cDNA microarray to analyse gene expression patterns in human cancer. *Nature Genetics. 14:* 457–460.

223. Reinhart, B.J., Slack, F.J. Basson, M.*, et al*. (2000). The 21-nucelotide let-7 RNA regulates developmental timing in *Caenorhabditis elegans*. *Nature, 403:* 901 – 906.

224. Reynoso, R., Laufer, N., Hackl, M., *et al.* (2014). MicroRNAs differentially present in the plasma of HIV elite controllers reduce HIV infection in vitro. *Scientific Reports, 4:* 5915, doi:10.1038/srep05915.

225. Riss, T.L., Moravec, R.A., Niles, A.L., et al. (2013). Cell Viability Assays. In Sittampalam, G.S., Coussens, N.P., Brimacombe, K., et al. (Eds). Assay Guidance Manual. Bethesda: Eli Lilly & Company & National Centre for Advancing Translational Sciences.

226. Roberts, A., Lewis, A., Jopling, C. (2011). The role of miRNAs in viral infection. Progress in Molecular Biology and Translational *Science, 102*: 101 – 139.

227. Robertus, J.L., Kluiver, J., Weggemans, C., *et al.* (2010). MiRNA profiling in B non-Hodgkins lymphoma a MYC-related miRNA profile characterises Burkitt lymphoma. *British Journal of Haematology, 149*(6): 896 – 899.

228. Roehle A., Hoefig, K.P., Repsilber, D., *et al*. (2008). MicroRNA signatures characterize diffuse large B-cell lymphomas and follicular lymphomas. *British Journal of Haematology, 142:* 732 – 744.

229. Rossio, J.L., Esser, M.T., Suryanarayan, K.*, et al*. (1998). Inactivation of Human Immunodeficiency Virus Type-1 infectivity with preservation of conformational and functional integrity of virion surface proteins. *Journal of Virology, 72*(10): 7992 – 8001.

230. Roth, W.W., Huang, M.B., Konadu, K.A., *et al.* (2016). MicroRNA in exosomes from HIV-1 infected macrophages. *International Journal of Environmental Research and Public Health, 13* (32): 1 – 9, doi:10.3390/ijerph12010032.

231. Roush, S., & Slack, F.J. (2008). The let-7 family of microRNAs. *Trends in Cellular Biology, 18:* 505–516.

232. Sampson, V.B., Rong, N.H., Han, J., *et al.* (2007). MicroRNA Let-7a down regulates MYC and reverts MYC-induced growth in Burkitt Lymphoma cells. *Cancer Research, 67* (20): 9762 – 9770.

233. Saparano, J.A. (2001). Clinical aspects and management of AIDS-related lymphoma. *European Journal of Cancer, 37:* 1296 – 1305.

234. Sand, M. (2014). The pathway of miRNA maturation. In Arenz, C (ed). *MiRNA Maturation: Methods & Protocols, Methods in Molecular Biology*. Springer Science & Business Media New York, *1095:* 1 – 10.

235. Sand, M., Skrygan, M., Georgas, D., *et al.* (2011). Expression levels of the microRNA maturing microprocessor complex component DGCR8 and the RNA-induced silencing complex (RISC) components Argonaute-1, Argonaute-2, PACT, TARBP1 and TARBP2 in epithelial skin cancer. *Molecular Carcinogenesis, 51:* 916 – 922.

236. Sandhu, S.K., Fassan, M., Volinia, S., *et al*. (2013). B-cell malignancies in microRNA Eμ-miR-17~92 transgenic mice. *Proceedings of National Academy of Science, 110* (45): 18208 – 18213.

237. Sassen, S., Miska, E.A., Caldas, C. (2008). MicroRNA – implications for cancer. *Virchows Archive, 452:* 1 – 10.

238. Schneider, C., Setty, M., Holmes, A.B., *et al.* (2014). microRNA 28 controls cell proliferation and is down-regulated in B-cell lymphomas. *Proceedings of the National Academy of Science, 111*(22): 8185 – 8190.

239. Schnittman, S.M., Clifford Lane, H., Higgins, S.E., *et al.* (1986). Direct polyclonal activation of human b lymphocytes by the acquired immune deficiency syndrome virus. *Science, 233* (4768): 1084 – 1086.

240. Schopman, N.C.T., Willemsen, M., Liu, Y.P., *et al.* (2012). Deep sequencing of virus-infected cells reveals HIV-encoded small RNAs. *Nucleic Acids Research, 40*(1): 414 – 427.

241. Seddiki, N., Phetsouphanh, C., Swaminathan, S., *et al.* (2013). The microRNA-9/B-lymphocyte-induced maturation protein-1/IL-2 axis is differentially regulated in progressive HIV infection. *European Journal of Immunology, 43:* 510 – 520.

242. Shepshelovich, D., Ram, R., Uziel, O., *et al.* (2015). MicroRNA signature is indicative of long term prognosis in diffuse large B-cell lymphoma. *Leukemia Research, 39:* 632 – 637.

243. Shipp, M.A., Harrington, D.P., Anderson, J.R. *et al*. (1993). A predictive model for aggressive Non-Hodgkin's Lymphoma, The International Non-Hodgkin's Lymphoma Prognostic Factors Project. *The New England Journal of Medicine, 329* (14): 987 – 994.

244. Skalsky, R. L. & Cullen, B. R. (2010). Viruses, microRNAs and host interactions. *Annual Review of Microbiology, 64:* 123 – 141.

245. Smith, P.K., Krohn, R.I., Hermanson, G.T., Mallia, A.K., Gartner, F.H., *et al*. (1985). Measurement of protein using bicinchoninic acid. *Analytical Biochemistry, 150*(1): 76 – 85.

246. Song, L., Liu, H., Gao, S., (2010). Cellular microRNAs inhibit replication of the H1N1 Influenza A virus in infected cells. *Journal of Virology, 84*(17): 8849 – 8860.

247. Spender, L.C., & Inman, G.J. (2014). Developments in Burkitt's lymphoma: novel cooperations in oncogenic MYC signalling. *Cancer Management and Research, 6:* 27 – 38.

248. Staudt, L.M. & Dave, S. (2005). The biology of human lymphoid malignancies revealed by gene expression profiling. *Advances in Immunology, 87*: 162 – 198.

249. Stinson, S., Lackner, M.R., Adai, A.T., *et al.* (2011). TRPS1 targeting by miR-221/222 promotes the epithelial-to-mesenchymal transition in breast cancer. *Science Signal*, *4*(177): 41.

250. Sun, Q., Zhang, J., Cao, W., Wang, X., Xu, Q., Yan, M., *et al.* (2013). Dysregulated miR-363 affects head and neck cancer invasion and metastasis by targeting podoplanin.

251. Sun, G., Li, H., Wu, X., *et al*. (2011). Interplay between HIV-1 infection and host miRNAs. *Nucleic Acids Research,* 1 – 16.

252. Sun, Y., Wu, J., Wu, S.H., Thakur, A., Bollig, A., Huang, Y., Joshua, L. D. (2008). Expression profile of microRNAs in c-Myc induced mouse mammary tumors. *Breast Cancer Research Treatment, 118:* 185 – 196.

253. Sung, T., & Rice, A. (2009). miR-198 inhibits HIV-1 gene expression and replication in monocytes and its mechanism of action appears to involve repression of cyclin T1. *Public Library of Science Pathology, 5:* e1000263.

254. Swaminathan, G, Navas-Martin, S., Martin-Garcia, J. (2013). MicroRNAs and HIV-1 Infection: Antiviral activities and beyond. *Journal of Molecular Biology, 426:* 1178 – 1197.

255. Swingler, S., Mann, A., Jacque, J., *et al.* (1999). HIV-1 Nef mediates lymphocyte chemotaxis and activation by infected macrophages. *Nature Medicine, 5* (9): 985–986.

256. Takamizawa, J., Konishi, H., Yanagisawa, K., *et al.* (2004). Reduced expression of the *let-7* microRNAs in human lung cancers in association with shortened postoperative survival. *Cancer Research, 64:* 3753 – 3756.

257. Tassano, E., Acquila, M., Tavella, E., Micalizzi, C., Panarello, C. and Morerio, C., (2010). MicroRNA-125b-1 and BLID upregulation resulting from a novel IGH translocation in childhood B-Cell precursor acute lymphoblastic leukemia. *Genes, Chromosomes and Cancer*, *49*(8): 682 – 687.

258. Tatarano, S., Chiyomaru, T., Kawakami, K., *et al.* (2011). miR-218 on the genomic loss region of chromosome 4p15.31 functions as a tumour suppressor in bladder cancer. *International Journal of Oncology, 39*: 13 – 21.

259. Taub, R., Kirsch, L., Morton, C., *et al*. (1982). Translocation of the c-myc gene into the immunoglobulin heavy chain locus in human Burkitt's lymphoma and murine plasmacytoma cells. *Proceedings of the National Academy of Sciences USA, 79* (24): 7837 – 7841.

260. Thapa, D.R., Li, X., Jamieson, B.D., *et al.* (2011). Overexpression of microRNAs from the miR-17-92 paralog clusters in AIDS-related non-Hodgkin's lymphomas. *Public Library of Science, 6* (6): e20781, doi:10.1371/journal.pone.0020781.

261. Thermo Fisher Scientific™. (2008). T009-TECHNICAL BULLETIN for NanoDrop 1000 & 8000. Available at http://www.nanodrop.com/Library/T009-NanoDrop%201000-&-NanoDrop% 208000-Nucleic-Acid-Purity-Ratios.pdf. Accessed 17 September 2015.

262. Thomson, D.W., Bracken, C.P. and Goodall, G.J. (2011). Experimental strategies for microRNA target identification. *Nucleic Acids Research*, *39*(16): 6845 – 6853.

263. Thornton, B., & Basu, C. (2011). Real-time PCR (qPCR) primer design using free online software. *Biochemistry and Molecular Biology Education, 39*(2): 145 – 154.

264. Titanji, K., De Milito, A., Cagigi, A., *et al.* (2006). Loss of memory B cells impairs maintenance of long-term serologic memory during HIV-1 infection. *Blood 108:* 1580–1587.

265. Troppan, K., Wenzl, K., Deutsch, A., *et al.* (2014). MicroRNAs in diffuse large B-cell lymphoma: Implications for pathogenesis, diagnosis, prognosis and treatment. *Anticancer Research, 34:* 557 – 564.

266. Triboulet, R., Mari, B., Lin, Y.L., *et al*. (2007). Suppression of microRNA-silencing pathway by HIV-1 during virus replication. *Science, 315:* 1579 – 1582.

267. Tsuji, S., Kawasaki, Y., Furukawa, S., Taniue, K., Hayashi, T., Okuno, M., Hiyoshi, M., Kitayama, J., Akiyama, T. (2014). The miR-363-GATA6-Lgr5 pathway is critical for colorectal tumourigenesis. *Nature Communications, 5*(3150): 1 – 12.

268. Udvardi, M.K., Czechowski, T., Scheible, W.R. (2008). Eleven golden rules of quantitative RT-PCR. *Plant Cell, 20:* 1736 – 1737.

269. United Nations AIDS. (2016). AIDS by the numbers – AIDS is not over, but it can be. Available from [http://www.unaids.org/en/resources/documents/2016/AIDS-by-the-numbers].

270. Vasilatou, D., Papageorgiou, S., Pappa, V., *et al.* (2009). The role of microRNAs in normal and malignant heamatopoiesis. *European Journal of Haematology, 84:* 1 – 16.

271. Vasudevan, S. (2011). Posttranscriptional upregulation by microRNAs. *Wiley Interdisciplinary Reviews: RNA, 3*(3): 311 – 330.

272. Viau, M., Veas, F., Zouali, M. (2007). Direct impact of inactivated HIV-1 virions on B lymphocyte subsets. *Molecular Immunology, 44:* 2124 – 2134.

273. Vishnu, P. & Aboulafia, D. M. (2012). AIDS-related non-Hodgkin's lymphoma in the era of highly active antiretroviral therapy. *Advances in Haematology*, 1 – 9,

274. Visione, R., Russo, L., Pallante, P., *et al.* (2007). MicroRNAs (miR)-221 and miR-222, both overexpressed in human thyroid papillary carcinomas, regulate p27Kip1 protein levels and cell cycle. *Endocrine Related Cancer, 14*:791 – 798.

275. Volinia, S., Calin, G.A., Liu, C.G.*, et al.* (2006). A microRNA expression signature of human solid tumors defines cancer gene targets. *Proceedings of the National Academy of Sciences USA, 103* (7): 2257 – 2261.

276. Von Ahlfen, S., and Schlumpberger, M. (2010). Effects of low A260/A230 ratios in RNA preparations on downstream applications. *QIAGEN Gene Expression Newsletter*, *15*: 6 – 7.

277. Wang, C., & Castillo, J.J. (2011). Management of HIV-associated lymphomas. *Medicine and Health/Rhode Island, 94* (1): 4 – 6.

278. Wang, W., Zhang, L., Zheng, K., & Zhang, X. (2016). miR-17-5p promotes the growth of osteosarcoma in a BRCC2-dependent mechanism. *Oncology Reports, 35*: 1473 – 1482.

279. Wang, H.W., Noland, C., Siridechadilok, B., *et al*. (2009). Structural insights into RNA processing by the human RISC-loading complex. *Nature Structural & Molecular Biology, 16:* 1148 – 1153.

280. Wang, B., Howel, P., Bruheim, S., Ju, J., Owen, L.B., *et al.* (2011). Systematic evaluation of three microRNA profiling platforms: microarray, beads array, and quantitative real time PCR array. *PLoS ONE, 6*(2): e17167.

281. Wang, B, Wang, X.F., Howell, P., Qian, X., Huang, K., *et al.* (2010). A personalised microRNA microarray normalised method using a logistic regression model. *Bioinformatics, 26:* 228 – 234.

282. Wang, B., & Xi, Y. (2013). Challenges for microRNA microarray data analysis. *Microarrays, 2:* 34 – 50.

283. Wang, H., Yan, C., Shi, X., *et al.* (2015). MicroRNA-575 targets BLID to promote growth and invasion of non-small cell lung cancer cells. *FEBS Letters, 589:* 805 – 811.

284. Whisnant, A.W., Bogerd, H.P., Flores, O., *et al.* (2013). In-depth analysis of the interaction of HIV-1 with cellular microRNA biogenesis and effector mechanisms. *Molecular Biosystems, 4* (2): e00193-13.

285. Witkos, T.M., Koscianska, E. and Krzyzosiak, J.W. (2011). Practical aspects of microRNA target prediction. *Current Molecular Medicine*, *11*(2): 93 – 109.

286. Witwer, K. W., Watson, A. K., Blankson, J. N., *et al.* (2012). Relationships of PBMC microRNA expression, plasma viral load, and CD41T-cell count in HIV- 1-infected elite suppressors and viremic patients. *Retrovirology 9:* 5.

287. Wong, W., Farr, R., Joglekar, M., Januszewski, A., Hardikar, A. (2015). Probe-based Real-time PCR Approaches for Quantitative Measurement of microRNAs. *Journal of Visualised. Experiments, 98:* e52586.

288. Wu, S., Huang, S., Ding, J., *et al.* (2010). Multiple microRNAs modulate p21Cip1/Waf1 expression by directly targeting its 3' untranslated region. *Oncogene, 29*(15): 2302 – 2308.

289. Xi, Q., Huang, M., Wang, Y., *et al*. (2015). The expression of CDK1 is associated with proliferation and can be a prognostic factor in epithelial ovarian cancer. *Tumor Biology*, *36*(7): 4939 – 4948.

290. Xue, M., Yao, S., Hu, M., *et al.* (2014). HIV-1 Nef and KSHC oncogene K1 synergistically promote angiogenesis by inducing cellular miR-718 to regulate the PTEN/AKT/mTOR signaling pathway. *Nucleic Acids Research*, doi:10.1093/nar/gku583.

291. Yamagishi, M., Katano, H., Hishima, T., *et al.* (2015). Coordinated loss of microRNA group causes defenseless signaling in malignant lymphoma. *Science Reports, 5*: 17868.

292. Yan, Q., Ma, X., Shen, C., *et al.* (2014). Inhibition of Kaposi's sarcoma-associated herpesvirus lytic replication by HIV-1 Nef and cellular microRNA has-miR-1258. *Journal of Virology, 88* (9): 4987 – 5000.

293. Yao, Y., Suo, A.L., Li, Z.F., *et al.* (2009). MicroRNA profiling of human gastric cancer. *Molecular Medicine Reports, 2*(6): 963 – 970.

294. Yekta, S., Shih, I.H., Bartel, D.P. (2004). MicroRNA-directed cleavage of HOXB8 mRNA. *Science, 304*(5670): 594 – 596.

295. Yin, Q., McBride, J., Fewell, C., Lacey, M., Wang, X., Lin, Z., Cameron, J., Flemington, E.K. (2008). MicroRNA-155 is an Epstein-Barr Virus-induced gene that modulates Epstein-Barr Virus-regulated gene expression pathways. *Journal of Virology, 82*(11): 5295 – 5306.

296. Yeung, M.L., Bennasser, Y., Myers, T.G., *et al.* (2005). Changes in microRNA expression profiles in HIV-1 transfected human cells. *Retrovirology, 2:* 81 – 89.

297. Yu, X., & Li, Z. (2015). BLID: A novel tumour-suppressor gene. *Oncology Research,*22: 333 – 338.

298. Yeung, M.L., Benasser, Y., Watashi, K., *et al*. (2009). Pyrosequencing of small non-coding RNAs in HIV-1 infected cells: evidence for the processing of a viral-cellular double-stranded RNA hybrid. *Nucleic Acids Research Advance,* 1 – 12, doi:10.1093/nar/gkp707.

299. Young, L., Sung, J., Stacey, G., Masters, J.R. (2010). Detection of Mycoplasma in cell cultures. Nature Protocols, 5(5): 929 – 934.

300. Zhang, Y., Fan, M., Gen, G., *et al.* (2014). A novel HIV-1 encoded microRNA enhances its viral replication by targeting the TATA box region. *Retrovirology, 11* (23): 1 – 15.

301. Zhang, Z., Gerhard, D.S., Nguyen, L., *et al.* (2005). Fine mapping and evaluation of candidate genes for cervical cancer on 11q23. *Genes, Chromosomes and Cancer*, *43*(1): 95 – 103.
302. Zhang, C.Z., Zhang, J.X., Zhang, A.L., Shi, Z.D., *et al.* (2010). miR-221 and miR-22 target PUMA to induce cell survival in glioblastoma. *Molecular Cancer, 9:* 229.
303. Zhao, J.J., Lin, J., Yang, H., *et al.* (2008). MicroRNA-221/222 negatively regulates estrogen receptor alpha and is associated with tamoxifen resistance in breast cancer. *Journal of Biological Chemistry, 283*: 31079-31086.
304. Zheng, Z., Li, X., Zhu, Y., Gu, W., Xie, X., Jiang, J. (2016). Prognostic significance of miRNA in patients with Diffuse Large B-Cell Lymphoma: a Meta-Analysis. *Cellular Physiology and Biochemistry, 39:* 1891 – 1904.
305. Zhou, P., Xu, W., Peng, X., *et al.* (2013a). Large-scale screens of miRNA-mRNA interactions unveiled that the 3′ UTR of a gene is targeted by multiple miRNAs. *PLoS One*, *8*(7): p.e68204.
306. Zhou, F., Xue, M., Qin, D., *et al*. (2013b). HIV-1 Tat promotes KSHV vIL-6-induced angiogenesis and tumourigenesis by regulating PI3K/PTEN/AKT/GSK-3β signalling pathway. *Public Library of Science ONE, 8* (1): e53145, doi:10.1371/journal.pone.0053145.
307. Ziegler, B.L. (1982). Burkitt's lymphoma. *Cancer Journal for Clinicians, 32* (3): 144 – 146.
308. Zhu, L., Qui, C., Qui, C., *et al.* (2012). MicroRNA profile identifies different outcomes of disease progression at later stage of HIV infection. XIX IAS Conference, Washington DC.
309. Zhu, Y., Peng, Q., Lin, Y., *et al.,* (2017). Identification of biomarker microRNAs for predicting the response of colorectal cancer to neoadjuvant chemotherapy based on microRNA regulatory network. *Oncotarget, 8*(2): 2233 – 2248

# APPENDIX

## APPENDIX A: RECIPES AND REAGENTS

### Tissue Culture

*Complete growth media for Ramos cell line*

Add 5 mL (10%) of FBS and 0.5 mL of P/S to a 50 mL Falcon tube

Fill up to 50 mL with RPMI media and mix

Store at 4°C until needed

*Complete growth media for L1439A cell line*

Add 10 mL (20%) of FBS and 0.5 mL of P/S to a 50 mL Falcon tube

Fill up to 50 mL with DMEM media and mix

Store at 4°C until needed

*Low serum media for pre-treatment*

Add 0.25 mL of FBS and 0.5 mL of P/S to a 50 mL Falcon tube

Fill up to 50 mL with RPMI media and mix before plating

*70% Ethanol*

Add 700 mL of 100% ethanol to a bottle and fill up to 1 L with autoclaved $H_2O$

*0.1% diethyl pyrocarbonate- (DEPC) treated water*

Fill a 5 L beaker with autoclaved water and add 1 mL of DEPC per 500 mL of $H_2O$

Add a magnetic stirrer bar and place on the stirrer for a few hours (3-5 hrs)

Place the beaker in the fume hood overnight, remove the stirrer bar and autoclave to inactivate the remaining DEPC

Store the $H_2O$ at room temperature until needed

*0.1% diethyl pyrocarbonate- (DEPC) to treat plasticware*

Fill 5 L beaker with $H_2O$ and add 1 mL of DEPC per 1 L of $H_2O$

Add stirrer bar and plasticware (pipette tips, centrifuge tubes)

Place in the stirrer for a few hours (3-5 hrs)

Place beaker in fume hood overnight

Remove the pipette tips from the $H_2O$ and allow to air dry before autoclaving

*Trypsin-EDTA*

Dissolve 8 g NaCl; 1,26 g $Na_2HPO_4$; 0,2 g KCl; 0.2 g $KH_2PO_4$; 0.5 g Trypsin and 0.5 g EDTA in 800 mL deionized $H_2O$

Adjust to pH 7.4

Filter using a 0.2 μM membrane

Aliquot into 250 mL bottles and autoclave

Store at 4°C

**Mycoplasma Testing**

*Fixative*

A ratio of 1:3 glacial acetic acid: Methanol

Store at 4°C

*Mounting Fluid*

Mix 22.2 mL 0.1 M citric acid; 27.8 mL 0.2 M $Na_2HPO_4.2H_2O$ and 50 mL glycerol

Adjust to pH 5.5

**RNA Extraction**

*10X Tris/Borate/EDTA (TBE) buffer*

108 g Tris

55 g Boric acid

Dissolve in 900 mL $H_2O$

Add 40 mL (0.5M pH 8)

Adjust to 1 L

Store at room temperature

*1X TBE*

Measure 100 mL of 10X TBE stock

Fill up to 1 L using autoclaved $H_2O$

*2X RNA loading buffer (1 mL)*

Add 900 µL formamide; 99 µL sucrose; 0.5 µL Bromophenol Blue and 0.5 µL Xylene Cyanol
Store at room temperature

*10X DNA loading dye*
Mix 0.025 g of Xylene cyanol; 0.025 g of Bromophenol Blue; 1.25 mL of 10% SDS; 12.5 mL of glycerol
Dissolve in 6.25 mL of $H_2O$
Store at room temperature

*1%/1.5% agarose gel*
Weigh 1 g/1.5 g agarose in 100 mL 1X TBE
Dissolve all the agarose by heating using a microwave
Allow to cool and then add 6 µL Ethidium Bromide (EtBr, 0.5mg/mL)
Pour gel on tray and allow to set

**Protein Extraction**
*RIPA Buffer (50 mL)*
Mix 1.5 mL 150 nM NaCl; 0.5 mL 1% Triton X100; 0.5 mL 0.1% SDS; 0.5 mL 10 mM Tris pH 7.5; 0.5 g 1% deoxycholate powder
Make up volume to 50 mL with deionized $H_2O$

*7X protease inhibitor*
Add 1 protease inhibitor tablet with 2.5 mL 1X PBS

*RIPA solution*
Combine 858 µL RIPA buffer with 142 µL 7X protease inhibitor

**SDS-PAGE Reagents**
*1.5M Tris pH 6.8*
Dissolve 60.5 g Tris base in 300 mL deionized $H_2O$
Adjust pH to 6.8 with concentrated HCl and volume to 500 mL with deionized $H_2O$
Store at 4°C

*1.5M Tris pH 8.8*

Dissolve 60.5 g Tris base in 300 mL deionized $H_2O$

Adjust pH to 8.8 with concentrated HCl and volume to 500 mL with deionized $H_2O$

Store at 4°C

*10% Sodium dodecyl sulphate (SDS)*

Dissolve 10 g sodium dodecyl sulphate crystals in 90 mL $H_2O$

Adjust volume to 100 mL with $H_2O$

Store at room temperature

*10% Ammonium persulfate (APS)*

Dissolve 0.1 g ammonium persulfate in $H_2O$

Adjust volume to 1 mL with deionized $H_2O$

Store at 4°C

*30% acryl-bisacrylamide mix (100 mL)*

Dissolve 29 g acrylamide and 1 g N.N'-methylenebisacrylamde in 60 mL $H_2O$

Heat the solution to 37°C to dissolve the chemicals

Adjust volume to 100 mL with $H_2O$

Filter through 0.45 μM membrane

Store at 4°C protected from light

*10X SDS-PAGE running buffer (1 L)*

Dissolve 10 g SDS; 30.3 g Tris and 144.1 g glycin in 800 mL $H_2O$

Adjust volume to 1 L with $H_2O$

Store at room temperature

*1X SDS-PAGE running buffer (1 L)*

Add 100 mL 10X SDS-PAGE running buffer to 900 mL deionized $H_2O$

Store at room temperature

*10X SDS-PAGE transfer buffer (1 L)*

Mix 144 g glycine and 38 g Tris and make up to 1 L with deionized $H_2O$

*1X SDS-PAGE transfer buffer (1 L)*

Mix 100 mL 10X transfer buffer; 700 mL deionized $H_2O$ and 200 mL isopropanol

Make fresh on day of running gel and store at 4°C

*1X Ponceau S staining solution (0.1% (w/v) Ponceau S in 5% acetic acid) (50 mL)*

Dissolve 0.1g Ponceau S in 5 mL acetic acid

Adjust volume to 50 mL with deionized $H_2O$ and protect from light

*15% resolving gel for SDS-PAGE (7,5 mL)*

Mix 1.65 mL $H_2O$; 3.75 mL 30% acryl-bisacrylamide mix; 1.95 mL 1.5M Tris (pH 8.8); 0.075 mL 10% SDS; 0.075 mL APS and 0.003 mL tetramethylethylenediamine (TEMED) (under hood)

Pour into 1 mm glass plate, minimise exposure to air

Add 1% SDS to set the top of the gel

*5% stacking gel for denaturing SDS-PAGE*

Mix 2.1 mL $H_2O$; 0.5 mL 30% acryl-bisacrylamide mix; 0.38 mL 1.5M Tris (pH 6.8); 0.03 mL 10% SDS; 0.03 mL APS and 0.003 mL tetramethylethylenediamine (TEMED) (under hood)

Pour into 1 mm glass plate which has the set resolving gel, add comb and leave to set

*5X SDS loading dye*

Mix 12.5 mL 2 M Tris HCl pH 6.8; 10 g 10% SDS; 30 mL 100% glycerol; 5 mL β-mercaptoethanol and 52 mL 0.04% Bromophenol Blue

Store at room temperature

**Western Blotting**

*10X PBS*

80 g NaCl

2 g KCl

26.8 g $Na_2HPO_4$-$7H_2o$ $KH_2PO_4$

Dissolve in 800 mL $H_2O$. Adjust pH to 7.4 with HCl and fill up to 1 L with $H_2O$.

Aliquot the PBS, sterilize by autoclaving for 20 minutes at 15 psi (1.05 kg/$cm^2$) on liquid cycle or by filter sterilisation and store at room temperature

*1X PBS*

Measure 100 mL of 10X PBS and add to 1 L bottle. Fill up to 1 L with $H_2O$

Aliquot as needed and store at room temperature

*1X PBS/0.1% Tween (PBST)*

Add 1 mL Tween 20 to 1X PBS made up to 1 L

Mix well with magnetic stirrer bar

Store at 4°C

*Blocking Solution*

Add 2.5 g non-fat powder milk (5%) and dissolve in 50 mL in PBST

Store at 4°C

*1M Tris-HCl (pH 6.7)*

Dissolve 24.22 g Tris base in 160 mL deionized $H_2O$

Adjust pH to 6.7 with concentrated HCl and adjust volume to 200 mL with deionized $H_2O$

Store at 4°C

*Stripping buffer (100 mL)*

Combine 0.69 mL 100 mM β-mercaptoethanol; 10 mL 2% SDS; 6,25 mL 62.5 mM Tris HCl (pH 6.7) adjusted with deionized $H_2O$ to 100 mL

Store at room temperature

**Protocol for using miScript primer assays**

The two-step process begins with cDNA synthesis using the miScript SYBR Green Kit II (Qiagen, Hilden, Germany). Briefly two samples (RNA extracted from Ramos cells treated with HIV-1 AT-2 of 91.47 ng/µL; RNA extracted from K562 sample of 500 ng/µL) were set up as described in Table A1 below for reverse transcription. The reactions were then incubated for 60 minutes at 37°C and then incubated for 5minutes at 95°C to inactivate the miScript reverse transcriptase mix and placed on ice. Thereafter single PCR 0.5 mL tubes were set up (Table A2) for qPCR using miScript primer assays (Qiagen, Hilden, Germany) for RNU6B for the two samples in triplicate with a no template control and a water control. The reaction was

run on the MultiGene$^{TM}$ Gradient PCR Thermal Cycling System (Labnet International, California, USA) as per cycling conditions (Table A3).

**Table A1: Components of the reverse transcription using miScript SYBR Green Kit II**

| **Reagent** | **Volume** (μL) |
|---|---|
| miScript HiSpec Buffer (5X) | 4.00 |
| miScript Nucleics Mix (10X) | 2.00 |
| Template RNA | 2.00 |
| miScript Reverse Transcriptase Mix | 2.00 |
| Nuclease-free water | 10.00 |
| **Total Volume** | **20.00** |

**Table A2: Components of the qPCR miScript primer assay**

| **Reagent** | **Volume** (μL) |
|---|---|
| QuantiTect SYBR Green PCR Master Mix (2X) | 5.00 |
| miScript universal primer (10X) | 1.00 |
| miScript primer assay (10X) | 1.00 |
| cDNA | 1.00 |
| Nuclease-free water | 2.00 |
| **Total Volume** | **10.00** |

**Table A3: Cycling conditions for miScript qPCR primer assays**

| **Stage** | **Temp** | **Time** | **Cycle** |
|---|---|---|---|
| **Initial activation step** | 95.0°C | 15 min | Hold |
| **Denaturation** | 94.0°C | 15 sec | 40 Cycles |
| **Annealing** | 55.0°C | 30 sec | |
| **Extension** | 70.0°C | 30 sec | |

## APPENDIX B: ADDITIONAL TABLES, IMAGES & DATA

**Table B1: miRNAs chosen for custom miRNA Taqman microarray profiling**

| miRNA | Reported Expression | Reference |
|---|---|---|
| let-7a-2-3p | DOWN | Bueno *et al.,* (2011); Jima *et al.,* (2010) |
| let-7a-1-3p | DOWN | Chang *et al.,* (2008) |
| let-7a-5p | DOWN | Jima *et al.,* (2010); Bueno *et al.,* (2011); Robertus *et al.,* (2010) |
| let-7b-5p | UP | Jima *et al.,* (2010) |
| let-7b-3p | DOWN | Chang *et al.,* (2008) |
| let-7c-5p | DOWN | Chang *et al.,* (2008) |
| let-7d-5p | DOWN | Bueno *et al.,* (2011); Robertus *et al.,* (2010); Chang *et al.,* (2008) |
| let-7e-5p | DOWN | Bueno *et al.,* (2011) |
| let-7e-3p | DOWN | Bueno *et al.,* (2011) |
| let-7f-5p | DOWN | Bueno *et al.,* (2011); Jima *et al.,* (2010) |
| let-7f-1-3p | DOWN | Chang *et al.,* (2008) |
| let-7g-5p | DOWN | Bueno *et al.,* (2011); Robertus *et al.,* (2010); Chang *et al.,* (2008); Jima *et al.,* (2010) |
| let-7i-5p | - | Cancer array (Lung, ovarian) |
| miR-100-5p | UP | Robertus *et al.,* (2010) |
| miR-100-3p | DOWN | Cancer array (Brain, pancreatic, ovarian); Bueno *et al.,* (2011) |
| miR-101-3p | UP | Jima *et al.,* (2010) |
| miR-103a-3p | DOWN | Leucci *et al.,* (2008); Jima *et al.,* (2010) |
| miR-105-5p | DOWN | Leucci *et al.,* (2008) |
| miR-105-3p | DOWN | Leucci *et al.,* (2008) |
| miR-106a-5p | UP | Bueno *et al.,* (2011) |
| miR-106a-3p | UP | Robertus *et al.,* (2010) |
| miR-106b-5p | UP | Robertus *et al.,* (2010) |
| miR-106b-3p | UP | Jima *et al.,* (2010) |
| miR-107 | DOWN | Leucci *et al.,* (2008) |
| miR-124-5p | UP/DOWN | Robertus *et al.,* (2010); Chang *et al.,* (2008) (DOWN) |
| miR-125b-5p | UP | Robertus *et al.,* (2010) |
| miR-126-3p | UP | Leucci *et al.,* (2010) |
| miR-126-5p | UP | Leucci *et al.,* (2010) |
| miR-127-3p | UP | Bueno *et al.,* (2011); Jima *et al.,* (2010) |
| miR-130b-3p | UP | Cancer array (skin, brain); Robertus *et al.,* (2010) |
| miR-132-3p | UP | Chiang *et al.,* (2013) |
| miR-133a-3p | DOWN | Bueno *et al.,* (2011); Robertus *et al.,* (2010) |
| miR-138-5p | DOWN | Robertus *et al.,* (2010) |
| miR-140-3p | UP | Jima *et al.,* (2010) |
| miR-141-3p | DOWN | Bueno *et al.,* (2011); Jima *et al.,* (2010) |
| miR-142-3p | DOWN | Leucci *et al.,* (2008); Jima *et al.,* (2010) |
| miR-142-5p | UP | Robertus *et al.,* (2010); Jima *et al.,* (2010) |
| miR-143-3p | UP | Robertus *et al.,* (2010) |
| miR-143-5p | - | - |
| miR-145-3p | DOWN | Bueno *et al.,* (2011) |
| miR-145-5p | DOWN | Bueno *et al.,* (2011); Robertus *et al.,* (2010); Chang *et al.,* (2008); Leucci *et al.,* (2008); Jima *et al.,* (2010) |
| miR-146a-3p | UP | Jima *et al.,* (2010) |
| miR-146b-3p | DOWN | Leucci *et al.,* (2008) |
| miR-146b-5p | DOWN | Bueno *et al.,* (2011); Jima *et al.,* (2010) |
| miR-148a-3p | UP | Cancer array (brain, prostate, skin); Robertus *et al.,* (2010) |
| miR-148a-5p | UP | Cancer array (brain, prostate, skin); Robertus *et al.,* (2010) |
| miR-149-5p | DOWN | Robertus *et al.,* (2013); Chang *et al*., (2008) |
| miR-150-5p | DOWN | Robertus *et al.,* (2010) |
| miR-150-3p | DOWN | Chang *et al.,* (2010) |

| | | |
|---|---|---|
| miR-151a-3p | DOWN | Bueno *et al.,* (2011); Robertus *et al.,* (2010); Leucci *et al.,* (2008); Jima *et al.,* (2010) |
| miR-155-5p | DOWN | Bueno *et al.,* (2011); Robertus *et al.,* (2010); Chang *et al.,* (2008); Jima *et al.,* (2010) |
| miR-155-3p | DOWN | Jima *et al.,* (2010) |
| miR-15a-3p | DOWN | Bueno *et al.,* (2011); Robertus *et al.,* (2010); Jima *et al.,* (2010) |
| miR-15b-5p | UP | Cancer array (Brain, head, neck, prostate, skin); Robertus *et al.,* (2010) |
| miR-16-5p | DOWN | Robertus *et al.,* (2010) |
| miR-17-5p | UP/DOWN | Bueno *et al.,* (2011); Jima *et al.,* (2010); Sampson *et al.,* (2007) (DOWN) |
| miR-17-3p | DOWN | Jima *et al.,* (2010) |
| miR-18a-5p | DOWN | Bueno *et al.,* (2011); Jima *et al.,* (2010) |
| miR-18b-5p | - | - |
| miR-185-5p | UP | Bueno *et al.,* (2011) |
| miR-188-5p | UP | Bueno *et al.,* (2011) |
| miR-191-5p | DOWN | Robertus *et al.,* (2010) |
| miR-192-5p | DOWN | Leucci *et al.,* (2008) |
| miR-193a-5p | DOWN | Leucci *et al.,* (2008) |
| miR-194-3p | UP | Jima *et al.,* (2010) |
| miR-194-5p | UP | Jima *et al.,* (2010) |
| miR-195-5p | DOWN | Chang *et al.,* (2008) |
| miR-195-3p | DOWN | Chang *et al.,* (2008) |
| miR-196a-5p | DOWN | Robertus *et al.,* (2010) |
| miR-196a-3p | DOWN | Robertus *et al.,* (2010) |
| miR-196b-5p | DOWN | Robertus *et al.,* (2010) |
| miR-197 | UP | Bueno *et al.,* (2011); Jima *et al.,* (2010) |
| miR-199a-3p | UP | Robertus *et al.,* (2010) |
| miR-19a-3p | UP | Bueno *et al.,* (2011); Jima *et al.,* (2010) |
| miR-19b-3p | UP | Bueno *et al.,* (2011); Jima *et al.,* (2010) |
| miR-20a-5p | DOWN | Robertus *et al*., (2010); Jima *et al.,* (2010) |
| miR-20b-5p | UP/DOWN | Bueno *et al.,* (2011); Leucci *et al.,* (2008) (DOWN) |
| miR-200c-3p | DOWN | Cancer array (prostate, pancreatic); Robertus *et al.,* (2010) |
| miR-202-5p | UP | Bueno *et al.,* (2011); Jima *et al.,* (2010) |
| miR-205-5p | UP | Bueno *et al.,* (2011); Jima *et al.,* (2010) |
| miR-21-5p | UP | Bueno *et al.,* (2011); Jima *et al.,* (2010) |
| miR-210-3p | DOWN | Robertus *et al.,* (2010); Jima *et al.,* (2010) |
| miR-214-3p | UP | Robertus *et al.,* (2010) |
| miR-215-5p | DOWN | Cancer array (liver); Robertus *et al.,* (2010) |
| miR-218-5p | - | Cancer array (brain, head, neck) |
| miR-22-3p | UP/DOWN | Bueno *et al.,* (2011); Chang *et al.,* (2008) (DOWN) |
| miR-221-3p | DOWN | Leucci *et al.,* (2008) |
| miR-222-3p | DOWN | Robertus *et al.,* (2010); Leucci *et al.,* (2008); Jima *et al.,* (2010); Imig *et al.,* (2010) (UP) |
| miR-223-5p | UP | Jima *et al.,* (2010) |
| miR-224-5p | DOWN | Robertus *et al.,* (2010) |
| miR-23a-3p | DOWN | Leucci *et al.,* (2008) |
| miR-23b-3p | DOWN | Bueno *et al.,* (2011); Leucci *et al.,* (2008) |
| miR-24-3p | UP | Jima *et al.,* (2010) |
| miR-25-3p | DOWN | Jima *et al.,* (2010) |
| miR-26a-5p | DOWN | Chang *et al.,* (2008); Jima *et al.,* (2010) |
| miR-26a-1-3p | DOWN | Leucci *et al.,* (2008) |
| miR-26b-5p | DOWN | Bueno *et al.,* (2011); Robertus *et al.,* (2010); Chang *et al.,* (2008); Leucci *et al.,* (2008); Jima *et al.,* (2010) |
| miR-26b-3p | DOWN | Leucci *et al.,* 2008 |
| miR-27a-3p | UP | Di Lisio *et al.,* 2012 |
| miR-27b-3p | DOWN | Bueno *et al.,* 2011 |
| miR-28-3p | DOWN | Bueno *et al.,* 2011; Robertus *et al.,* 2010; Jima *et al.,* 2010 |
| miR-29a-3p | DOWN | Bueno *et al.,* 2011; Robertus *et al.,* 2010; Chang *et al.,* 2008; Jima *et al.,* 2010 |

| | | |
|---|---|---|
| miR-29b-3p | DOWN | Bueno *et al.,* 2011; Leucci *et al.,* 2008 |
| miR-29c-3p | DOWN | Chang *et al.,* 2008; Jima *et al.,* 2010 |
| miR-296-3p | UP | Bueno *et al.,* 2011; Jima *et al.,* 2010 |
| miR-30a-3p | DOWN/UP | Robertus *et al.,* 2010; Jima *et al.,* 2010 (UP); Leucci *et al.,* 2008 |
| miR-30a-5p | UP | Jima *et al.,* 2010 |
| miR-30b-3p | DOWN | Jima *et al.,* 2010 |
| miR-30c-5p | DOWN | Jima *et al.,* 2010; Chang et *al.,* 2008 |
| miR-30d-5p | DOWN | Robertus *et al.,* 2010; Jima *et al.,* 2010; Leucci *et al.,* 2008 |
| miR-30e-3p | DOWN | Robertus *et al.,* 2010; Jima *et al.,* 2010 |
| miR-30e-5p | DOWN | Chang *et al.,* 2008 |
| miR-301a-3p | DOWN | Bueno *et al.,* 2011 |
| miR-31-5p | DOWN | Robertus *et al.,* 2010 |
| miR-32-5p | DOWN | Robertus *et al.,* 2010; Jima *et al.,* 2010 |
| miR-320a | UP | Bueno *et al.,* 2011; Jima *et al.,* 2010 |
| miR-324-3p | DOWN | Leucci *et al.,* 2008 |
| miR-324-5p | DOWN | Leucci *et al.,* 2008 |
| miR-326 | DOWN | Robertus *et al.,* 2010; Leucci *et al.,* 2008 |
| miR-328-3p | DOWN | Leucci *et al.,* 2008; Jima *et al.,* 2010 |
| miR-331-3p | DOWN | Bueno *et al.,* 2011; Robertus *et al.,* 2010; Jima *et al.,* 2010 |
| miR-339-3p | DOWN | Robertus *et al.,* 2010 |
| miR-339-5p | DOWN | Leucci *et al.,* 2008 |
| miR-340-5p | DOWN | Leucci *et al.,* 2008 |
| miR-342-5p | DOWN | Robertus *et al.,* 2010; Jima *et al.,* 2010 |
| miR-342-3p | DOWN | Leucci *et al.,* 2008 |
| miR-345-5p | UP | Jima *et al.,* 2010 |
| miR-34a-5p | DOWN | Chang *et al.,* 2008 |
| miR-34b-5p | DOWN | Leucci *et al.,* 2008 |
| miR-361-5p | UP | Jima *et al.,* 2010 |
| miR-363-3p | DOWN | Bueno *et al.,* 2011 |
| miR-365a-3p | UP | Di Lisio *et al.,* 2012 |
| miR-370-3p | UP | Bueno *et al.,* 2011 |
| miR-374a-5p | UP | Robertus *et al.,* 2010 |
| miR-422a | UP | Bueno *et al.,* 2011 |
| miR-423-5p | UP | Jima *et al.,* 2010 |
| miR-425-5p | UP | Jima *et al.,* 2010 |
| miR-429 | DOWN | Leucci *et al.,* 2008 |
| miR-448 | DOWN | Leucci *et al.,* 2008 |
| miR-454-3p | DOWN | Bueno *et al.,* 2011 |
| miR-455-3p | DOWN | Robertus *et al.,* 2010 |
| miR-483-3p | DOWN | Leucci *et al.,* 2008 |
| miR-484-3p | UP | Bueno *et al.,* 2011 |
| miR-485-3p | DOWN | Leucci *et al.,* 2008 |
| miR-486-5p | UP | Jima *et al.,* 2010 |
| miR-494-3p | UP | Bueno *et al.,* 2011 |
| miR-497-5p | DOWN | Leucci *et al.,* 2008 |
| miR-513a-3p | DOWN | Bueno *et al.,* 2011 |
| miR-516b-3p | UP | Di Lisio *et al.,* 2012 |
| miR-520d-3p | UP | Di Lisio *et al.,* 2012 |
| miR-520d-5p | UP | Di Lisio *et al.,* 2012 |
| miR-520f-5p | - | - |
| miR-520f-3p | - | - |
| miR-532-5p | UP | Jima *et al.,* 2010 |
| miR-563 | DOWN | Robertus *et al.,* 2010 |
| miR-573 | UP | Di Lisio *et al.,* 2012 |
| miR-574-3p | UP | Bueno *et al.,* 2011 |
| miR-575 | UP | Bueno *et al.,* 2011 |
| miR-582-3p | DOWN | Bueno *et al.,* 2011; Robertus *et al.,* 2010 |
| miR-582-5p | DOWN | Bueno *et al.,* 2011; Robertus *et al.,* 2010 |

| | | |
|---|---|---|
| miR-590-3p | UP | Di Lisio *et al.,* 2012 |
| miR-595 | DOWN | Robertus *et al.,* 2010 |
| miR-624-5p | DOWN | Robertus *et al.,* 2010 |
| miR-624-3p | DOWN | Robertus *et al.,* 2010 |
| miR-627-3p | DOWN | Robertus *et al.,* 2010 |
| miR-627-5p | DOWN | Robertus *et al.,* 2010 |
| miR-628-5p | UP | Robertus *et al.,* 2010; Di Lisio *et al.,* 2012; Jima *et al.,* 2010 |
| miR-629-5p | DOWN | Robertus *et al.,* 2010 |
| miR-634 | - | - |
| miR-650 | - | - |
| miR-660-5p | UP | Bueno *et al.,* 2011; Robertus *et al.,* 2010; Di Lisio *et al.,* 2012; Jima *et al.,* 2010 |
| miR-7-2-3p | DOWN | Robertus *et al.,* 2010 |
| miR-765 | DOWN | Robertus *et al.,* 2010 |
| miR-766-3p | DOWN | Robertus *et al.,* 2010 |
| miR-769-5p | UP | Bueno *et al.,* 2011 |
| miR-9-3p | UP | Leucci *et al.,* 2008; Jima *et al.,* 2010 |
| miR-9-5p | UP | Bueno *et al.,* 2011; Di Lisio *et al.,* 2012; Jima *et al*., 2010 |
| miR-92a-3p | UP | Jima *et al.,* 2010 |
| miR-92a-1-5p | DOWN | Jima *et al.,* 2010 |
| miR-92a-2-5p | DOWN | Jima *et al.,* 2010 |
| miR-93-3p | UP | Bueno *et al.,* 2011; Jima *et al.,* 2010 |
| miR-95-3p | DOWN | Robertus *et al.,* 2010 |
| miR-96-3p | DOWN/UP | Bueno *et al.,* 2011; Sampson *et al.,* 2007 (UP); Jima *et al.,* 2010 |
| miR-98-5p | DOWN | Chang *et al.,* 2008 |
| miR-99a-5p | DOWN | Malumbres *et al.,* 2009; Chang *et al.,* 2008 |
| RNU6B | CONTROL | Malumbres *et al.,* 2009 |
| RNU48 | CONTROL | Forte *et al.,* 2012 |
| RNU44 | CONTROL | Linda *et al.,* 2010 |

miR – microRNA; RNU – small nucleolar RNA; - Added onto array based on availability of the assay

**Table B2: Stem loop primers for miRNA PCR Array**

| miRNa | Target Sequence |
|---|---|
| hsa-miR-218-5p | UUGUGCUUGAUCUAACCAUGU |
| hsa-miR-30c-5p | UGUAAACAUCCUACACUCUCAGC |
| hsa-miR-365a-3p | UAAUGCCCCUAAAAAUCCUUAU |
| hsa-miR-532-3p | CAUGCCUUGAGUGUAGGACCGU |
| hsa-miR-9-5p | UCUUUGGUUAUCUAGCUGUAUGA |
| hsa-miR-100-3p | CAAGCUUGUAUCUAUAGGUAUG |
| hsa-miR-143-3p | UGAGAUGAAGCACUGUAGCUC |
| hsa-miR-192-5p | CUGACCUAUGAAUUGACAGCC |
| hsa-miR-22-3p | AAGCUGCCAGUUGAAGAACUGU |
| hsa-miR-30d-5p | UGUAAACAUCCCCGACUGGAAG |
| hsa-miR-370-3p | GCCUGCUGGGGUGGAACCUGGU |
| hsa-miR-563 | AGGUUGACAUACGUUUCCC |
| hsa-miR-92a-3p | UAUUGCACUUGUCCCGGCCUGU |
| hsa-miR-101-3p | UACAGUACUGUGAUAACUGAA |
| hsa-miR-145-3p | GGAUUCCUGGAAAUACUGUUCU |
| hsa-miR-193a-5p | UGGGUCUUUGCGGGCGAGAUGA |
| hsa-miR-221-3p | AGCUACAUUGUCUGCUGGGUUUC |
| hsa-miR-30e-5p | UGUAAACAUCCUUGACUGGAAG |
| hsa-miR-374a-5p | UUAUAAUACAACCUGAUAAGUG |
| hsa-miR-573 | CUGAAGUGAUGUGUAACUGAUCAG |
| hsa-miR-92a-1-5p | AGGUUGGGAUCGGUUGCAAUGCU |
| hsa-miR-103a-3p | AGCAGCAUUGUACAGGGCUAUGA |
| hsa-miR-145-5p | GUCCAGUUUUCCCAGGAAUCCCU |
| hsa-miR-194-5p | UGUAACAGCAACUCCAUGUGGA |
| hsa-miR-222-3p | AGCUACAUCUGGCUACUGGGU |
| hsa-miR-30e-3p | CUUUCAGUCGGAUGUUUACAGC |
| hsa-miR-422a | ACUGGACUUAGGGUCAGAAGGC |

| | |
|---|---|
| hsa-miR-574-3p | CACGCUCAUGCACACACCCACA |
| hsa-miR-92a-2-5p | GGGUGGGGAUUUGUUGCAUUAC |
| hsa-miR-105-5p | UCAAAUGCUCAGACUCCUGUGGU |
| hsa-miR-146a-5p | UGAGAACUGAAUUCCAUGGGUU |
| hsa-miR-194-3p | CCAGUGGGGCUGCUGUUAUCUG |
| hsa-miR-223-5p | CGUGUAUUUGACAAGCUGAGUU |
| hsa-miR-423-5p | UGAGGGGCAGAGAGCGAGACUUU |
| hsa-miR-575 | GAGCCAGUUGGACAGGAGC |
| hsa-miR-93-3p | ACUGCUGAGCUAGCACUUCCCG |
| hsa-miR-105-3p | ACGGAUGUUUGAGCAUGUGCUA |
| hsa-miR-146b-3p | UGCCCUGUGGACUCAGUUCUGG |
| hsa-miR-195-3p | CCAAUAUUGGCUGUGCUGCUCC |
| hsa-miR-224-5p | CAAGUCACUAGUGGUUCCGUU |
| hsa-miR-301a-3p | CAGUGCAAUAGUAUUGUCAAAGC |
| hsa-miR-425-5p | AAUGACACGAUCACUCCCGUUGA |
| hsa-miR-582-3p | UAACUGGUUGAACAACUGAACC |
| hsa-miR-95-3p | UUCAACGGGUAUUUAUUGAGCA |
| hsa-miR-106a-5p | AAAAGUGCUUACAGUGCAGGUAG |
| hsa-miR-146b | UGAGAACUGAAUUCCAUAGGCU |
| hsa-miR-195-5p | UAGCAGCACAGAAAUAUUGGC |
| hsa-miR-23a-3p | AUCACAUUGCCAGGGAUUUCC |
| hsa-miR-31-5p | AGGCAAGAUGCUGGCAUAGCU |
| hsa-miR-429 | UAAUACUGUCUGGUAAAACCGU |
| hsa-miR-582-5p | UUACAGUUGUUCAACCAGUUACU |
| hsa-miR-96-3p | AAUCAUGUGCAGUGCCAAUAUG |
| hsa-miR-106a-3p | CUGCAAUGUAAGCACUUCUUAC |
| hsa-miR-148a-5p | AAAGUUCUGAGACACUCCGACU |
| hsa-miR-196a-5p | UAGGUAGUUUCAUGUUGUUGGG |
| hsa-miR-23b-3p | AUCACAUUGCCAGGGAUUACC |
| hsa-miR-32-5p | UAUUGCACAUUACUAAGUUGCA |
| hsa-miR-448 | UUGCAUAUGUAGGAUGUCCCAU |
| hsa-miR-590-3p | UAAUUUUAUGUAUAAGCUAGU |
| hsa-miR-98-5p | UGAGGUAGUAAGUUGUAUUGUU |
| hsa-miR-106b-5p | UAAAGUGCUGACAGUGCAGAU |
| hsa-miR-148a-3p | UCAGUGCACUACAGAACUUUGU |
| hsa-miR-196a-3p | CGGCAACAAGAAACUGCCUGAG |
| hsa-miR-24-3p | UGGCUCAGUUCAGCAGGAACAG |
| hsa-miR-320a | AAAAGCUGGGUUGAGAGGGCGA |
| hsa-miR-454-3p | UAGUGCAAUAUUGCUUAUAGGGU |
| hsa-miR-595 | GAAGUGUGCCGUGGUGUGUCU |
| hsa-miR-99a-5p | AACCCGUAGAUCCGAUCUUGUG |
| hsa-miR-107 | AGCAGCAUUGUACAGGGCUAUCA |
| hsa-miR-149-5p | UCUGGCUCCGUGUCUUCACUCCC |
| hsa-miR-196b-5p | UAGGUAGUUUCCUGUUGUUGGG |
| hsa-miR-25-3p | CAUUGCACUUGUCUCGGUCUGA |
| hsa-miR-324-3p | ACUGCCCCAGGUGCUGCUGG |
| hsa-miR-455-5p | UAUGUGCCUUUGGACUACAUCG |
| hsa-miR-624-3p | CACAAGGUAUUGGUAUUACCU |
| hsa-let-7a-5p | UGAGGUAGUAGGUUGUAUAGUU |
| hsa-let-7a-3p | CUAUACAAUCUACUGUCUUUC |
| hsa-let-7a-2-3p | CUGUACAGCCUCCUAGCUUUCC |
| hsa-let-7b-5p | UGAGGUAGUAGGUUGUGUGGUU |
| hsa-let-7b-3p | CUAUACAACCUACUGCCUUCCC |
| hsa-miR-124-5p | CGUGUUCACAGCGGACCUUGAU |
| hsa-miR-125b-5p | UCCCUGAGACCCUAACUUGUGA |
| hsa-miR-126-3p | UCGUACCGUGAGUAAUAAUGCG |
| hsa-miR-126-5p | CAUUAUUACUUUUGGUACGCG |
| hsa-miR-127-3p | UCGGAUCCGUCUGAGCUUGGCU |
| hsa-miR-150-5p | UCUCCCAACCCUUGUACCAGUG |
| hsa-miR-150-3p | CUGGUACAGGCCUGGGGGACAG |
| hsa-miR-151-3p | CUAGACUGAAGCUCCUUGAGG |
| hsa-miR-155-5p | UUAAUGCUAAUCGUGAUAGGGGU |
| hsa-miR-155-3p | CUCCUACAUAUUAGCAUUAACA |
| hsa-miR-197-3p | UUCACCACCUUCUCCACCCAGC |
| hsa-miR-199a-3p | ACAGUAGUCUGCACAUUGGUUA |
| hsa-miR-19a-3p | UGUGCAAAUCUAUGCAAAACUGA |

| | |
|---|---|
| hsa-miR-19b-3p | UGUGCAAAUCCAUGCAAAACUGA |
| hsa-miR-26a-5p | UUCAAGUAAUCCAGGAUAGGCU |
| hsa-miR-26a-1-3p | CCUAUUCUUGGUUACUUGCACG |
| hsa-miR-26b-5p | UUCAAGUAAUUCAGGAUAGGU |
| hsa-miR-26b-3p | CCUGUUCUCCAUUACUUGGCUC |
| hsa-miR-27a-3p | UUCACAGUGGCUAAGUUCCGC |
| hsa-miR-324-5p | CGCAUCCCCUAGGGCAUUGGUGU |
| hsa-miR-326 | CCUCUGGGCCCUUCCUCCAG |
| hsa-miR-328-3p | CUGGCCCUCUCUGCCCUUCCGU |
| hsa-miR-331-3p | GCCCCUGGGCCUAUCCUAGAA |
| hsa-miR-339-3p | UGAGCGCCUCGACGACAGAGCCG |
| hsa-miR-483-3p | UCACUCCUCUCCUCCCGUCUU |
| hsa-miR-484 | UCAGGCUCAGUCCCCUCCCGAU |
| hsa-miR-485-3p | GUCAUACACGGCUCUCCUCUCU |
| hsa-miR-486-5p | UCCUGUACUGAGCUGCCCCGAG |
| hsa-miR-624-5p | UAGUACCAGUACCUUGUGUUCA |
| hsa-miR-627-5p | GUGAGUCUCUAAGAAAAGAGGA |
| hsa-miR-629-5p | UGGGUUUACGUUGGGAGAACU |
| hsa-miR-628-5p | AUGCUGACAUAUUUACUAGAGG |
| hsa-miR-let-7e-5p | UGAGGUAGGAGGUUGUAUAGUU |
| hsa-let-7c-5p | UGAGGUAGUAGGUUGUAUGGUU |
| hsa-let-7d-5p | AGAGGUAGUAGGUUGCAUAGUU |
| hsa-let-7e-3p | CUAUACGGCCUCCUAGCUUUCC |
| hsa-let-7f-5p | UGAGGUAGUAGAUUGUAUAGUU |
| hsa-miR-130b-3p | CAGUGCAAUGAUGAAAGGGCAU |
| hsa-miR-132-3p | UAACAGUCUACAGCCAUGGUCG |
| hsa-miR-133a-3p | UUUGGUCCCCUUCAACCAGCUG |
| hsa-miR-138-5p | AGCUGGUGUUGUGAAUCAGGCCG |
| hsa-miR-140-3p | UACCACAGGGUAGAACCACGG |
| hsa-miR-15a-5p | UAGCAGCACAUAAUGGUUUGUG |
| hsa-miR-15b-5p | UAGCAGCACAUCAUGGUUUACA |
| hsa-miR-16-5p | UAGCAGCACGUAAAUAUUGGCG |
| hsa-miR-17-5p | CAAAGUGCUUACAGUGCAGGUAG |
| hsa-miR-17-3p | ACUGCAGUGAAGGCACUUGUAG |
| hsa-miR-200c-3p | UAAUACUGCCGGGUAAUGAUGGA |
| hsa-miR-202-5p | UUCCUAUGCAUAUACUUCUUUG |
| hsa-miR-205-5p | UCCUUCAUUCCACCGGAGUCUG |
| hsa-miR-20a-5p | UAAAGUGCUUAUAGUGCAGGUAG |
| hsa-miR-20b-5p | CAAAGUGCUCAUAGUGCAGGUAG |
| hsa-miR-27b-3p | UUCACAGUGGCUAAGUUCUGC |
| hsa-miR-28-3p | CACUAGAUUGUGAGCUCCUGGA |
| hsa-miR-29a-3p | UAGCACCAUCUGAAAUCGGUUA |
| hsa-miR-29b-3p | UAGCACCAUUUGAAAUCAGUGUU |
| hsa-miR-29c-3p | UAGCACCAUUUGAAAUCGGUUA |
| hsa-miR-339-5p | UCCCUGUCCUCCAGGAGCUCACG |
| hsa-miR-340-5p | UUAUAAAGCAAUGAGACUGAUU |
| hsa-miR-342-3p | UCUCACACAGAAAUCGCACCCGU |
| hsa-miR-342-5p | AGGGGUGCUAUCUGUGAUUGA |
| hsa-miR-494 | UGAAACAUACACGGGAAACCUC |
| hsa-miR-497-5p | CAGCAGCACACUGUGGUUUGU |
| hsa-miR-500-3p | AUGCACCUGGGCAAGGAUUCUG |
| hsa-miR-513-3p | UAAAUUUCACCUUUCUGAGAAGG |
| hsa-miR-634 | AACCAGCACCCCAACUUUGGAC |
| hsa-miR-650 | AGGAGGCAGCGCUCUCAGGAC |
| hsa-miR-660-5p | UACCCAUUGCAUAUCGGAGUUG |
| hsa-let-7f-1-3p | CUAUACAAUCUAUUGCCUUCCC |
| hsa-let-7g-5p | UGAGGUAGUAGUUUGUACAGUU |
| hsa-let-7i-5p | UGAGGUAGUAGUUUGUGCUGUU |
| hsa-miR-100-5p | AACCCGUAGAUCCGAACUUGUG |
| hsa-miR-141-3p | UAACACUGUCUGGUAAAGAUGG |
| hsa-miR-142-3p | UGUAGUGUUUCCUACUUUAUGGA |
| hsa-miR-142-5p | CAUAAAGUAGAAAGCACUACU |
| hsa-miR-143-5p | GGUGCAGUGCUGCAUCUCUGGU |
| hsa-miR-185-5p | UGGAGAGAAAGGCAGUUCCUGA |
| hsa-miR-188-5p | CAUCCCUUGCAUGGUGGAGGG |
| hsa-miR-18a-5p | UAAGGUGCAUCUAGUGCAGAUAG |

| | |
|---|---|
| hsa-miR-18b-5p | UAAGGUGCAUCUAGUGCAGUUAG |
| hsa-miR-191-5p | CAACGGAAUCCCAAAAGCAGCUG |
| hsa-miR-21-5p | UAGCUUAUCAGACUGAUGUUGA |
| hsa-miR-210-3p | CUGUGCGUGUGACAGCGGCUGA |
| hsa-miR-214-3p | ACAGCAGGCACAGACAGGCAGU |
| hsa-miR-215-5p | AUGACCUAUGAAUUGACAGAC |
| hsa-miR-296-3p | GAGGGUUGGGUGGAGGCUCUCC |
| hsa-miR-30a-3p | CUUUCAGUCGGAUGUUUGCAGC |
| hsa-miR-30a-5p | UGUAAACAUCCUCGACUGGAAG |
| hsa-miR-30b-5p | UGUAAACAUCCUACACUCAGCU |
| hsa-miR-345-5p | GCUGACUCCUAGUCCAGGGCUC |
| hsa-miR-34a-5p | UGGCAGUGUCUUAGCUGGUUGU |
| hsa-miR-34b -5p | UAGGCAGUGUCAUUAGCUGAUUG |
| hsa-miR-361-5p | UUAUCAGAAUCUCCAGGGGUAC |
| hsa-miR-363-3p | AAUUGCACGGUAUCCAUCUGUA |
| hsa-miR-516-3p | GAGUGCCUUCUUUUGGAGCGUU |
| hsa-miR-520d-3p | AAAGUGCUUCUCUUUGGUGGGU |
| hsa-miR-520d-5p | CUACAAAGGGAAGCCCUUUC |
| hsa-miR-520f-3p | AAGUGCUUCCUUUUAGAGGGUU |
| hsa-miR-520f-5p | CCUCUAAAGGGAAGCGCUUUCU |
| hsa-miR-7-2-3p | CAACAAAUCCCAGUCUACCUAA |
| hsa-miR-765 | UGGAGGAGAAGGAAGGUGAUG |
| hsa-miR-766-3p | ACUCCAGCCCCACAGCCUCAGC |
| hsa-miR-769-5p | UGAGACCUCUGGGUUCUGAGCU |
| hsa-miR-9-3p | AUAAAGCUAGAUAACCGAAAGU |

hsa – *Homo sapiens*; miR – microRNA

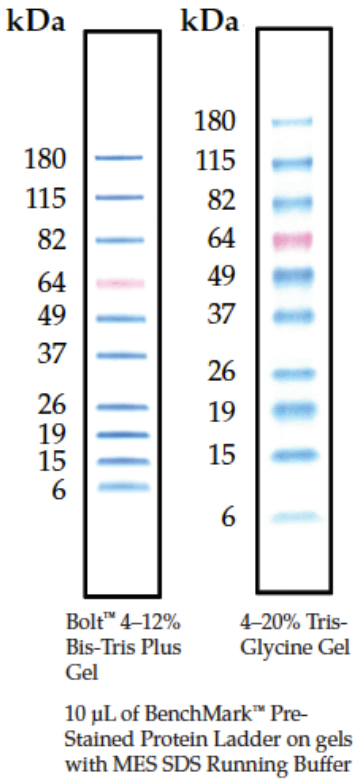


**Figure B1: BenchMark™ Pre-Stained Protein Ladder**

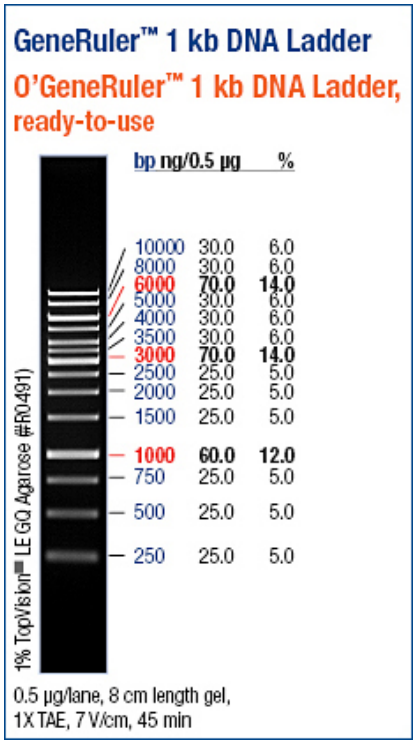


**Figure B2: 1kB DNA ladder**

**Table B3: Raw data – expression of miR-575 in fold change, in the Ramos cell line normalised to the endogenous controls**

| Sample | RNU6B | RNU48 |
|---|---|---|
| **Rep. 1.1** | 1.049* | 0.654* |
| **Rep. 1.2** | 0.609* | 0.765* |
| **Rep. 2.1** | 0.993* | 0.804* |
| **Rep. 2.2** | 0.644* | 0.623* |

Rep – replicate

* $p \leq 0,05$ when compared with microvesicle treated control cells

**Table B4: Raw data - Cut-off values for validation of miR-363-3p and miR-222-3p and miR-200c-3p in the Ramos cell line**

| Sample | miR-363-3p | | miR-200c-3p | | miR-222-3p | | miR-575 | |
|---|---|---|---|---|---|---|---|---|
| | Rep. 1 | Rep.2 | Rep. 1 | Rep. 2 | Rep. 1 | Rep. 2 | Rep. 1 | Rep. 2 |
| **MV1** | 40 | 31.380 | 35.534 | 34.121 | 36.623 | 33.509 | 34.166 | 38.289 |
| **MV2** | 40 | 32.426 | 38.255 | 36.846 | 34.420 | 35.221 | 35.352 | 34.767 |
| **HIV1** | 40 | 31.748 | 35.688 | 33.809 | 40 | 39.105 | 34.841 | 33.411 |
| **HIV2** | 40 | 31.479 | 34.368 | 33.702 | 34.995 | 40 | 33.839 | 34.718 |

Rep – replicate

**Table B5: Raw data – expression of miR-363-3p, miR-222-3p, miR-575, and miR-200c-3p as fold changes in the L1439A cell line**

| Sample | miR-363-3p | | miR-200c-3p | | miR-222-3p | | miR-575 | |
|---|---|---|---|---|---|---|---|---|
| | RNU6B | RNU48 | RNU6B | RNU48 | RNU6B | RNU48 | RNU6B | RNU48 |
| **Rep. 1.1** | 0.900 | 0.834 | 0.925 | 0.864 | 0.645 | 0.602 | 0.563 | 0.526 |
| **Rep. 1.2** | 1.337 | 0.878 | 0.810 | 0.806 | 1.045 | 1.041 | 0.967 | 0.963 |
| **Rep. 2.1** | 1.395 | 0.848 | 0.669 | 0.701 | 0.947 | 0.993 | 0.423 | 0.443 |
| **Rep. 2.2** | 0.862 | 0.863 | 0.120 | 0.994 | 0.712 | 0.632 | 1.287 | 1.142 |

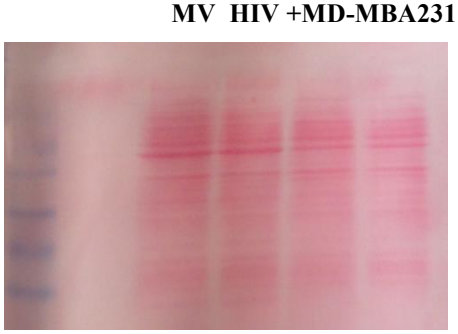


**Figure B3: Ponceau S stained membrane representing successful protein transfer for western blotting**
HIV – HIV-1 treated cells, MV – microvesicle treated cells; +MD-MBA231 – positive control cells

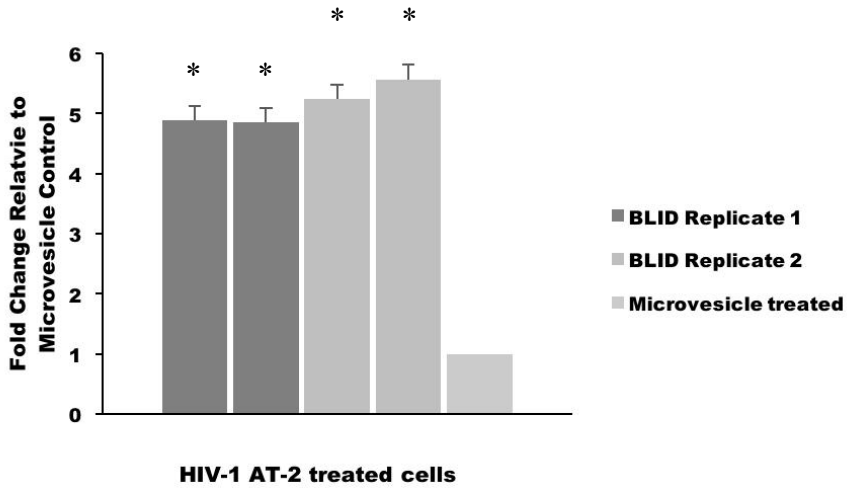


**Figure B4: *BLID* mRNA is upregulated after HIV-1 AT-2 treatment in Ramos cells relative to microvesicle treated control cells.** Upregulation of *BLID* mRNA expressed as fold changes in HIV-treated cells relative to microvesicle-treated control cells, which has been normalised to one. The housekeeping gene, GAPDH was used as the endogenous control. Two independent experiments with each sample performed in duplicate. Error bars represent the standard deviation. An upregulated fold change was observed ranging from 4,857-5,578 ($p \leq 0,05$)* when compared to microvesicle treated control cells (Prism 7, Graphpad, USA).

**Table B6: Heatmap of miRNA differential expression after microarray profiling**

| MiRNA | FC |
|---|---|
| hsa-miR-92a-2#-002138 | 90.213 |
| hsa-miR-98-000577 | 25.296 |
| hsa-miR-520d-3p-002743 | 13.268 |
| hsa-miR-143-002249 | 13.243 |
| hsa-miR-342-5p-002147 | 9.523 |
| hsa-miR-513-3p-002091 | 7.907 |
| hsa-miR-22-000398 | 7.226 |
| hsa-miR-222-002276 | 6.735 |
| hsa-miR-423-5p-002340 | 5.928 |
| hsa-miR-218-000521 | 5.676 |
| hsa-let-7a-2#-121214_mat | 5.546 |
| hsa-miR-202#-002362 | 5.376 |
| hsa-miR-23b-000400 | 5.143 |
| hsa-miR-575-001617 | 4.519 |
| hsa-miR-520f-001120 | 4.268 |
| hsa-miR-194-000493 | 4.167 |
| hsa-miR-30b-000602 | 3.566 |
| hsa-miR-363-001271 | 3.496 |
| hsa-miR-326-000542 | 3.319 |
| hsa-miR-100-000437 | 3.308 |
| hsa-let7c-000379 | 3.247 |
| hsa-miR-485-3p-001277 | 3.006 |
| hsa-miR-132-000457 | 2.808 |
| hsa-miR-563-001530 | 2.791 |
| hsa-miR-370-002275 | 2.782 |

| | |
|---|---|
| hsa-miR-194#-002379 | 2.691 |
| hsa-miR-448-001029 | 2.688 |
| hsa-miR-101-002253 | 2.604 |
| hsa-miR-100#-002142 | 2.337 |
| hsa-miR-365-001020 | 2.046 |
| hsa-miR-196a-241070_mat | 2.038 |
| hsa-miR-221-000524 | 1.992 |
| hsa-miR-214-002306 | 1.973 |
| hsa-miR-105-002167 | 1.957 |
| hsa-miR-7-2#-002314 | 1.943 |
| hsa-miR-455-001280 | 1.884 |
| hsa-miR-345-002186 | 1.784 |
| hsa-miR-765-002643 | 1.731 |
| hsa-miR-192-000491 | 1.690 |
| hsa-miR-146b-001097 | 1.681 |
| hsa-miR-483-002339 | 1.655 |
| hsa-miR-340-002258 | 1.648 |
| hsa-miR-141-000463 | 1.634 |
| hsa-miR-301-000528 | 1.614 |
| hsa-miR-31-002279 | 1.503 |
| hsa-miR-422a-002297 | 1.476 |
| hsa-miR-328-000543 | 1.474 |
| hsa-miR-99a-000435 | 1.469 |
| hsa-miR-32-002109 | 1.368 |
| hsa-miR-145-002278 | 1.331 |
| hsa-miR-155#-002287 | 1.317 |
| hsa-let-7a-000377 | 1.289 |
| hsa-miR-590-3p-002677 | 1.284 |
| hsa-miR-125b-000449 | 1.273 |
| hsa-let-7a#-002307 | 1.257 |
| hsa-miR-let-7e-002406 | 1.250 |
| hsa-miR-486-001278 | 1.242 |
| hsa-miR-142-3p-000464 | 1.228 |
| hsa-miR-34a-000426 | 1.205 |
| hsa-miR-30a-5p-000417 | 1.193 |
| hsa-miR-331-000545 | 1.168 |
| hsa-let-7d-002283 | 1.111 |
| hsa-miR-29b-000413 | 1.102 |
| hsa-miR-516-3p-001149 | 1.086 |
| hsa-miR-766-001986 | 1.060 |
| hsa-miR-425-5p-001516 | 1.046 |
| hsa-miR-96#-002140 | 1.035 |
| hsa-miR-126#-000451 | 1.034 |
| hsa-miR-193a-5p-002281 | 1.016 |
| hsa-miR-223#-002098 | 0.987 |
| hsa-miR-342-3p-002260 | 0.982 |
| hsa-miR-24-000402 | 0.980 |
| hsa-miR-106b-000442 | 0.966 |
| hsa-miR-339-3p-002184 | 0.955 |
| hsa-miR-429-001024 | 0.929 |
| hsa-miR-23a-000399 | 0.927 |

| | |
|---|---|
| hsa-miR-520f-5p-466371_mat | 0.927 |
| hsa-miR-500-001046 | 0.916 |
| hsa-miR-151-002254 | 0.909 |
| hsa-miR-20b-001014 | 0.894 |
| hsa-miR-146a-000468 | 0.881 |
| hsa-miR-148a-000470 | 0.880 |
| hsa-miR-29a-002112 | 0.880 |
| hsa-miR-124#-002197 | 0.852 |
| hsa-miR-7-000391 | 0.846 |
| hsa-miR-30c-000419 | 0.840 |
| hsa-miR-17-002308 | 0.840 |
| hsa-miR-339-5p-002257 | 0.836 |
| hsa-miR-191-002299 | 0.823 |
| hsa-miR-195#-002107 | 0.823 |
| hsa-let-7i-002221 | 0.821 |
| hsa-miR-18a-002422 | 0.817 |
| hsa-miR-20a-000580 | 0.816 |
| hsa-miR-484-001821 | 0.801 |
| hsa-miR-130b-000456 | 0.797 |
| hsa-miR-26b-000407 | 0.793 |
| hsa-miR-374-000563 | 0.793 |
| hsa-miR-574-3p-002349 | 0.791 |
| hsa-miR-19a-000395 | 0.788 |
| hsa-miR-150-000473 | 0.785 |
| hsa-miR-155-002623 | 0.784 |
| hsa-miR-138-002284 | 0.772 |
| hsa-miR-19b-000396 | 0.770 |
| hsa-miR-210-000512 | 0.765 |
| hsa-miR-21-000397 | 0.763 |
| hsa-miR-103-000439 | 0.763 |
| hsa-miR-28-3p-002446 | 0.760 |
| hsa-let-7e#-002407 | 0.756 |
| hsa-miR-34b-000427 | 0.751 |
| hsa-miR-497-001043 | 0.751 |
| hsa-miR-520d-5p-002393 | 0.751 |
| hsa-miR-624-002430 | 0.751 |
| hsa-miR-660-001515 | 0.720 |
| hsa-miR-93#-002139 | 0.719 |
| hsa-miR-30d-000420 | 0.718 |
| hsa-miR-106a-002169 | 0.718 |
| hsa-miR-197-000497 | 0.712 |
| hsa-miR-26a-000405 | 0.703 |
| hsa-miR-140-3p-002234 | 0.702 |
| hsa-miR-25-000403 | 0.688 |
| hsa-miR-205-000509 | 0.683 |
| hsa-miR-196a#-002336 | 0.668 |
| hsa-miR-30a-3p-000416 | 0.665 |
| hsa-let-7f-000382 | 0.660 |
| hsa-miR-320-002277 | 0.659 |
| hsa-miR-582-3p-002399 | 0.654 |
| hsa-miR-92a-000431 | 0.653 |

| | |
|---|---|
| hsa-miR-15b-000390 | 0.639 |
| hsa-miR-18b-002217 | 0.624 |
| hsa-miR-107-000443 | 0.622 |
| hsa-miR-185-002271 | 0.599 |
| hsa-miR-324-5p-000539 | 0.592 |
| hsa-let-7g-002282 | 0.587 |
| hsa-miR-149-002255 | 0.565 |
| hsa-miR-26b#-002444 | 0.561 |
| hsa-miR-15a-000389 | 0.559 |
| hsa-miR-17#-002421 | 0.548 |
| hsa-miR-195-000494 | 0.543 |
| hsa-miR-454-002323 | 0.541 |
| hsa-miR-126-002228 | 0.524 |
| hsa-miR-92a-1#-002137 | 0.504 |
| hsa-miR-150#-002637 | 0.503 |
| hsa-miR-143#-002146 | 0.492 |
| hsa-miR-215-000518 | 0.486 |
| hsa-miR-573-001615 | 0.481 |
| hsa-miR-196b-002215 | 0.468 |
| hsa-miR-224-002099 | 0.464 |
| hsa-miR-133a-002246 | 0.458 |
| hsa-miR-634-001576 | 0.442 |
| hsa-miR-296-3p-002101 | 0.436 |
| hsa-miR-127-000452 | 0.434 |
| hsa-miR-95-000433 | 0.424 |
| hsa-miR-142-5p-002248 | 0.423 |
| hsa-miR-532-001518 | 0.344 |
| hsa-miR-650-001603 | 0.320 |
| hsa-let-7b-002619 | 0.297 |
| hsa-miR-26a-1#-002443 | 0.283 |
| hsa-miR-148a#-002134 | 0.275 |
| hsa-miR-199a-3p-002304 | 0.272 |
| hsa-miR-188-002320 | 0.263 |
| hsa-miR-627-466888_mat | 0.234 |
| hsa-miR-494-002365 | 0.232 |
| hsa-miR-628-5p-002433 | 0.224 |
| hsa-miR-146b-3p-002361 | 0.222 |
| hsa-miR-106a#-002170 | 0.213 |
| hsa-miR-27b-000409 | 0.204 |
| hsa-miR-30e-3p-000422 | 0.201 |
| hsa-miR-582-5p-001983 | 0.200 |
| hsa-let-7b#-002404 | 0.197 |
| hsa-miR-324-3p-002161 | 0.194 |
| hsa-let-7f-1#-002417 | 0.185 |
| hsa-miR-30e-002223 | 0.171 |
| hsa-miR-27a-000408 | 0.171 |
| hsa-miR-200c-002300 | 0.151 |
| hsa-miR-29c-000587 | 0.144 |
| hsa-miR-769-5p-001998 | 0.084 |
| hsa-miR-624-001557 | 0.080 |
| hsa-miR-595-001987 | 0.080 |

| | |
|---|---|
| hsa-miR-361-000554 | 0.061 |
| hsa-miR-145#-002149 | 0.050 |
| hsa-miR-9#-002231 | 0.030 |
| hsa-miR-629-002436 | 0.029 |
| hsa-miR-105#-002168 | 0.026 |
| hsa-miR-9-000583 | 0.020 |
| hsa-miR-627-001560 | 0.007 |

FC – fold change

Expression level:

\+ -

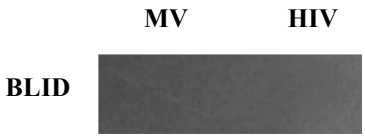


**Figure B5: BLID expression in L1439A cells relative to microvesicle treated control cells.** Western blot analysis displaying BLID expression (~11.8 kDa) in the normal B-cell line which could not be detected. 5 µL of 5X SDS loading dye and 1 µL of DTT was added to 20 µg of protein (varying volumes) in RIPA buffer and boiled at 95 °C for five minutes before being loaded and separated on a 15 % SDS-PAGE gel at 100 V for 2 hours in 1X running buffer. The protein was then transferred onto a nitrocellulose membrane (Bio-Rad, California, USA) for 1 hour at 100 V in 1X transfer buffer. This was then detected using the Clarity™ Western ECL Blotting Substrate (Bio-Rad, USA). To detect BLID, mouse anti-BLID antibody (Novus Biologicals, Singapore, Malaysia) was used, with a HRP bound goat anti-mouse secondary antibody (Bio-Rad, California, USA). BLID – BH3-like motif containing inducer of cell death; HIV – HIV-AT2 treated cells; MV – microvesicle treated control; + - positive control

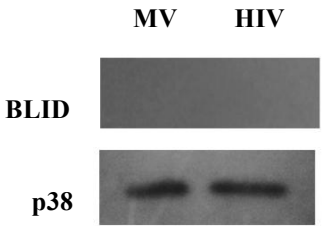


**Figure B6: BLID expression in Ramos cells relative to microvesicle treated control cells.** Western blot analysis displaying BLID expression (~11.8 kDa) in the Ramos cell line which could not be detected. 5 µL of 5X SDS loading dye and 1 µL of DTT was added to 25 µg of protein (varying volumes) in RIPA buffer and boiled at 95 °C for five minutes before being loaded and separated on a 15 % SDS-PAGE gel at 100 V for 2 hours in 1X running buffer. The protein was then transferred onto a nitrocellulose membrane (Bio- Rad, California, USA) for one hour at 100 V in 1X transfer buffer. This was then detected using the Clarity™ Western ECL Blotting Substrate (Bio-Rad, California, USA). To detect BLID, mouse anti-BLID antibody (Novus Biologicals, Singapore, Malaysia) was used, with a HRP bound goat anti-mouse secondary antibody (Bio-Rad, California, USA). The p38 protein was used as a loading control and detected using rabbit anti-p38 antibody (Sigma-Aldrich, Mossouri, USA) and the HRP bound goat anti-rabbit secondary antibody (Bio-Rad, California, USA). BLID – BH3-like motif containing inducer of cell death; HIV – HIV-AT2 treated cells; MV – microvesicle treated control; + - positive control

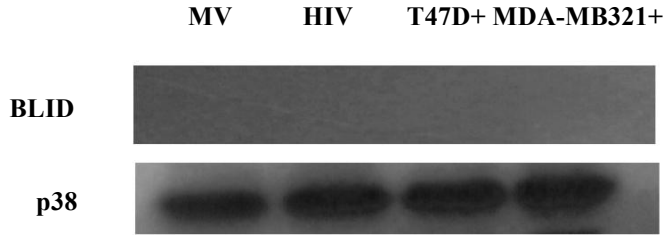


**Figure B7: BLID expression in normal B-cells relative to microvesicle treated control cells.** Western blot analysis displaying BLID expression in the L1439A cell line which could not be detected. 5 µL of 5X SDS loading dye and 1 µL of DTT was added to 25 µg of protein (varying volumes) in RIPA buffer and boiled at 95 °C for five minutes before being loaded and separated on a 15 % SDS-PAGE gel at 100 V for two hours in 1X running buffer. The protein was then transferred onto a nitrocellulose membrane (Bio-Rad, California, USA) for 1 hour at 100 V in 1X transfer buffer. This was then detected using the Clarity™ Western ECL Blotting Substrate (Bio-Rad, California, USA). To detect BLID, mouse anti-BLID antibody (Novus Biologicals, Singapore, Malaysia) was used, with a HRP bound goat anti-mouse secondary antibody (Bio-Rad, California, USA). The p38 protein was used as a loading control and detected using the rabbit anti-p38 antibody (Sigma-Aldrich, Missouri, USA) and the HRP bound goat anti-rabbit secondary antibody (Bio-Rad, California, USA). BLID – BH3-like motif containing inducer of cell death; HIV – HIV-AT2 treated cells; MV – microvesicle treated control; + - positive control

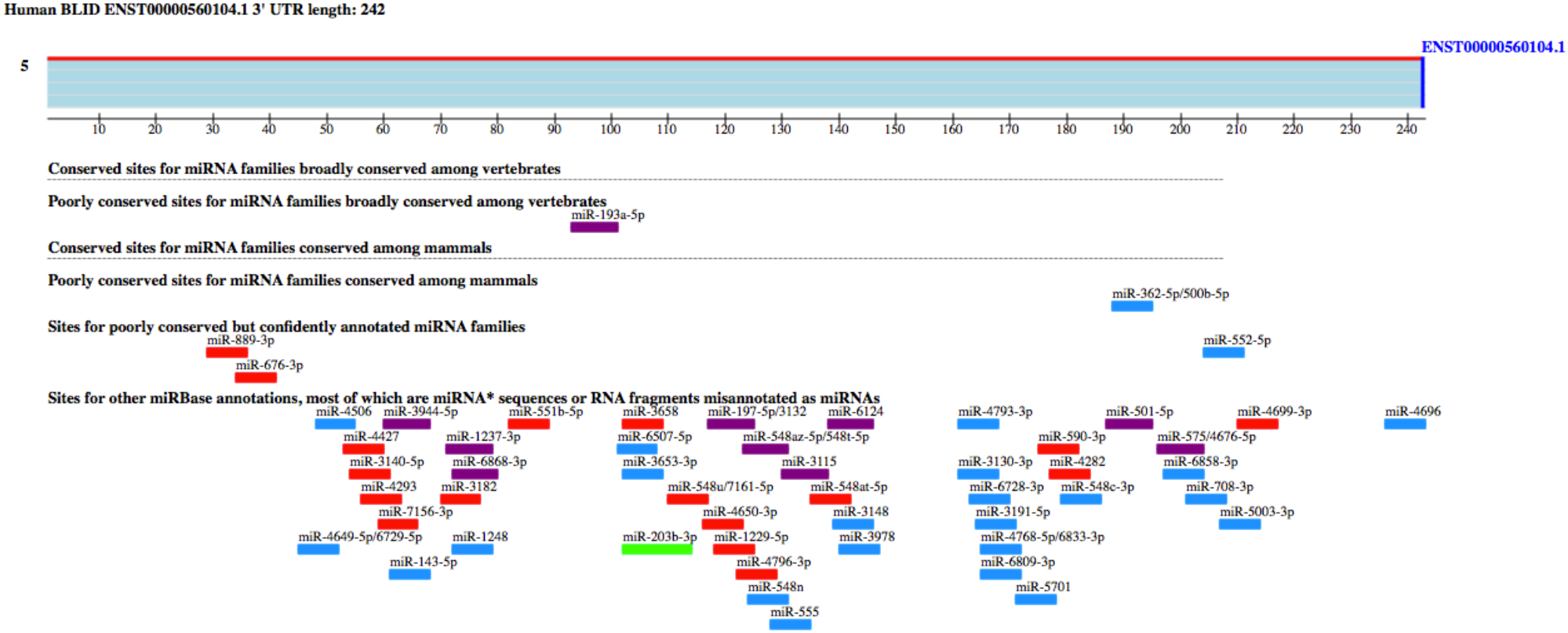


**Figure B5: Output from TargetScan for the mRNA:miRNA possible interaction between miR-575 and BLID**

## APPENDIX C: ADDITIONAL STATISTICAL DOCUMENT

CPGR | CENTRE FOR PROTEOMIC & GENOMIC RESEARCH

# Analytical Report

| | |
|---|---|
| **Report to** | **Dr Shaheen Mowla**<br>**Division of Haematology**<br>**University of Cape Town** |
| **Document Number** | **BIX03022015-001** |
| **Version** | **1.0** |
| **Status** | **Final** |
| **Date** | **5 February 2015** |
| **Project ID** | **0679BIX_SMOWLA_EXHIV** |
| **Author:** | **Wendy Kröger**<br>**Bioinformatics Analyst** |
| **Reviewers** | **Ida van Jaarsveld**<br>**Lead Bioinformatician**<br>**And**<br>**Nicki Adams**<br>**qRT-PCR Platform Manager** |

## Table of Contents

## 1. Background and Samples Submitted

The aim of this study is to investigate the differential expression of miRNA in a B cell lymphoma cell line treated with attenuated HIV, compared to microvesicle treated and untreated negative controls, as measured by an Applied Biosystems Custom TaqMan® MicroRNA qRT-PCR Assay by the CPGR (project ID 0530ABI_MOWLA_RT_PCR). The sample preparation and assay QC were reported in document 13012015_001.

A brief summary of the experiment reported herein is as follows: Nine B cell cancer cell line samples (Table 1) were submitted by the client to the CPGR for RNA extraction and gene expression analysis via qRT-PCR array. The client provided all materials and reagents and CPGR provided assistance with experimental analysis.

**Table 1. B cell cancer cell line RNA samples and details submitted by the client.**

| Sample ID | Details | Categorical comparison group |
|---|---|---|
| **HIV1** | HIV treated | HIV |
| **HIV2** | HIV treated | HIV |
| **HIV3** | HIV treated | HIV |
| **MV1** | Microvesicle treated control | MV |
| **MV2** | Microvesicle treated control | MV |
| **MV3** | Microvesicle treated control | MV |
| **UT1** | Untreated control (1) | - |
| **UT2** | Untreated control (2.3) | - |
| **No-RT** | No-RT control | - |

The SDS output files were converted to plain text using Applied Biosystem's RQ Manager (version 1.2), which served as input for the remainder of the differential expression experiment. Bioconductor's HTqPCR package (Dvinge & Bertone, 2009) was used in R (R Development Core Team, 2013) to analyse the qRT-PCR data. It is expected that the samples treated with HIV will exhibit a different expression profile to the microvesicle treated controls.

## 2. Abbreviations

| | |
|---|---|
| **Ct** | Cycle threshold |
| **ddCt** | method to analyse relative changes in qRT-PCR data, if target and calibrator gene amplification efficiencies are approximately equal (Pfaffl, 2001) |
| **FDR** | false discovery rate (Benjamini-Hochberg/false discovery rate (0.06) multiple testing correction for *p*-value) (Benjamini & Hochberg, 1995) |
| **miRNA** | microRNA |
| **PCA** | Principal Component Analysis |
| **qRT-PCR** | quantitative real-time PCR |
| **adjusted *p*-value** | FDR adjusted (0.1) *p*-value |
| **SDS** | file output format from the Applied Biosystem's qRT-PCR instrument ABI7900HT |

## 3. Analysis Synopsis

Applied Biosystems qRT-PCR Ct values generated from 384 well plates (1 plate per sample) were analysed with Bioconductor's HTqPCR package (Dvinge & Bertone, 2009) in R (R Development Core Team, 2013) to determine differentially expressed miRNA's in B cell cancer cell lines treated with HIV compared to controls. Raw data quality was assessed and normalised. Differential expression of miRNA's in the HIV-treated cells was compared to that in the MV controls. Untreated samples were not included in the differential expression analysis as there were not enough replicates to calculate significance. Significance was determined by an FDR adjusted *p*-value < 0.06, corrected for multiple testing.

## 4. Detailed Analysis

qRT-PCR allows the simultaneous detection and relative quantitation of a target through measurement of the amplification of this sequence. Sufficient presence of the target DNA molecule in a given sample results in an increase in fluorescent signal over a set number of PCR cycles (usually 40). Ct values are measured as the cycle number at which point the curve intersects a fluorescence threshold (set to exceed baseline noise). The amount of target template contained within a sample is therefore inversely proportional to the Ct value, i.e. lower Ct values are indicative of a large amount of target present and *vice versa*. In general, Ct values of below 29 are characteristic of strong positive amplifications suggesting abundant target molecule present in the sample. Those Ct values of between 30 and 37 are indicative of positive reactions characterising moderate levels of target molecule present in the sample. Ct values of above 38 are characteristic of weak amplification suggesting minimal amounts or lack of target molecule present within the respective sample.

### Raw data visualisation

HIV1_21102014, HIV2_21102014, HIV3_21102014, MV1_22102014, MV2_22102014, MV3_22102014, Untreated1_21102014, Untreated2.3_22102014 and Test2_noRT 02102014.txt files were loaded into R using the HTqPCR package. Overall the raw Ct values were quite high or "Undetermined" indicating a low level of target present. This was probably due to the low amount of RNA template that was used in the experiment (see document number 13012015_001).

The average Ct values for all features across all samples revealed an overall similar pattern as expected (see Appendix). Spatial visualisation of the raw Ct values (see Appendix) indicated there were a large number of "Undetermined" Ct values (grey circles) on each plate, suggesting minimal or no target present in the samples. Measured Ct values ranged mostly from 20 – 40; however it should be highlighted that lower Ct values may in fact be a result of peak noise from the baseline and raw data should be consulted before drawing any conclusions from these findings. The no-RT control indicated generally very high Ct values for all wells as expected, however it is important to note that there were 35 features that displayed Ct values of < 40 (see Appendix). These features also need to be considered when interpreting any findings from this study.

Concordance between feature replicates within samples was not good, with a number of feature replicates indicating large variation between replicates (more than 20% difference from their means) (Table 2 and see Appendix). Boxplot comparisons of standard deviations of the raw data revealed a similar pattern between sample groups (excluding the no-RT control; Figure 1) and variation versus mean plots for each sample revealed a few outlying features within each sample (see Appendix).

**Table 2. Number of features with large variation between replicates (more than 20% difference from their means)**

| Sample ID | Number of features |
|---|---|
| **HIV1** | 11 |
| **HIV2** | 20 |
| **HIV3** | 16 |
| **MV1** | 16 |
| **MV2** | 20 |
| **MV3** | 13 |
| **UT1** | 18 |
| **UT2** | 17 |
| **No-RT** | 10 |

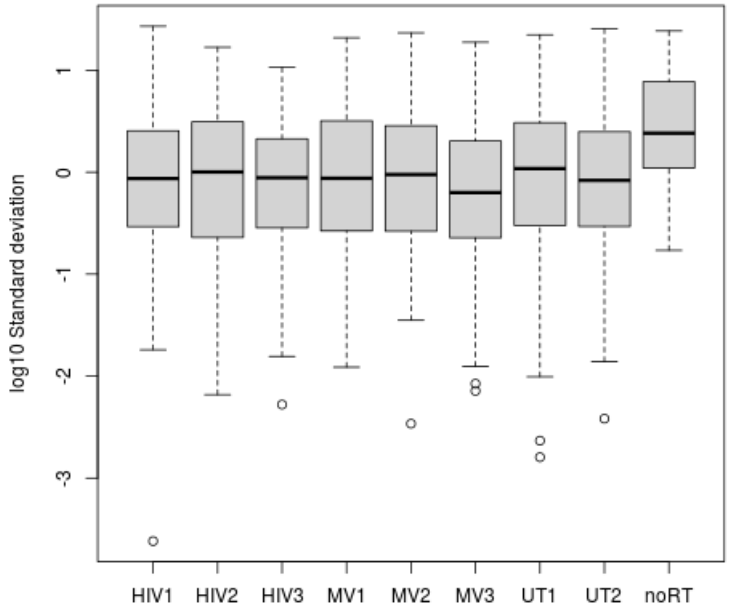


**Figure 1. Summary of standard deviation between raw replicated features within samples.**

The HTqPCR package allows us to assign a reliability category of "OK", "Undetermined" or "Unreliable" to each Ct value. All features are still tested for differential expression; however each feature result is flagged accordingly (see below). The "Undetermined" flag is automatically assigned to any features with Ct values undetermined by the qRT-PCR instrument. An "Unreliable" category is assigned to feature replicates displaying large variation or extremely low values that may be problematic (set in this case for a Ct of below 3). Based on the amplification curves we observed in

RQ Manager, we filtered these data using minimum and maximum Ct thresholds of 3 and 40 respectively with a 90% confidence interval. Figure 2A demonstrates the breakdown of features into their "OK", "Undetermined" and "Unreliable" categories after this filtering, demonstrating that more than half of the features within each sample retained an "OK" flag. Figure 2B stratifies this information per feature set. We have also included these figures containing only HIV and MV sample comparisons in the Appendix.

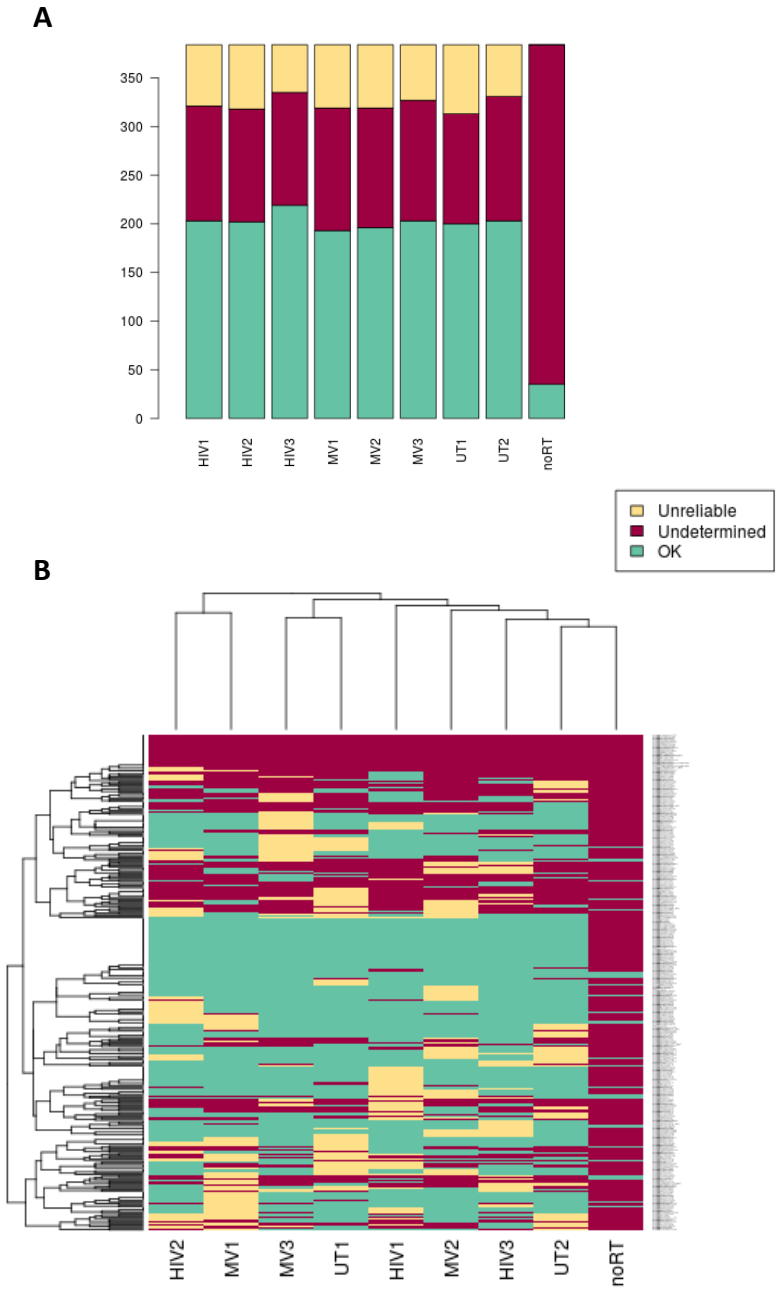


**Figure 2. Summary of the categories after filtering either for (A) each sample individually or (B) each sample stratified by feature class.**

## Normalisation and quality assessment

Because the Student's t-test requires at least three replicates for significance testing, and the triplicate MV controls better represent a true control for the triplicate HIV treated samples compared to the UT controls (only 2 samples), we continued our differential expression analysis with only the HIV and MV control samples. HIV1-3 and MV1-3 sample data were reloaded alone into HTqPCR and normalised using the geometric mean (Mestdagh et al., 2009), delta Ct, quantile and rank invariant methods. As each method has its own advantages and disadvantages, it can be useful to use more than one method of normalisation to see how the data best fits a normalisation algorithm. Quality assessment of raw and normalised Ct values for each method (Figure 3) suggest that all methods work well for larger Ct values, with the Geometric mean and Delta Ct methods displaying the most similar patterns to the raw data for all Ct values. Quantile and Rank invariant methods showed some large deviations from the raw data for Ct values below 25, which suggests a possibility of over-normalisation using these methods. Boxplot summaries of normalised results are available in Figure 4.

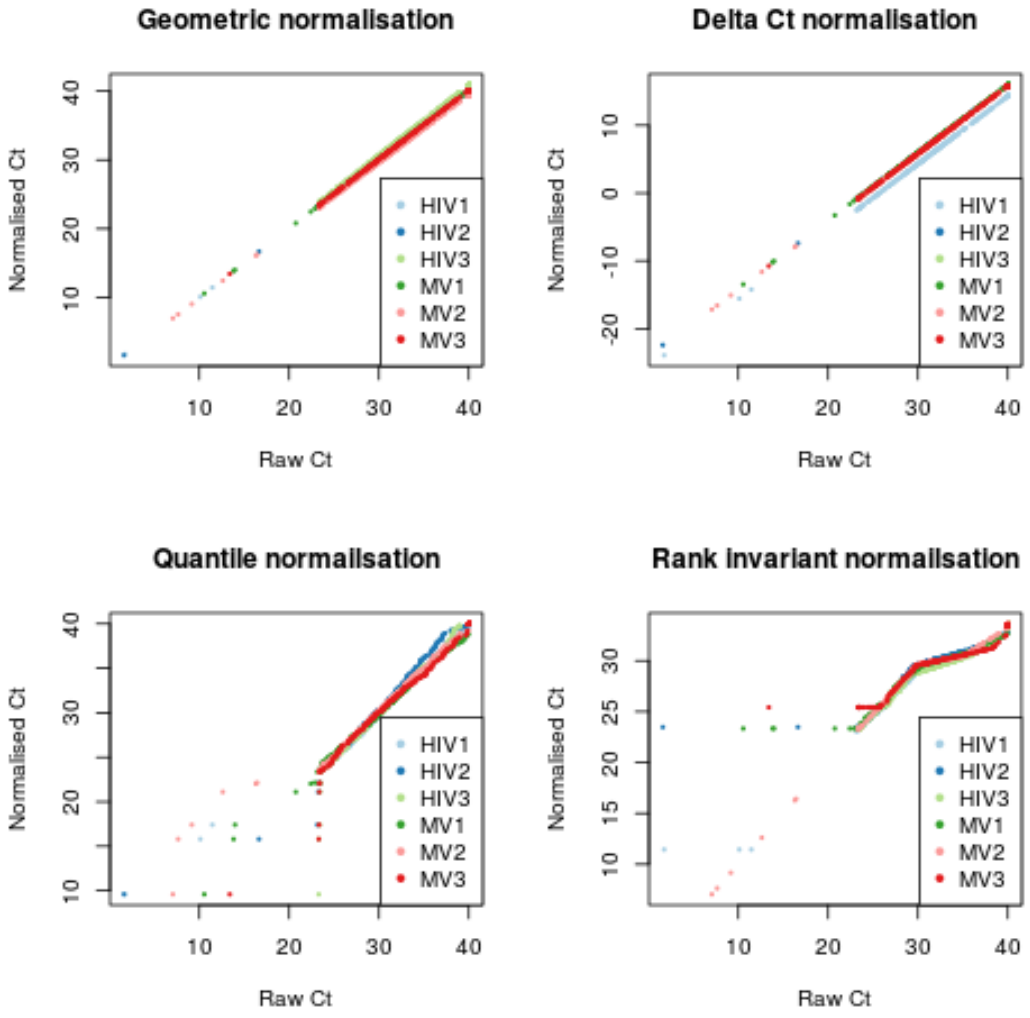


**Figure 3. Normalised versus raw Ct data for each normalisation method performed.**

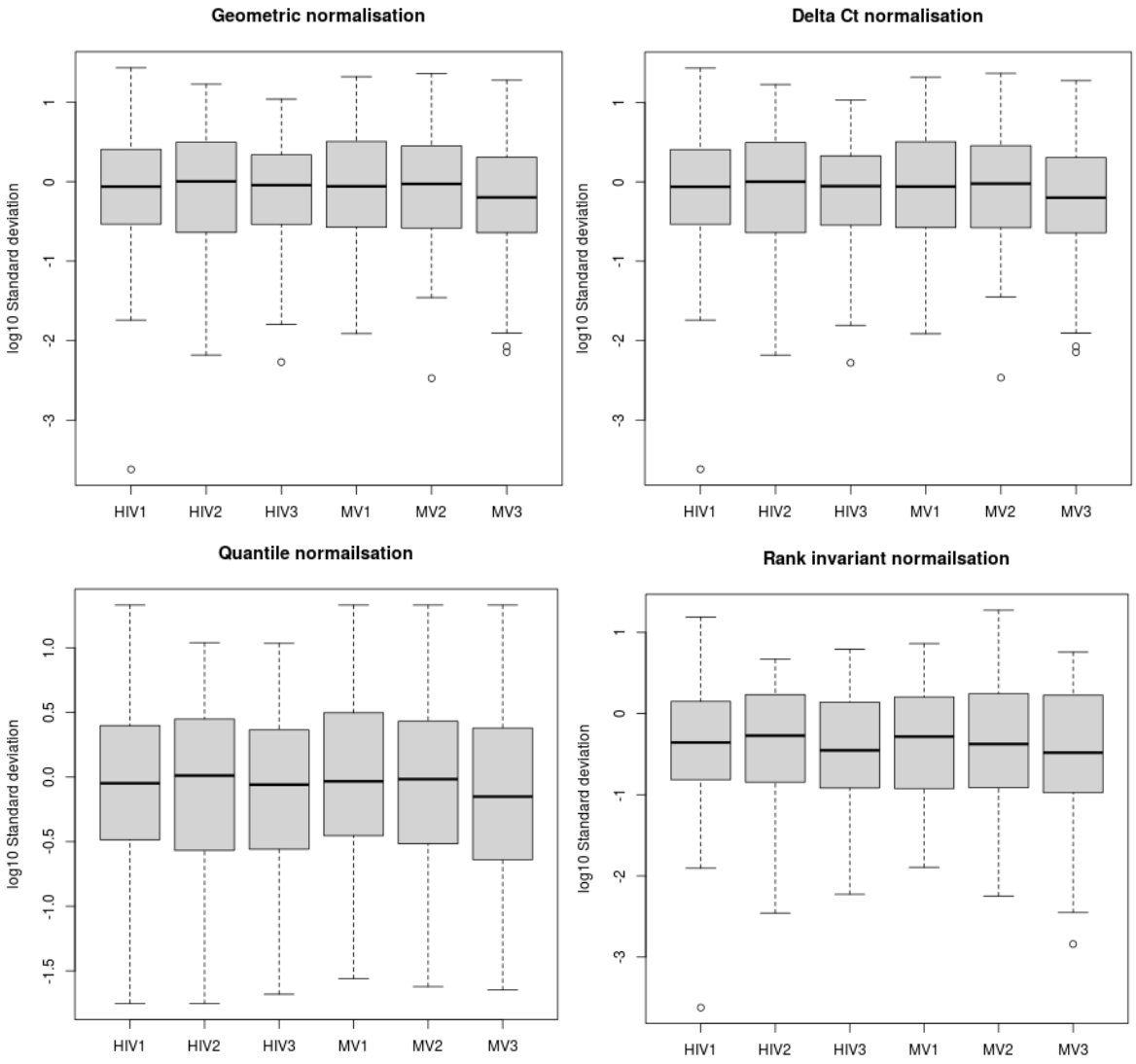


**Figure 4. Summary of standard deviation between each normalised set of replicated features within samples.**

Correlation between samples for raw and normalised data sets (Figure 5) indicated some correlation within sample groups (please note that 1 minus the correlation is plotted). Quantile normalisation resulted in the highest correlation between samples with a dendrogram structure most fitting of the sample groups. Rank invariant normalisation resulted in the lowest correlation between samples compared to the other normalisation methods and raw data.

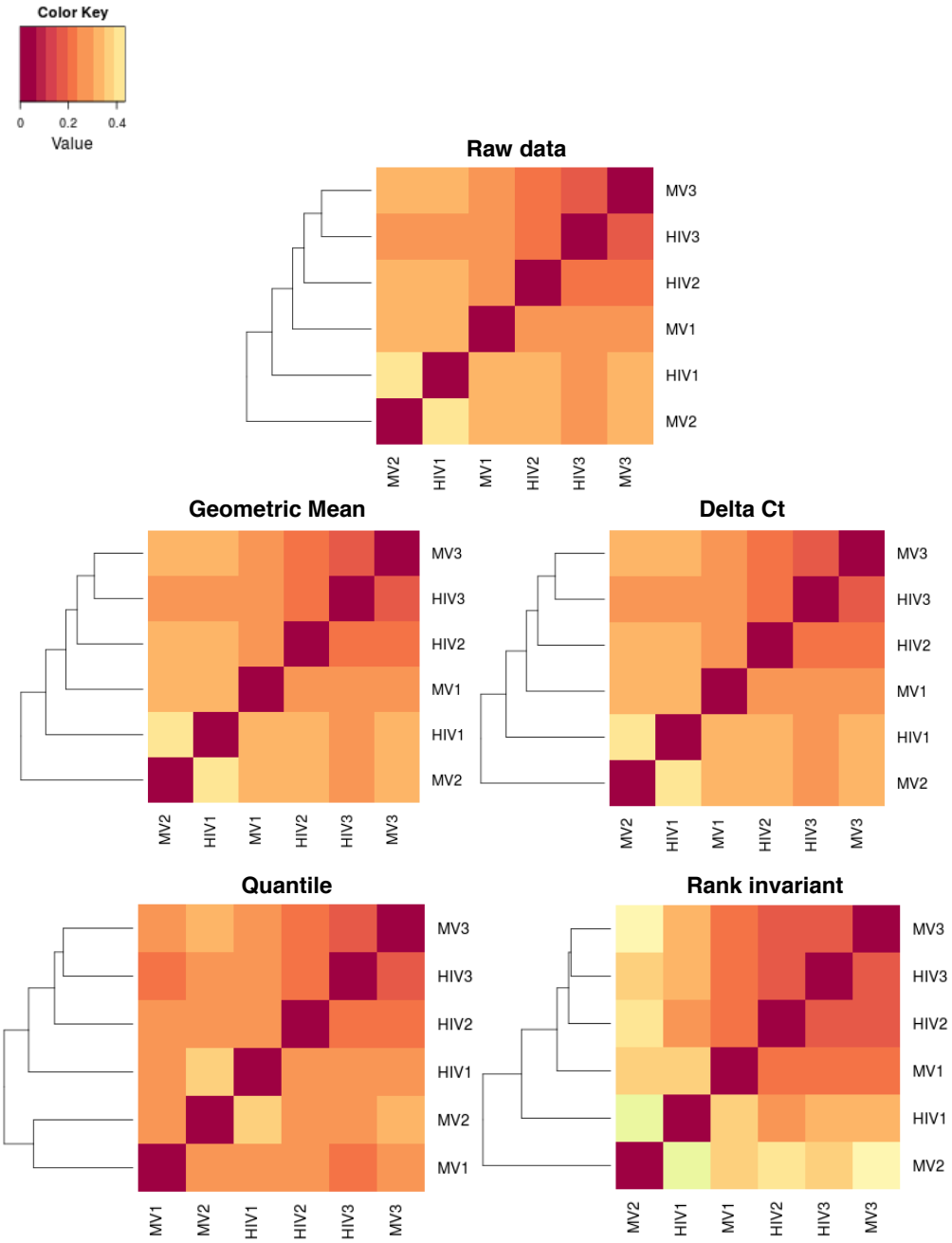


**Figure 5. Correlation between samples for the raw data and each normalisation method between Ct values (1 minus the correlation is plotted).**

## Initial analysis of normalised qRT-PCR data

The distributions of Ct values are similar for all datasets (raw and normalised) and are plotted in Figure 6. Please note that the peak at Ct = 40 for all of the plots is due to the large number of "Undetermined" Ct values which are automatically assigned a value of 40 for the generation of this plot. These plots therefore suggest a normal-like distribution of the data, albeit with a possible right skew. Scatterplots for all pairwise comparisons between samples were also generated (see Appendix).

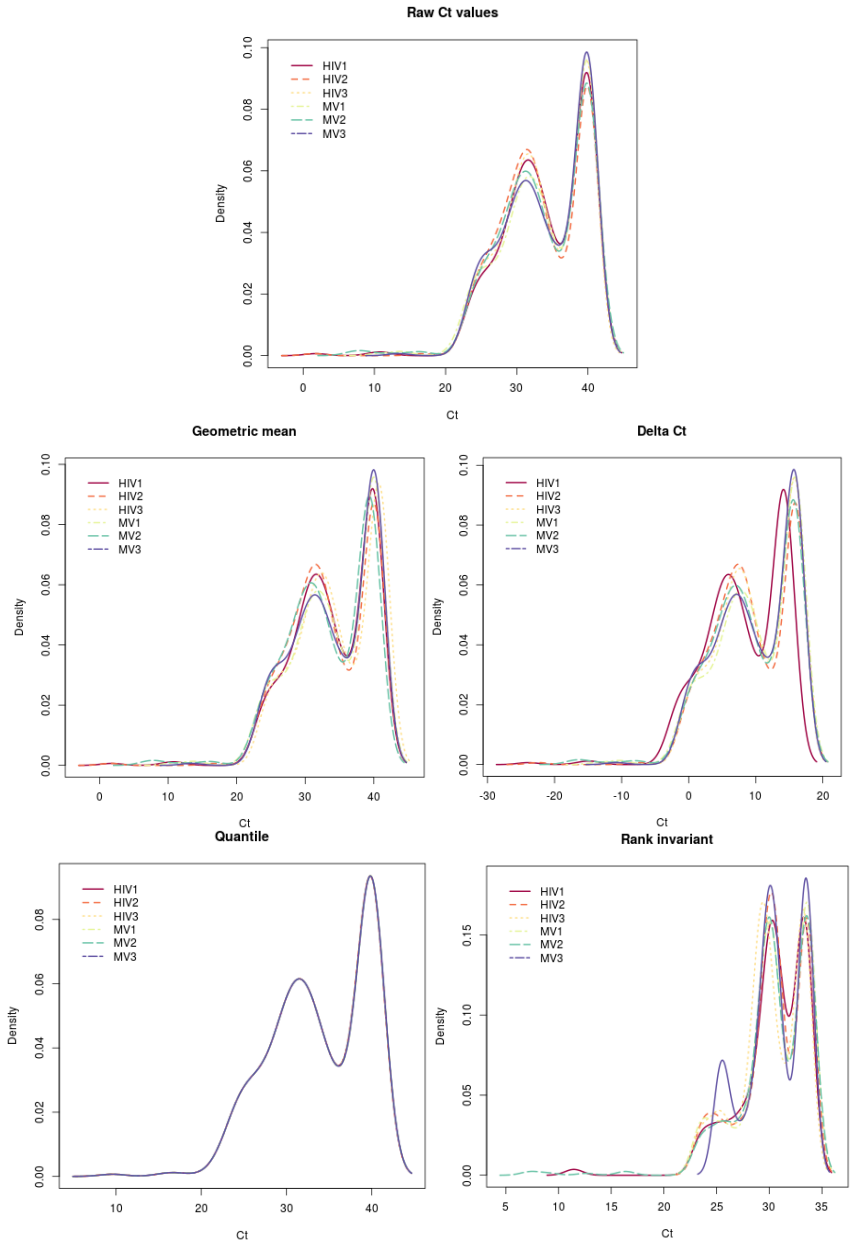


**Figure 6. Distribution of Ct values for the individual samples before and after each normalisation method. The large number of "Undetermined" features are automatically assigned a Ct of 40 in this function, resulting in the large peak at the high end of the x-axis scale.**

Heatmaps generated to visualise the Euclidean distance clustering of features and samples (Figure 7; please see Appendix for Pearson correlation clustering), as well as PCA plots (Figure 8), revealed that sample groups did not cluster together as expected, suggesting large variation between replicates.

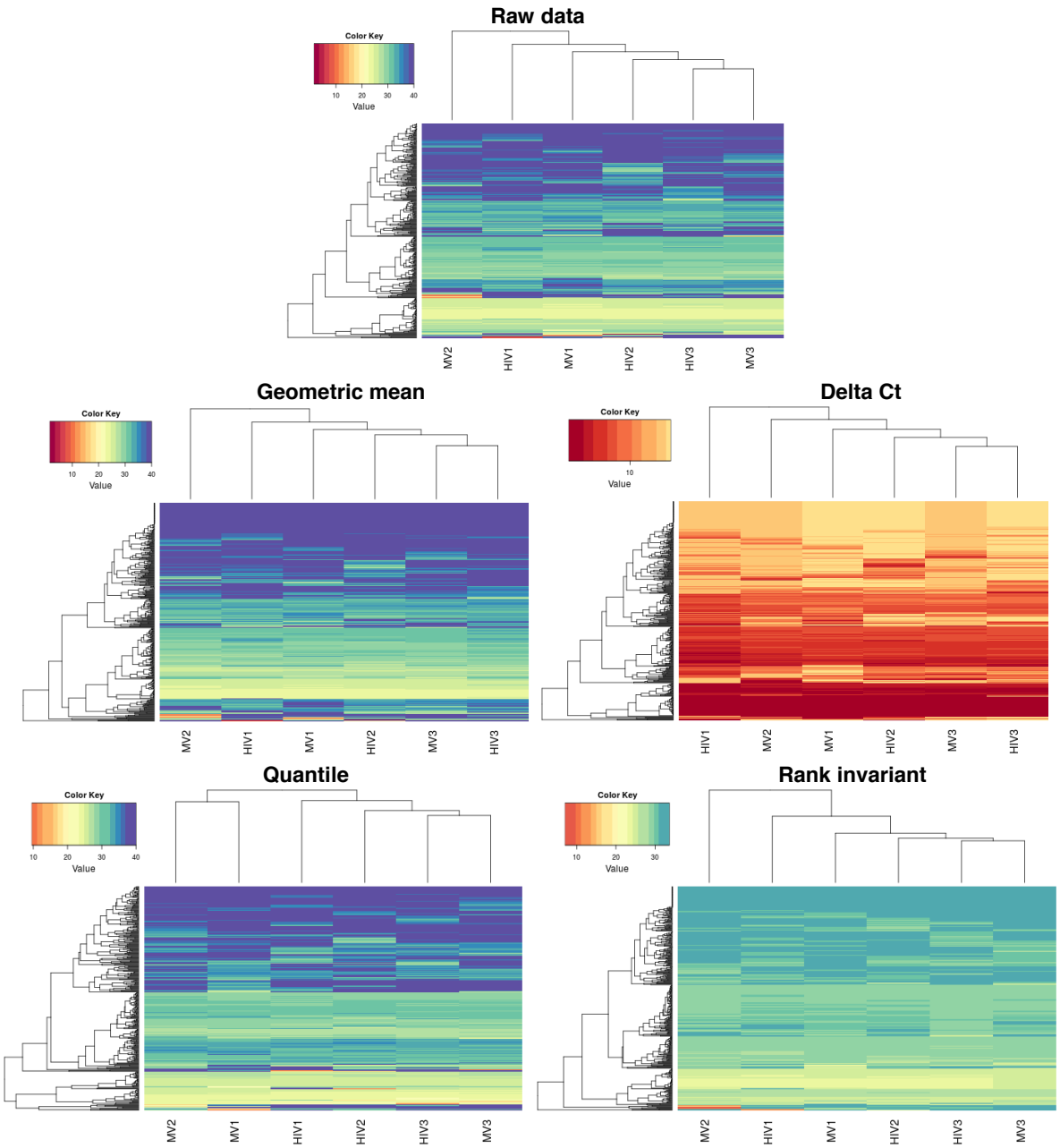


**Figure 7. Heatmaps for raw and normalised data sets based on Euclidean distance clustering between Ct values revealing no clustering of sample groups.**

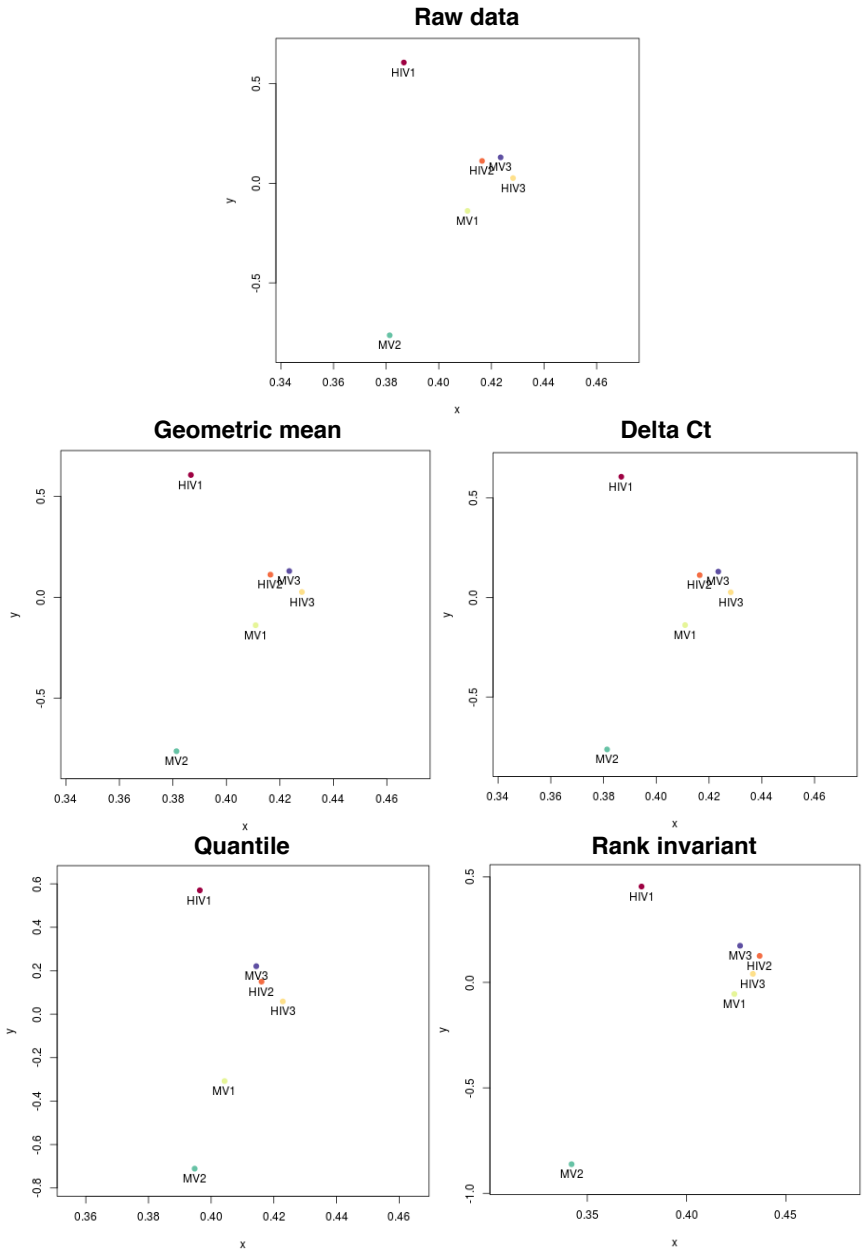


**Figure 8. PCA plots of raw and normalised samples revealing no clustering of sample groups.**

Overall, the quality assessment of each of the normalisation methods suggests that Quantile normalisation will be the most reliable method due to the concordance between samples and the clustering of the data. It should be noted that there is some indication that for low Ct values the data may be slightly over-normalised with Quantile normalisation (Figure 3), and the raw data should be consulted before drawing any conclusions from these findings. We should also point out that the HTqPCR documentation mentions that there is some suggestion that Geometric mean normalisation has some advantages over others particularly for miRNA studies (Dvinge & Bertone, 2009; Mestdagh et al., 2009). Based on these quality assessments, we feel that Rank invariant normalisation seems to be the least reliable method, and this normalised data set was therefore omitted from subsequent differential expression analyses.

## Determining differentially expressed genes

The samples loaded into the HTqPCR for normalisation (above; HIV1-3 and MV1-3) were assigned into the categorical comparison groups "HIV" (target) and "MV" (calibrator). Comparison groups were designated by biological replication, and replicates were assigned to their respective groups (see Table 1). As the data displayed a normal-like distribution (Figure 6), the Student's t-test was used to test for significance of differences in Ct values between the microvesicle treated controls and the HIV treated cells. All features are included in the t-test calculation regardless of reliability flag, however each feature result indicates its reliability with an "OK" or "Undetermined" category flag for each sample group (categoryHIV and categoryMV); the latter indicating that at least a single feature within at least a single sample contained an "Undetermined" or "Unreliable" flag for that sample group.

The results are provided in spreadsheet format, with each normalisation method analysed on an individual sheet within the spreadsheet (see Appendix). Each sheet is provided in order of increasing adjusted *p*-value (adj.p.value in the spreadsheet), and can be manipulated by sorting according to a field of interest by clicking on the down arrow in the header of that field. Other fields include the t statistic (t.test), the raw *p*-value not adjusted for multiple testing (p.value), delta delta Ct (ddCt; (Pfaffl, 2001)), the fold change (FC) calculated from ddCt using the Pfaffl method (Pfaffl, 2001), and the log of this fold change (log(FC)). It is important to note that while the Pfaffl method is extremely convenient to calculate fold change from Ct values, it is only completely accurate when the amplification efficiency of both the target and the calibrator sequences are approximately equal. Therefore all conclusions made from these findings (and confirmed with the raw data) need to be experimentally validated. Log(FC) values are coloured by scale (blue and red for respective decreases and increases in fold change), and features with "Undetermined" or "OK" Ct value flags are indicated in red and green respectively for HIV (categoryHIV) and MV (categoryMV) samples.

The t-test revealed significant (FDR adjusted *p*-value < 0.06), albeit modest, differential expression for hsa-miR-532-001518 and hsa-miR-342-3p-002260 from the quantile normalised data set (Table 3 and see Appendix for full t-test results table; FDR adjusted *p*-values < 0.06 are indicated in yellow). There was no significant differential expression observed from the t-tests of the geometric mean and delta Ct normalised data sets, both of which displayed more similar distributions to the raw data compared to Quantile normalisation. It is important to remember that the lower Ct values may have been over-normalised using certain normalisation algorithms, and that the raw data and category flags should be consulted before drawing any conclusions from these results.

**Table 3. Significantly differentially expressed miRNA's as determined by Quantile normalised qRT-PCR array data (adjusted *p*-value < 0.1) (An "Undetermined" flag indicates undetermined or unreliable Ct values were obtained for one or more feature Ct's within that sample group).**

| miRNA | FDR adjusted *p*-value | Fold change | HIV flag | MV flag |
|---|---|---|---|---|
| **hsa-miR-532-001518** | 0.0584 | 0.432 | OK | Undetermined |
| **hsa-miR-342-3p-002260** | 0.0584 | 1.630 | OK | OK |

## Minimal differential expressed gene list mitigation

We would also like to highlight that there were a number of genes that, while not significantly differentially regulated, demonstrated fold changes which may be of interest (please see the full t-test results table which is currently ordered from smallest to largest adjusted *p*-value, but can easily be ordered by largest increase to largest decrease in FC by clicking the small down arrow in the FC or log(FC) header). For example, in the t-test results for all three normalised data sets, hsa-miR-92a-2#-002138 demonstrated the highest increase of between 1.955 and 2.21 fold, while hsa-miR-627-001560 and hsa-miR-9-000583 displayed the largest decreases of between of more than 1.45 fold (see Appendix). These large fold changes do warrant further investigation as their non-significant adjusted *p*-values may be due to a single outlying sample contributing large variation to the sample group. As mentioned above however, it is also very important to note that the raw data and category flags for each feature should be consulted before drawing any conclusions from these results.

## 5. Deviations

Because the Student's t-test requires at least three replicates for significance testing and the UT controls only contained two biological replicates, differential expression was only analysed in HIV treated samples compared to MV controls and not HIV treated compared to untreated controls.

As not much significant differential expression was identified from these analyses, a secondary approach was suggested whereby fold change is assessed without consideration for adjusted *p*-value, or significance. This was in order to extract as much biological information from the study as possible, despite the above being an invalid methodology which is not publishable. It is important to highlight that one needs to consult the individual feature Ct flags and the raw data before drawing any conclusions from these results, whether significant or not.

## 6. Enquiries

Your application specialist on this project is Wendy Kröger; do not hesitate to contact her on 021 447 5669 or wendy.kroger@cpgr.org.za, for additional discussion or information on this report. Please feel free to contact us to organise a meeting to come and have a look at your raw data on our RQ Manager software once you have had a chance to analyse our findings.

## 7. References


Benjamini, Y., & Hochberg, Y. (1995). Controlling the False Discovery Rate: A Practical and Powerful Approach to Multiple Testing. *Journal of the Royal Statistical Society. Series B (Methodological)*, *57*(1), 289 – 300. doi:10.2307/2346101

Dvinge, H., & Bertone, P. (2009). HTqPCR: high-throughput analysis and visualization of quantitative real-time PCR data in R. *Bioinformatics (Oxford, England)*, *25*(24), 3325–6. doi:10.1093/bioinformatics/btp578

Mestdagh, P., Van Vlierberghe, P., De Weer, A., Muth, D., Westermann, F., Speleman, F., & Vandesompele, J. (2009). A novel and universal method for microRNA RT-qPCR data normalization. *Genome Biology*, *10*(6), R64. doi:10.1186/gb-2009-10-6-r64

Pfaffl, M. W. (2001). A new mathematical model for relative quantification in real-time RT-PCR. *Nucleic Acids Research*, *29*(9), e45. Retrieved from

http://www.pubmedcentral.nih.gov/articlerender.fcgi?artid=55695&tool=pmcentrez&rendertype=abstract

R Development Core Team. (2013). R: A language and environment for statistical computing. R Foundation for Statistical Computing, Vienna, Austria. URL http://www.R-project.org/. *R Foundation for Statistical Computing, Vienna, Austria.*

# 8. Appendices

## Data visualisation

The files detailed below are provided in the `data_visualisation/` folder:

| | |
|---|---|
| **spatial_layout** | Spatial visualisation of each array in PDF format (grey = Undetermined Ct). |
| **noRT_features_over40** | Features found on the no-RT control array with Ct values below 40. |
| **average_Ct/** | See below |
| **concordance/** | See below |
| **variation/** | See below |
| **feature_categories/** | See below |

The files detailed below are provided in the `data_visualisation/average_Ct` folder:

| | |
|---|---|
| **ave_Ct** | Plot of average Ct values for each feature and all samples (provided in PDF and PNG formats). |

The files detailed below are provided in the `data_visualisation/concordance` folder:

| | |
|---|---|
| **replicate_ concordance** | Concordance between duplicated Ct values in all samples, marking features differing > 20% from their mean in PDF format. |
| **reps_diff_more_than_20/** | Text files containing feature names for all feature replicates differing > 20% from their mean. |

The files detailed below are provided in the `data_visualisation/variation` folder:

| | |
|---|---|
| **SD_of_reps** | Summary of standard deviation between raw replicated features within samples (in PDF and PNG formats). |
| **var_vs_mean** | Variation versus mean plots for each sample (in PDF and PNG formats; Figure 1). |

The files detailed below are provided in the `data_visualisation/feature_categories` folder:

| | |
|---|---|
| **feature_categories** | Summary of the categories after filtering either for each sample individually (in PDF and PNG formats; Figure 2A). |
| **feature_categories _by_feature** | Summary of the categories after filtering either for each sample stratified by feature class individually (in PDF and PNG formats; Figure 2B). |

## Normalisation and quality assessment

The files detailed below are provided in the `QC_normalised/` folder:

| | |
|---|---|
| **raw_vs_norm** | Normalised versus raw Ct data for each normalisation method (in PDF and PNG formats; Figure 3). |
| **SD_of_reps** | Summary of standard deviation between each normalised set of replicated features within samples (in PDF and PNG formats; Figure 4). |
| **correlation/** | Correlation between samples for the raw data and each normalisation method between Ct values. 1 minus the correlation is plotted in PNG format (Figure 5). |
| **Ct_distributions/** | Distribution of Ct values for the individual samples before and after each normalisation method in PNG format (Figure 6). |
| **heatmaps/** | Heatmaps based on Euclidean distance (Figure 7) and Pearson correlation clustering. |
| **PCA/** | PCA plots raw and normalised data in PNG format (Figure 8). |

## Differentially expressed genes

The files detailed below are provided in the `differential_expression/` folder:

| | |
|---|---|
| **`t_test/`** | Directory containing tab separated plain text files for t-test results on data sets from each normalisation method. Please see section entitled **"**Determining differentially expressed genes" for explanation of field headers. |
| **`t_test_results.xlsx`** | Spreadsheet with all t-test results with each normalisation method on an individual sheet. Please see section entitled **"**Determining differentially expressed genes" for explanation of field headers. |


CPGR
WORLD CLASS
BIO-TECH
MADE IN
AFRICA